



**Michigan
Technological
University**

**Michigan Technological University
Digital Commons @ Michigan Tech**

Dissertations, Master's Theses and Master's Reports

2019

EFFECTS OF VARIABLE VALVE ACTUATION ON EXHAUST ENTHALPY AND ENGINE OUT EMISSIONS

Zakarie Parker

Michigan Technological University, zrparker@mtu.edu

Copyright 2019 Zakarie Parker

Recommended Citation

Parker, Zakarie, "EFFECTS OF VARIABLE VALVE ACTUATION ON EXHAUST ENTHALPY AND ENGINE OUT EMISSIONS", Open Access Master's Thesis, Michigan Technological University, 2019.
<https://digitalcommons.mtu.edu/etdr/883>

Follow this and additional works at: <https://digitalcommons.mtu.edu/etdr>



Part of the [Automotive Engineering Commons](#)

EFFECTS OF VARIABLE VALVE ACTUATION ON EXHAUST ENTHALPY AND
ENGINE OUT EMISSIONS

By
Zakarie Parker

A THESIS

Submitted in partial fulfillment of the requirements for the degree of
MASTER OF SCIENCE
In Mechanical Engineering

MICHIGAN TECHNOLOGICAL UNIVERSITY

2019

© 2019 Zakarie R. Parker

This thesis has been approved in partial fulfillment of the requirements for the Degree of MASTER OF SCIENCE in Mechanical Engineering.

Department of Mechanical Engineering – Engineering Mechanics

Thesis Advisor: *Dr. Jeremy Worm*

Committee Member: *Dr. Jeffrey S. Allen*

Committee Member: *Dr. Scott A Miers*

Department Chair: *Dr. William W. Predebon.*

Table of Contents

List of figures.....	vi
List of tables.....	x
Acknowledgments.....	xi
Definitions.....	xii
List of abbreviations	xiii
Abstract.....	xv
1 Introduction.....	1
1.1 Emissions.....	1
1.1.1 EPA Dynamometer Drive Cycles	1
1.1.2 Updates to Emissions Standards	3
1.2 Current Methods for Meeting Emissions Standards.....	4
1.2.1 Catalytic Converter Operation	4
1.2.2 Current Catalyst Light-Off Strategies	5
1.3 Motivation	6
2 Literature Review.....	7
2.1 Cold Start Emissions	7
2.2 Catalyst Light-Off	9
2.2.1 Retarded Ignition Timing.....	9
2.2.2 Electric heating elements	9
2.2.3 Exhaust Afterburners/Burner	9
2.2.3.1 Afterburner.....	9
2.2.3.2 Burner	10
2.3 Valve Activation.....	10
2.4 Crevice HC Emissions.....	11
3 Goals and Objectives	12
3.1.1 Test New Hypothesis	12
3.1.1.1 Valve Deactivation.....	12
3.1.1.2 Longer Exhaust Cam Duration	12
4 Research Methodology	13
4.1 Camshafts	14
4.1.1 Mid-Duration	14

4.1.1.1	Maintaining Opening and Closing Profiles.....	14
4.1.1.2	Pushing EVC As Late As Possible	14
4.1.1.3	Maximum Output At 6,000 RPM	15
4.1.1.4	Design Process	15
4.1.2	Long Duration	19
4.2	Test Matrix	20
4.3	Test Procedure.....	21
4.3.1	Testing.....	21
4.3.2	Engine Cleaning Procedures	22
5	Experimental Setup.....	23
5.1	Engine Test Bed	23
5.1.1	Engine	23
5.1.2	Fluids.....	24
5.1.2.1	Fuel	24
5.1.2.2	Oil	24
5.1.2.3	Coolant.....	24
5.1.3	Engine Controller.....	24
5.1.3.1	Split Injection.....	24
5.2	Instrumentation.....	25
5.2.1	Engine Dynamometer	25
5.2.2	Test Cell Control and Low-Speed DAQ.....	25
5.2.3	In-Cylinder Pressure Transducers.....	26
5.2.4	Combustion Analyzer	26
5.3	Emissions Equipment.....	26
5.3.1	Fast Response Analyzers	26
5.3.1.1	Fast FID	26
5.3.1.2	Fast CO/CO2.....	27
5.3.2	PM/PN.....	29
5.3.3	Horiba 5-Gas.....	29
5.3.4	Cummins NOx Sensor	30
5.3.5	Probe Location	31
5.4	Camshaft Procurement	32
5.4.1	Camshaft Install	36
5.5	Valve Deactivation	38
5.6	Operational Temperatures	39
5.7	Parameterization	40
5.7.1	SOI Sweep	40
5.7.2	Lambda Sweep.....	42

6	Results.....	45
6.1	Rate of Exhaust Enthalpy	45
6.1.1	Single valve vs Dual valve.....	45
6.1.1.1	CA50.....	45
6.1.1.2	COV IMEP.....	47
6.1.2	Exhaust Enthalpy	49
6.1.2.1	Temperature	49
6.1.2.1.1	Heat Transfer	51
6.1.2.1.2	Increased Expansion Work	53
6.1.2.1.3	EGT Measurement	55
6.1.2.2	Mass Flow Rate.....	55
6.1.2.3	Specific Heat.....	57
6.1.2.4	Residuals.....	58
6.1.3	Combined Effects of Port Deactivation and Longer Duration Camshaft on Rate of Enthalpy.....	59
6.2	Emissions.....	62
6.2.1	Single valve vs. Dual valve.....	62
6.2.2	Combined Effects of Port Deactivation and Cam Duration Increase on Emissions.....	67
6.3	Mass Fraction Burn Analysis	71
7	Conclusions.....	73
8	Future Work.....	75
	Reference List	76
	Appendix A: Fuel Properties	79
9	Appendix B: Crank Position Encoder.....	80
10	Appendix C: Combustion Fast Analyzer Specifications.....	82
11	Appendix D: Copyright Documentation.....	83
11.1	Permission to use screen images and plots from GT-Power and GT-Post software produced by Gamma Technologies Incorporated	83
11.2	Permission to use Equation 1, Table 1, and Figure 2 from [8].....	84
11.3	Permission to use the image from [27].....	85

List of figures

Figure 1: FTP Drive Cycle [2]	2
Figure 2: Timeline for the federal test procedure [2].....	2
Figure 3: Three-way catalyst conversion efficiency as a function of lambda [6].....	4
Figure 4: Conversion efficiency for CO and HC as a function of temperature for a catalytic converter [7]	5
Figure 5: Cause-and-effect diagram of the fundamental difficulties of cold-start operation at low ambient temperatures [8]	8
Figure 6: HC post catalyst emissions comparison between cold and hot start [9]	8
Figure 7: Cold start warmup example [17].....	13
Figure 8: Mass-scaled HC flow at exhaust port septum for fully retarded stock camshaft and dual valve operation at various CA50s	15
Figure 9: Valve lift profile comparison	16
Figure 10: Valve to piston clearance from later EVC cause by longer duration camshaft	17
Figure 11: NMEP at 6,000 RPM with different max lift dwell duration increases	18
Figure 12: Cam lift profile comparison between stock exhaust camshaft and mid duration camshaft	18
Figure 13: NMEP comparison between final mid duration camshaft design and stock camshaft at different engine speeds	19
Figure 14: CA90 analysis to determine long duration camshaft duration increase	20
Figure 15: Alternative injector wiring	25
Figure 16: Combustion HFR500 Fast FID.....	27
Figure 17: Combustion NDIR500 Fast CO/CO2	28
Figure 18: TSI EEPS 3090.....	29
Figure 19: NOx reading of Horiba 5-Gas bench vs OEM Cummins NOx sensor.....	30
Figure 20: NOx reading comparison between Horiba 5-Gas bench and Cummins OEM NOx sensor for a lambda sweep	31

Figure 21: Emissions probe locations	31
Figure 22: RoC diagram [27].....	33
Figure 23: Acceleration curve for mid duration camshaft and stock RoC	34
Figure 24: Mass flow rate at exhaust valve port comparing different RoC.....	34
Figure 25: LogP-LogV diagram from GT-Power to verify RoC change doesn't cause other issues.....	35
Figure 26: Measured valve lift with the camshaft in the home position.....	37
Figure 27: Measured valve lift with the camshaft the fully retarded position	37
Figure 28: Valvetrain diagram [28]	38
Figure 29: Welded lash adjuster and hold down.....	39
Figure 30: PN from TSI EEPS for SOI sweep.....	40
Figure 31: Particle mass from TSI EEPS for SOI Sweep.....	41
Figure 32: CO from 5-Gas for particle sweep	41
Figure 33: CO ₂ and NO _x from 5-Gas for SOI sweep	42
Figure 34: HC and lambda from 5-Gas for SOI sweep	42
Figure 35: CO ₂ and NO _x for lambda sweep	43
Figure 36: HC and CO for lambda sweep.....	44
Figure 37: CA50 Sweep with stock cams without cam retard.....	46
Figure 38: Enthalpy comparison for stock cam single valve and dual valve operation with CA50 as x-axis. Top: Camshaft in home position Middle: Camshaft retarded by 25° Bottom: Camshaft retarded by 50°	47
Figure 39: Enthalpy on a COV of IMEP basis for stock cam single valve and dual valve operation. Top: Camshaft in home position Middle: Camshaft retarded by 25° Bottom: Camshaft retarded by 50° Note: Low enthalpy and high COV point for dual valve operation is due to the engine approaching misfire limit when approaching MBT.	48
Figure 40: Left- Post-turbine EGTs Right- Port EGTs.....	50

Figure 41: GT-Power heat transfer coefficient comparison	51
Figure 42: Diagram of port area after valve deactivation	53
Figure 43: LogP-LogV Diagram of experimental engine for fully retarded exhaust cam and a CA50 of 60° CA	54
Figure 44: EGT drop from port to post-turbine	55
Figure 45: Mass flow comparison for stock cam single valve and dual valve operation. Top: Camshaft in home position Middle: Camshaft retarded by 25° Bottom: Camshaft retarded by 50°	56
Figure 46: LogP-LogV with cam retarded by 50° and CA50 of 60° to show pumping losses	57
Figure 47: Enthalpy comparison for single valve and dual valve with the stock and 60° camshafts Top: Camshaft in home position Middle: Camshaft retarded by 25° Bottom: Camshaft retarded by 50°	60
Figure 48: Mass flow comparison for single valve and dual valve with the stock and 60° camshafts Top: Camshaft in home position Middle: Camshaft retarded by 25° Bottom: Camshaft retarded by 50°	61
Figure 49: HC emissions comparison for single valve and dual valve with the stock camshaft Top: Camshaft in home position Middle: Camshaft retarded by 25° Bottom: Camshaft retarded by 50°	63
Figure 50: CO emissions comparison for single valve and dual valve with the stock camshaft Top: Camshaft in home position Middle: Camshaft retarded by 25° Bottom: Camshaft retarded by 50°	64
Figure 51: NOx emissions comparison for single valve and dual valve with the stock camshaft Top: Camshaft in home position Middle: Camshaft retarded by 25° Bottom: Camshaft retarded by 50°	65
Figure 52: HC emissions comparison for single valve and dual valve with the stock and 60° camshafts Top: Camshaft in home position Middle: Camshaft retarded by 25° Bottom: Camshaft retarded by 50°	68
Figure 53: CO emissions comparison for single valve and dual valve with the stock and 60° camshafts Top: Camshaft in home position Middle: Camshaft retarded by 25° Bottom: Camshaft retarded by 50° Error! Bookmark not defined.	

Figure 54: NOx emissions comparison for single valve and dual valve with the stock and 60° camshafts Top: Camshaft in home position Middle: Camshaft retarded by 25° Bottom: Camshaft retarded by 50°	70
Figure 55: CAS CA50 comparison with post-processed CA50.....	71
Figure 56: Home position, stock cam, dual valve operation CA50 sweep.....	72
Figure 57: Specifications for Combustion Fast Analyzers [21].....	82

List of tables

Table 1: Tier 3 emissions standards, FTP for 150,000 miles [4].....	3
Table 2: Tier 1 emissions standards, FTP for 50,000 mi/5 years [4].....	4
Table 3: Approximate fleet average cold-start equivalent distances gamma for Euro 4 Stroke SI and CI vehicles [8].....	7
Table 4: Project test matrix.....	21
Table 5: Test engine physical dimensions.....	23
Table 6: Combustion Span Gases.....	28
Table 7: Camshaft procurement summary.....	36
Table 8: Temperature set points.....	39
Table 9: Cam Residual Comparison. All Values are in % The green and red plots correspond to lowest and highest values, respectively. The blue and red colors in the delta table correspond to decreased residuals from dual to single valve and increased residuals, respectively. Dual valve operation with stock, 35° duration increase, and 60° duration increase.....	58
Table 10: Residuals comparison for all configurations All values are in %. The green and red plots correspond to lowest and highest values, respectively. The blue and red colors in the delta table correspond to decreased residuals from dual to single valve and increased residuals, respectively. Left: dual valve operation with stock, 35° duration increase, and 60° duration increase Middle: single valve operation with stock, 35° duration increase, and 60° duration increase Right: Difference between dual valve and single valve operation with stock, 35° duration increase, and 60° duration increase.....	62
Table 11: Final summary of results.....	74

Acknowledgments

This project is the culmination of the support of many, all of whom I am grateful.

This project was sponsored by the APS Labs Light Duty Engine Consortium, made up of BorgWarner, Fiat Chrysler Automobiles, Ford Motor Company, and General Motors. Each of the members was engaged in the project and their input at meetings was appreciated. I would like to say an additional thank you to GM for the redesign and donation of the two prototype camshafts used in testing.

Siddarth Gopujkar, a Ph.D. candidate at APS LABS was always ready to jump in and help with GT-Power simulations or help understand the physics behind what was happening. Joel Duncan, Research Engineer at APS LABS helped a great deal with teaching me how to operate the test cell and helping to fabricate components when needed. Tucker Alsup, Research Engineer at APS LABS for the assistance in commissioning all of the emissions test benches. Paul Dice and Alex Normand of APS LABS for always being willing to help. Lastly, I would like to thank Dr. Shahbakhti for lighting the fire that drove my interest in thermodynamics and wanting to better understand the principles behind the operation of engines.

Dr. Worm, my advisor for this project and the head of the consortium that funded this research was instrumental in both the generation of and continued support during the project. If it weren't for him, I never would have pursued graduate education.

I would like to also thank my committee members Dr. Allen and Dr. Miers for taking the time to serve on my committee as well as answering some of my crazy questions throughout the time I spent in their classes.

Definitions

A	Area
A_c	Valve curtain area – the area represented by the non-circular area of the cylinder formed between the valve seat and the valve
c_p	Specific heat at constant pressure
$c_{p,i}$	Specific heat at constant pressure of constituents
D	Diameter
h	Specific exhaust enthalpy
h_c	Heat transfer coefficient
H	Rate of exhaust enthalpy
k	Thermal conductivity
K	Constant
\dot{m}	Mass flow rate
n	Polytropic exponent
Nu	Nusselt number
Pr	Prandtl number
Q	Heat transfer
Re	Reynolds number
T	Temperature
V	Volume
x	Mass fraction
x_i	Mass fraction of constituent
λ	Lambda - Air/fuel ratio divided by stoichiometric air/fuel ratio
ρ	Density

List of abbreviations

A/F	Air/fuel ratio
ATDC	After top-dead-center
BTDC	Before top-dead-center
CA	Crank angle
CA50	Crank angle of 50% charge mass burn after TDCc
CAN	Controller Area Network bus protocol
CO	Carbon monoxide
CO ₂	Carbon dioxide
COV	Coefficient of variance
ECCL	Exhaust cam centerline
EEPS	Engine Exhaust Particle Sizer Spectrometer
EGT	Exhaust gas temperature
EPA	Environmental Protection Agency
EVC/EVO	Exhaust valve closing, opening
FID	Flame ionization detector
FMEP	Frictional mean effective pressure
FTP	Federal test procedure
H ₂	Hydrogen
H ₂ O	Water
HC	Unburned hydrocarbons
IVC/IVO	Inlet valve closing, opening
IMEP	Indicated mean effective pressure
LDV	Light duty vehicle

MAP	Manifold absolute pressure
MEP	Mean effective pressure
N ₂	Nitrogen
NDIR	Nondispersive infrared sensor
NMEP	Net mean effective pressure
NMHC	Non-methane hydrocarbon emissions
NO	Nitric oxide
NO ₂	Nitrogen dioxide
NO _x	Combined NO+NO ₂
NVH	Noise, vibration, and harshness
O ₂	Oxygen
PM	Particulate matter
PMEP	Pumping mean effective pressure
Re	Reynolds number
RoC	Radius of curvature
RPM	Revolutions per minute
SI	Spark ignited
SOI	Start of injection
TDC _c	Top-dead-center crank position – compression stroke
THC	Total hydrocarbon emissions
TPS	Throttle position
VE	Volumetric efficiency
VVT	Variable valve timing
WOT	Wide open throttle

Abstract

Vehicle emissions standards are becoming increasingly more strict as time progresses. Once all of the emissions devices are in their operational stage, these standards can be met with reasonable effort in powertrain design and calibration. However, the core of this system, the three-way catalyst, is non-operational until it has reached 200-350°C. Because of this, cold-start catalyst heating is extremely important in new vehicles. The objective of this project was to improve catalyst heating without increasing engine-out emissions. It was decided that the sensible heat portion of the exhaust enthalpy would be the best metric to judge differences between the different strategies. This is because catalyst-in temperatures ignore the energy flow increase with an increase in mass flow and exergy relates to a state that simply doesn't exist in application.

The two strategies tested were the deactivation of one exhaust valve and an increase in exhaust cam duration. While neither strategy proved to be particularly effective on their own, the combination of both could be a viable option for increased exhaust enthalpy and a minimal increase in engine-out emissions. Interestingly, the key to these changes was mostly due to changes in the re-breathing of the engine.

1 Introduction

4-stroke SI engines have been around since the late 1800s [1] and will continue to exist for the foreseeable future. They are fantastic energy converters in that they are scale-able, power dense, operate over a range of conditions, produce NVH levels that are tolerable, have a long service life, are relatively simple in operation, are relatively inexpensive to manufacture, have good source to propulsion efficiency compared to alternatives such as EV, and good overall emissions including criteria and non-criteria emissions. In the past, they have met emissions regulations set by the EPA, but these regulations are changing, adding complexity and cost to the manufacture of these engines. Because of this, a consortium hosted by the Michigan Tech Advanced Power Systems Lab (MTU APS Labs) that includes Borg Warner, FCA, Ford, and GM chose this catalyst light off project from a list for the 2017-2018 project cycle.

1.1 Emissions

Automotive emissions are regulated through multiple means. One of the most common of these is through drive cycle testing at EPA regulated test facilities. [2] Every new production vehicle sold in the United States must pass these tests before it is allowed to be sold. In the past, the emissions standards were met for SI engines by using a three-way catalytic converter and operating under specific control conditions. Over time, these regulations have become more stringent and, therefore, more difficult to meet.

1.1.1 EPA Dynamometer Drive Cycles

There are several different drive cycles used for light-duty vehicle emissions testing. Currently, there are 3 of these driving schedules that must be met. These cycles are performed on chassis dynamometers with professional drivers following the speed of the drive cycles set by the EPA standards. The first of these is the FTP, seen in figures 1 & 2.

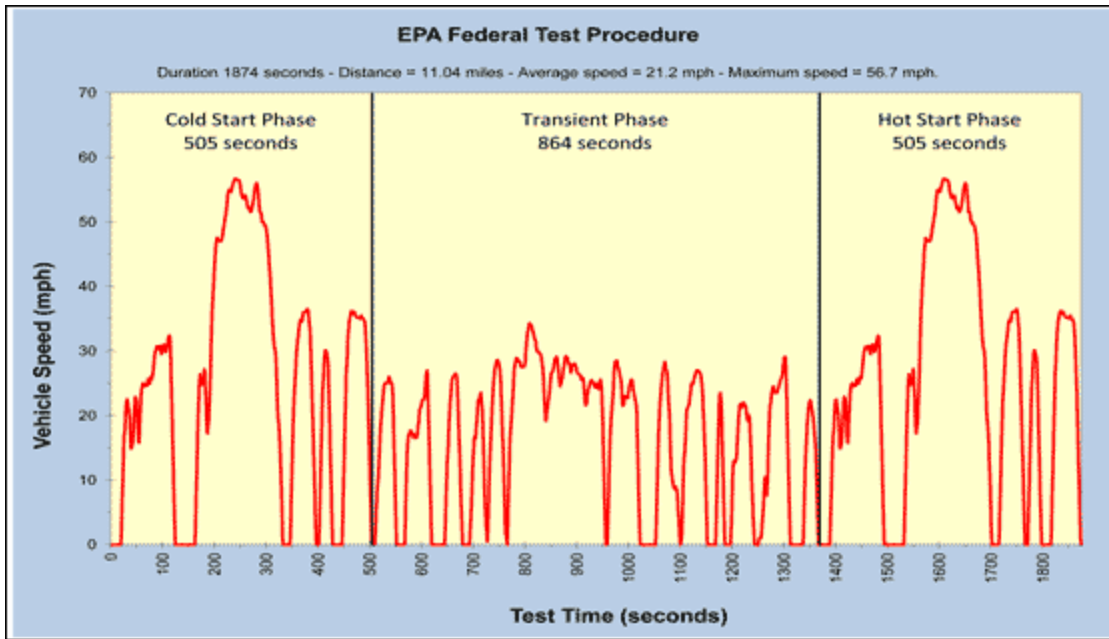


Figure 1: FTP Drive Cycle [2]

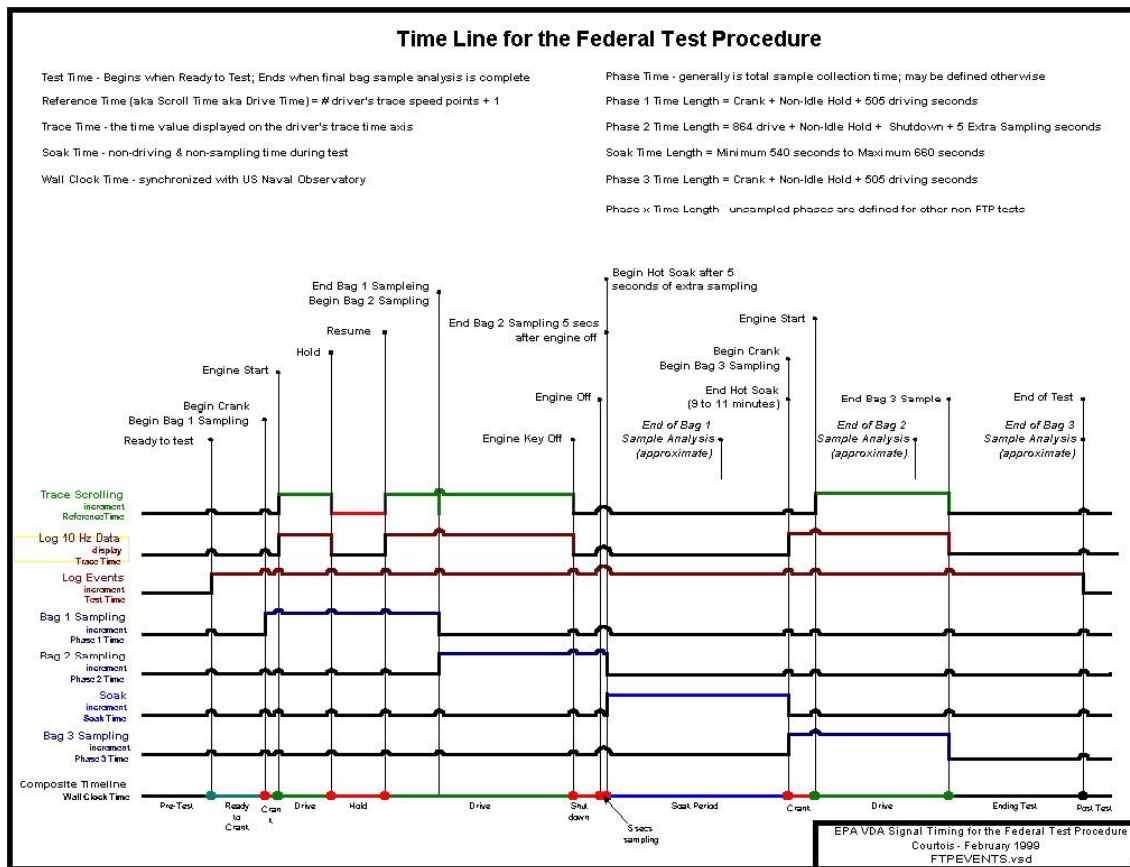


Figure 2: Timeline for the federal test procedure [2]

1.1.2 Updates to Emissions Standards

Over time, emissions standards have become more stringent and more difficult to meet. This has been done through 3 tiers of new emissions standards, starting in 1991. As can be seen in table 1, emissions in 1991 were measured in g/mi and only for 50,000 miles/5 years and 100,000 miles/10 years. Tier 3 emissions are currently being phased in and must be completely met by 2025.

These tier 3 emissions are far more stringent. For example, the most strict standard set for NMOG+NO_x in tier 1 was 0.91 g/mi, whereas the 2025 requirement is for the fleet average to meet the bin 30 requirements of 0.03 g/mi. This is a 97% reduction in NMOG+NO_x. [3] Furthermore, there is a requirement of a 99.5% reduction in HC output across all vehicles, regardless of the bin they fall into. The reduction in CO is not as drastic, but it still ranges 0-76%, depending on the bin the vehicle is in. In addition, these requirements must be warranted to be met for 3-times as long. (50,000 to 150,000 miles) All of these requirements can be seen in detail in tables 1 and 2. [4]

Meeting these new requirements has been difficult, but manageable in the past. However, reductions of 97% or more in exhaust constituents means that the systems must be functioning perfectly from startup. A single misfire or the catalyst taking too long to reach operational temperature will cause an immediate emissions failure of a new vehicle.

Table 1: Tier 3 emissions standards, FTP for 150,000 miles [4]

Standard ¹		MY Fully Implemented Tier/LEV	Vehicles	Emission Limits at Full Useful Life ²				
				Maximum Allowed Grams Per Mile				
				NO _x + NMOG	CO	PM (Tier/LEV) ³		HCHO
Bin 0	N/A ⁴	2025/2015	LDV, LDT, MDPV	0	0	0	0	0
Bin 20	SULEV20	2025/2015	LDV, LDT, MDPV	0.02	1	0.003	0.01	0.004
Bin 30	SULEV30	2025/2015	LDV, LDT, MDPV	0.03	1	0.003	0.01	0.004
Bin 50	ULEV50	2025/2015	LDV, LDT, MDPV	0.05	1.7	0.003	0.01	0.004
Bin 70	ULEV70	2025/2015	LDV, LDT, MDPV	0.07	1.7	0.003	0.01	0.004
Bin 125	ULEV125	2025/2015	LDV, LDT, MDPV	0.125	2.1	0.003	0.01	0.004
Bin 160	LEV160	2025/2015	LDV, LDT, MDPV	0.16	4.2	0.003	0.01	0.004

Table 2: Tier 1 emissions standards, FTP for 50,000 mi/5 years [4]

LDV	1994 2003	LDV	0.91	4.2	0.01	--
LDT1	1994 2003	LDT1	0.91	4.2	0.01	0.8
LDV diesel	1994 2003	LDV	1.56	4.2	0.01	--
LDT1 diesel	1994 2003	LDT1	1.56	4.2	0.01	0.8
LDT2	1994 2003	LDT2	1.37	5.5	0.01	0.8
LDT3	1994 2003	LDT3	1.44	6.4	0.01	0.8
LDT4	1994 2003	LDT4	2.09	7.3	0.12	0.8

1.2 Current Methods for Meeting Emissions Standards

1.2.1 Catalytic Converter Operation

A three-way catalyst is relatively (90+%) efficient at converting CO, HC, and NO_x to CO₂, H₂O, and N₂. However, this is only the case over a narrow range of operation. As can be seen in figure 3, lean operation leads to a significant decrease in the conversion efficiency of NO_x. (Note, the x-axis on this plot should be lambda, not AFR.) This is because the catalyst saturates with oxygen, and so it becomes less reactive to the NO_x, limiting its ability to convert the NO_x to N₂ and O₂. However, fuel-rich mixtures lead to a similar, but opposite, problem. The catalyst becomes saturated with carbon, and there is a shortage of oxygen for that carbon to react with. Because of this, the engine is run in a switching pattern around $\lambda = 0.998$. [5]

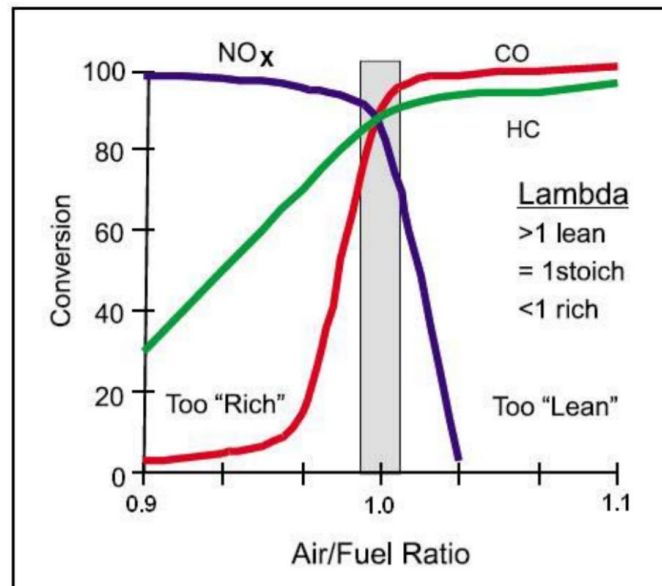


Figure 3: Three-way catalyst conversion efficiency as a function of lambda [6]. X-axis should be “Lambda, not Air/Fuel Ratio”

This operating metric is only useful once the catalyst is at the temperature needed for these reactions to start. As you can see in figure 4, the catalyst only begins to be effective at converting CO and HC at around 300°C. For it to efficiently convert HC it must be heated to over 400°C. In other words, the catalyst must be heated from an ambient temperature of 25°C to its 400°C operational temperature. The catalysts themselves are rather dense with the rare metals that are in them, so the energy required to reach their operating temperature is very high, and to reach this energy requirement quickly the exhaust enthalpy and temperatures must be as high as possible.

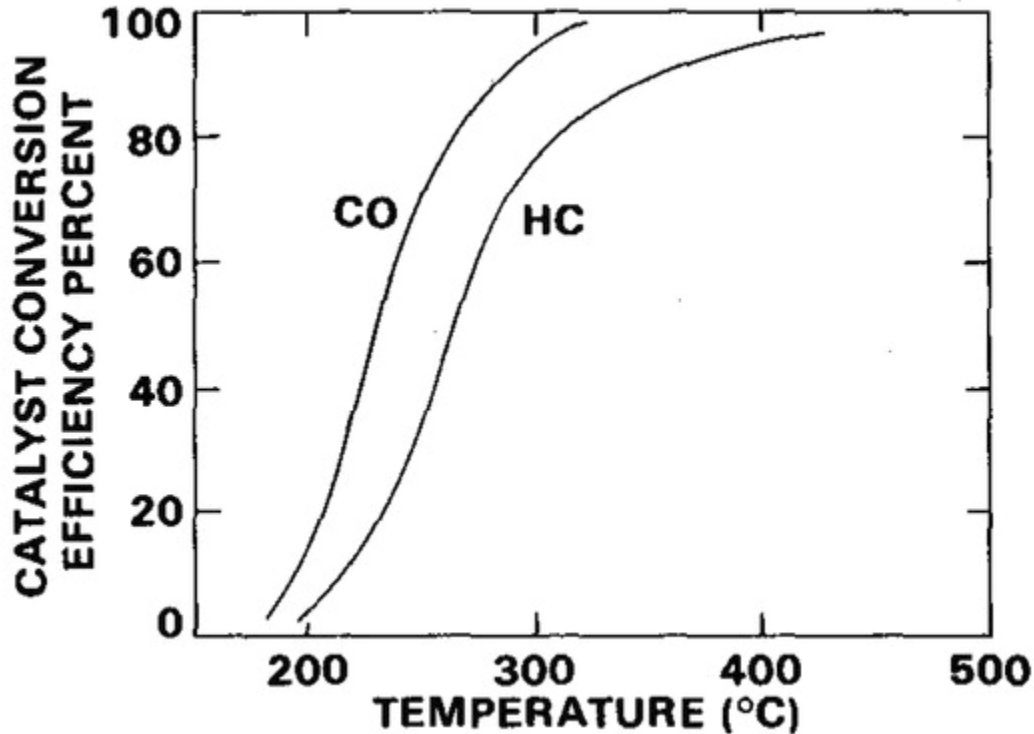


Figure 4: Conversion efficiency for CO and HC as a function of temperature for a catalytic converter [7]

1.2.2 Current Catalyst Light-Off Strategies

There are several strategies to help light the catalyst faster that have been examined in the past. However, each of these strategies comes with their own set of issues. These range from increases in some emissions to added system complexity and cost. Four of these will be covered in the literature review:

1. Retarded ignition timing
2. Electric heating elements
3. Exhaust afterburner
4. Exhaust burner

1.3 Motivation

As emissions become more stringent, passing the requirements becomes significantly more difficult. The industry has hit a point of diminishing returns in that the emissions output of modern vehicles is already so low that even one misfire on cold start will cause a failure. Once the vehicle is running and the catalyst is at operational temperature, it can act as a capacitor to absorb any inconsistencies in firing. All of this means that cold start emissions are now the core target of engine calibration and technologies related to emissions. In other words, even small improvements in this area lead to a direct improvement in overall emissions output. Additionally, exiting this cold catalyst state as quickly as possible is critical and the focus of quite a lot of research. If the exhaust enthalpy can be increased enough to decrease catalyst light-off time, without increasing engine-out emissions, this can be accomplished.

2 Literature Review

2.1 Cold Start Emissions

A very clear indication of the drastic difference in cold start emissions compared to the emissions produced during the warm operation of a vehicle can be seen below. In table 3, [8] points out a factor that correlates the emissions of a cold start to this warm operation:

$$\gamma = \frac{EE_{cold}}{EE_{hot}} \quad (1)$$

EE_{cold} = cold start exhaust emissions (g/start)

EE_{hot} = warmed emissions factors (g/km)

Using this factor and table 3, it can be seen that the emissions during cold start are equivalent to as much as 2600, 185, and 12 kilometers traveled during warm operation for HC, CO, and NO_x, respectively. This is caused by a combination of factors, with the largest being that the catalyst is cold and non-functioning during this time.

Table 3: Approximate fleet average cold-start equivalent distances gamma for Euro 4 Stroke SI and CI vehicles [8]

Vehicle type	Temperature (°C)	γ (HC) (km)	γ (CO) (km)	γ (NO _x) (km)	γ (CO ₂) (km)
SI (Euro 4)	23	400*	25	8	0.3
	-7	1900 [†]	130	12	0.9
	-20	2670 [†]	185*	9	0.8
CI (Euro 4)	23	15	17	-2.4	0.7
	-7	0	43	0.8	1.8
	-20	15	70	1.6	1.7

* γ more than 10 times further than 18 km.

[†] γ more than 100 times further than 18 km.

In [8], there is a fantastic diagram that shows the fundamental issues with cold start emissions. As can be seen in figure 5, the lower ambient temperature causes several issues at once. First, the engine is physically cold. This causes an increase in friction from differences in tolerances and increased oil viscosity. The increase in friction leads to a necessary increase in fuel energy that is being introduced into the system. This increase in fuel leads to a direct increase in CO₂. Second, the viscosity of the fuel is greater, leading to poor atomization and reduced homogeneity of the mixture. Third, the cylinder wall temperatures are lower, increasing flame quenching. Fourth, The lower intake air temperatures reduce the flame speed. The net result of the last 3 causes is that the combustion efficiency is reduced, leading to an increase in HC and CO emissions. This further necessitates the increase in fuel energy input, resulting in increased CO₂.

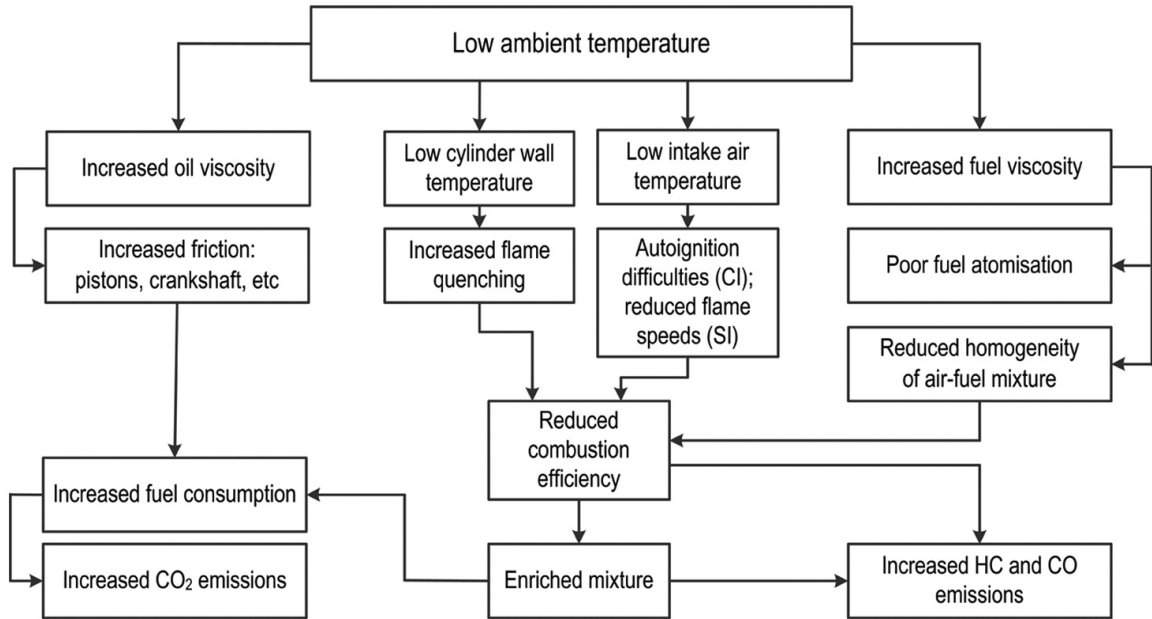


Figure 5: Cause-and-effect diagram of the fundamental difficulties of cold-start operation at low ambient temperatures [8]

To reiterate the drastic difference in HC for a cold start one final time, figure 9, from [9], shows the difference in diluted PPM for cold start HC emissions compared to hot start HC emissions. Again, while all of the other conditions cause an increase in emissions, the most significant contributor is the fact that the catalyst is too cold to function. The cold start line on this plot is with a cold catalyst, whereas the hot start line is with a warm catalyst that is operating correctly. For reference, this data was taken during the first 160 seconds of the FTP drive cycle on a BMW 3 series.

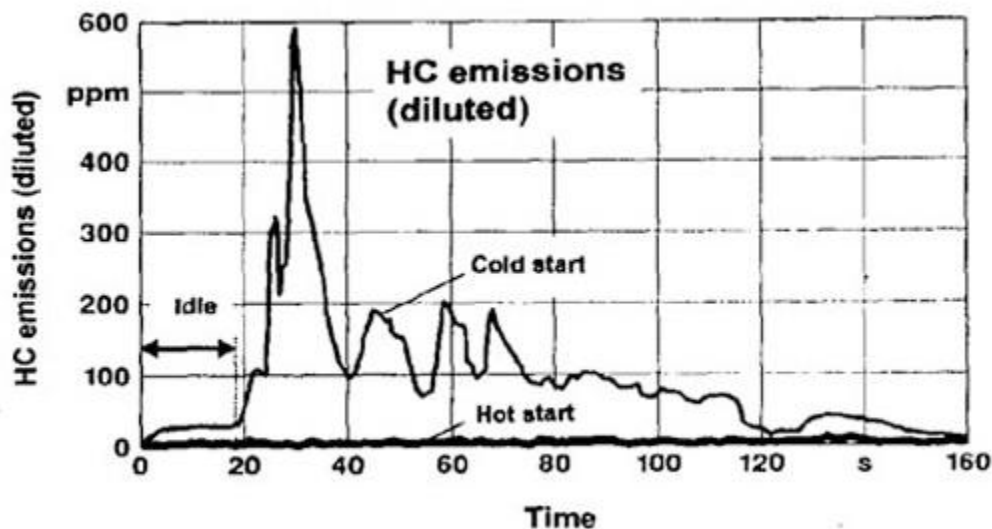


Figure 6: HC post catalyst emissions comparison between cold and hot start [9]

2.2 Catalyst Light-Off

2.2.1 Retarded Ignition Timing

The standard method used for catalyst light-off is to retard ignition timing. This does several things at once that lead to an increase in exhaust enthalpy. First, it makes the engine less efficient, so mass flow increases. Second, combustion is potentially still happening at EVO, leading to continued burn in the exhaust. Third, there is less expansion work done in the cylinder, so temperatures are potentially higher at EVO. [10] The disadvantage, from an emissions standpoint, of this method is that HC emissions are increased for the duration of the catalyst light-off strategy. [10] Additionally, the engine is extremely inefficient with this late combustion phasing, and so there is a penalty to the vehicle's mileage and overall efficiency as well.

2.2.2 Electric heating elements

Another method that has been examined, but not commonly implemented in production vehicles is the use of electric heating elements. The idea behind this is to use an electric heating element inside the catalyst to preheat the catalyst before startup or to help heat the catalyst faster after startup. [11] There have even been designs that pass reasonable durability requirements. However, while this method does improve light off times and, therefore, emissions, it comes with its own set of disadvantages. The first of which is that it requires a source that is capable of outputting 1-3 kW of power for a relatively long period of time.

Assuming a heating time of 30 seconds at 2 kW, an environmental temperature of 0°F, and that the battery started at 12V and drained linearly to 7.2V for the duration of the heating time, the battery would need an additional cold cranking amp rating of approximately 210 CCA on top of the original battery size. [12] [13] Assuming a common battery size of 600 CCA, that is a 35% increase in battery reserve, leading to increased packaging issues, increased vehicle mass, and increased cost to manufacture. This sort of drain on a typical car battery would lower the charge to the point that it would be difficult to properly start the engine or the size of the batteries in vehicles would have to increase significantly.

2.2.3 Exhaust Afterburners/Burner

2.2.3.1 Afterburner

There have been multiple projects focused on the use of exhaust afterburners or burners. The objective with these is to introduce a fuel and air mixture into the exhaust before that catalyst that can be burned for the sole purpose of heating the catalyst to operational temperature. There are two fundamental versions of this that can be implemented.

The first, an exhaust afterburner, was implemented by [14] in 1992 and followed up by [9] in a comparison between technologies in 1994. This method requires the addition of a secondary air system, an afterburner chamber, and an ignition source to the exhaust. During startup, the engine operates under extremely fuel-rich ($\lambda=0.55$) [9] conditions. This excess fuel mixes in the afterburner chamber with the air introduced by the secondary air system and is ignited. The energy released by this burn is then fed directly into the catalyst in an effort to heat it rapidly. This calibration for the afterburning chamber can potentially be switched off after 20 seconds [9] of operation due to the significantly higher heating capacity of the unit. This method is very similar to the one used in the 70's and 80's secondary air injection systems, but with more control via a more advanced EFI system and the addition of the burn chamber to the exhaust.

However, this method comes with several drawbacks. Because the engine must be operated in such a rich operating zone, idle stability may be affected. This method also becomes unpredictable and difficult to regulate after repeated starts at short intervals due to the nature of the engine running so rich. Additionally, this method is unusable at any operating condition besides idle due to the extremely rich mixture and its inherent instability under part load conditions.

2.2.3.2 *Burner*

The second, an exhaust burner, was examined by [9] and was found to have many of the benefits of the afterburner system, without as many drawbacks. This system is actually very similar to the afterburner system except for the addition of a fuel source. Because the fuel has a dedicated source, the engine can be operated using much more favorable conditions, namely much closer to stoichiometric fuel/air mixtures. The general concept of introducing fuel and air in the exhaust and igniting it directly in front of the catalyst is the same as the afterburner system. The addition of the fuel source in the exhaust also means that the engine can be used in conditions outside of idle without any significant penalties to combustion.

Both of these systems, however, have a few major drawbacks. The addition of the extra equipment means that the systems add complexity to the vehicle and the cost to manufacture them is higher. Additionally, there were safety and durability concerns that still needed to be addressed before these systems could be considered for use in a production vehicle.

2.3 Valve Activation

[15] performed a similar study to this one in 2012. However, the engine in their study was of a much higher geometric compression ratio, was operated at 1.7 bar IMEP at 1,200 RPM, and used split injection. In [15] they expected an increase in exhaust

temperature and a decrease in HC emissions with an earlier EVO and a similar EVC. These would be helpful for both catalyst light-off as well as meeting emissions. There was, however, concerns about an increase in NOx from a theorized increase in peak temperatures from the increase in charge mass required to meet the load requirements. The end result of the earlier EVO was that the catalyst heating was directly related to the difference in charge mass, HC increases with earlier EVO, and earlier EVO leads to a decrease in NOx.

They also deactivated one of the exhaust valves. The theory in [15] was that the decrease in the wetted port area, the surface area which the exhaust flow stream has contact with, would lead to a decrease in heat transfer to the port walls. This decrease in heat transfer would lead to an increase in EGT and, therefore, higher exhaust enthalpy. Through the experiments in [15], it was observed that the EGTs did, in fact, increase with the smaller port area and this was at a lower specific fuel consumption. It was also observed that the emissions tradeoff between HC and NOx was more acceptable in that the HC emissions were reduced, but the increase in NOx was lower at earlier EVO.

2.4 Crevice HC Emissions

An additional theorized advantage to switching to one valve operation was the decrease in crevice volume from the deactivated exhaust valve. Heywood says that the crevice volume of the head gasket and valve seats is negligible in [16] compared to the piston crevice regions. However, they later test for the differences caused by alterations of the head gasket, coming to the conclusion that they are, in fact, important in factoring in crevice volume. Adding to that the fact that this study was performed in 1994 when regulations were far more lax than they are today, and the difference in crevice volume caused by deactivating a valve became relevant for this project again.

3 Goals and Objectives

The goal of this project is very simple:

1. Increase the rate of exhaust enthalpy to decrease catalyst light-off time
2. Maintain or decrease engine-out HC
3. Maintain or decrease engine-out CO
4. Maintain or decrease engine-out NO_x
5. Maintain or decrease engine-out PM

The objective was to see how the different valve activation strategies affected these outputs. While [15] was a great study on these effects, there are several different aspects of this project that were not published in the paper. The first of these is the use of a more conventional valvetrain. The “UniAir” technology used in [15] is still expensive and relatively difficult to implement in a vehicle compared to the valvetrain used in this project. Second, the compression ratio in [15] was 13:1 which is on the higher end of a modern SI engine. The compression ratio of the test bed in this project of 9.2:1 is fairly standard for a modern turbocharged engine. Third, the load used in [15] was only 170 kPa IMEP, which is far short of the load in this project of 250 kPa NMEP; a more realistic load for the operation of accessories on a 2.0 L engine in a modern vehicle. Lastly, the engine used for [15] was a single cylinder, whereas the engine in this project was a multi-cylinder configuration which was also more realistic for the application. Additionally, [15] did not include a detailed analysis of the different effects that each configuration was causing.

3.1.1 Test New Hypothesis

3.1.1.1 Valve Deactivation

It was hypothesized that with a decrease in the wetted area of the exhaust port there would be less heat transfer in the port. This would, in theory, lead to higher EGTs and, assuming roughly the same efficiency, a correlated increase in exhaust enthalpy.

3.1.1.2 Longer Exhaust Cam Duration

The hypothesis for a longer cam duration was three-fold. First, the earlier EVO would allow for less expansion work to be performed, increasing EGTs, which would increase exhaust enthalpy. Second, this decrease in expansion work would lead to an increase in mass flow requirements to meet load, increasing exhaust enthalpy. Third, the later EVC would lead to greater rebreathing (backflow from the exhaust stream back into the cylinder), which would result in lower HC emissions.

4 Research Methodology

This project was performed through a combination of experimentation and GT-Power, a 1-D computer simulation using a production model of the LHU engine provided by GM. Every point tested was simulated, except for the latest combustion phasing because the true combustion phasing was unknown for these points due to a significant portion of the burn occurring in the exhaust.

Experimentation is the only way to truly observe the results of the hardware changes made. There are simply too many variables involved to accurately simulate the results of this experiment. This is especially true with topics involving heat transfer, emissions, or combustion variation. However, simulation was used to develop the new camshafts as well as to better understand what was happening inside the engine leading to the observed results.

Because the purpose of this project was to test the effects of each of these different configurations on the portion of cold-start that is for catalyst light off, the flair at the initial start was ignored and the engine was operated at a steady state. By running steady state, the number of variables in testing is also significantly lessened. This chosen condition represents the time from 3 to 15 seconds in figure 7.

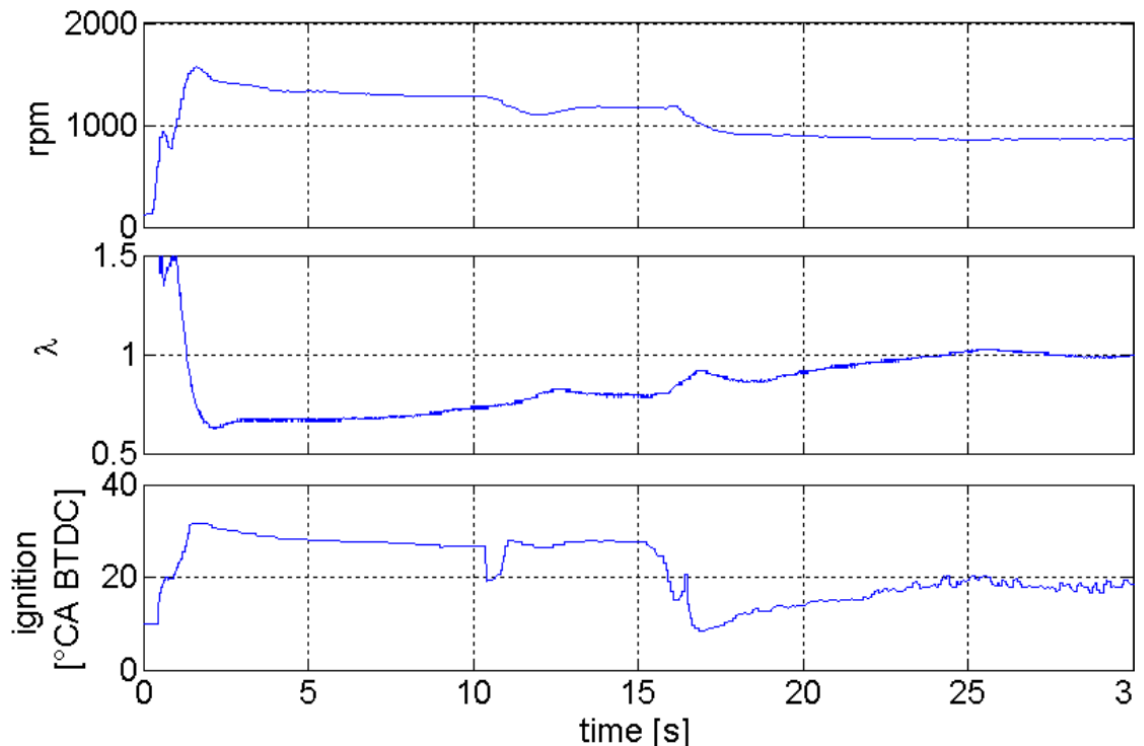


Figure 7: Cold start warmup example [17]

4.1 Camshafts

Testing included 3 different exhaust camshafts. The first of these was the production cam, PN 12629743. The second cam tested was a mid-duration camshaft with a 35° increase in duration. Lastly, there was a long duration camshaft with a 60° increase in duration.

4.1.1 Mid-Duration

When designing the mid-duration camshaft, there were several objectives:

1. Maintain opening and closing profiles
2. Push EVC as late as possible
3. Determine the duration increase that provided maximum output at 6,000 RPM to match and increase the engine's original operating condition for peak power.

4.1.1.1 *Maintaining Opening and Closing Profiles*

The fundamental objective behind retaining identical opening and closing profiles was to ensure the results were only from the change in duration. Second, by using the same profiles, there should be no ill effects on valvetrain dynamics that could cause other issues. However, the dynamics of the valvetrain were far less critical than ensuring the results were only from the duration increase as the camshaft was only going to be used for a short period of time and at low speeds.

4.1.1.2 *Pushing EVC As Late As Possible*

Pushing EVC as late as possible was desired to help maximize the potential for rebreathing. This rebreathing would, in theory, allow for the recapture and burning of HC in the exhaust. This backflow is caused by the lower cylinder pressures of the downstroke just before the exhaust valve closes. This pressure delta across the exhaust valve causes the closest exhaust gases to reenter the cylinder. Figure 8 shows a sample of this rebreathing at different angles of exhaust camshaft retard.

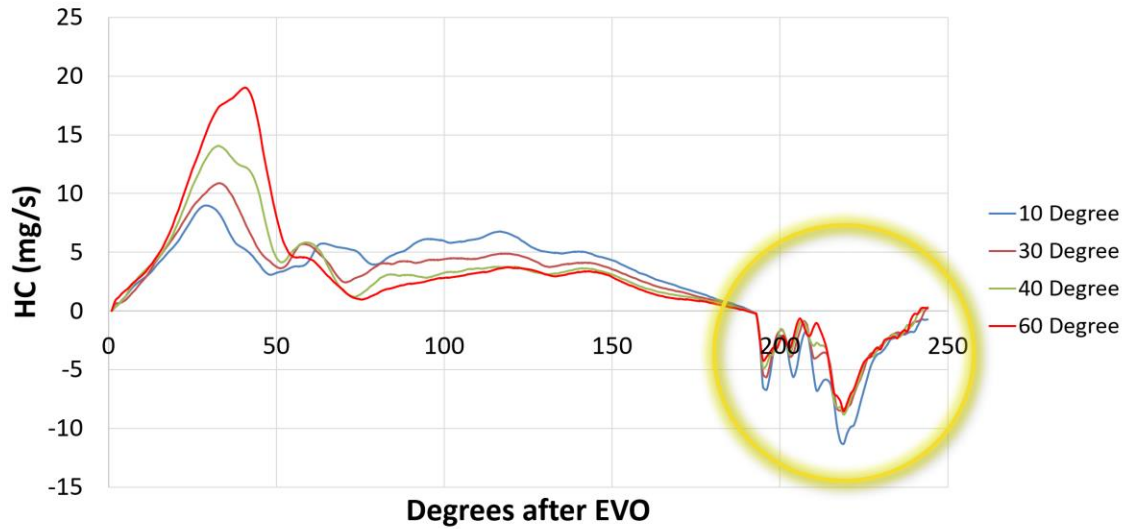


Figure 8: Mass-scaled HC flow at exhaust port septum for fully retarded stock camshaft and dual valve operation at various CA50s

4.1.1.3 Maximum Output At 6,000 RPM

The cam profile was also designed to allow for the maximum engine output at 6,000 RPM. Ideally, the longer duration could be used for both startup and maximum output operation, helping to justify the additional hardware required for the multi-lobe cam.

4.1.1.4 Design Process

The first stage of the actual design process was to use the valve lift profiles provided in the GT Power to design and simulate the increased duration on the exhaust cam. To do this, the lobe was split at peak lift and the dwell was increased in 10° increments up to an increase of 100°. A few examples of the valve lift profiles that were simulated can be seen in figure 9.

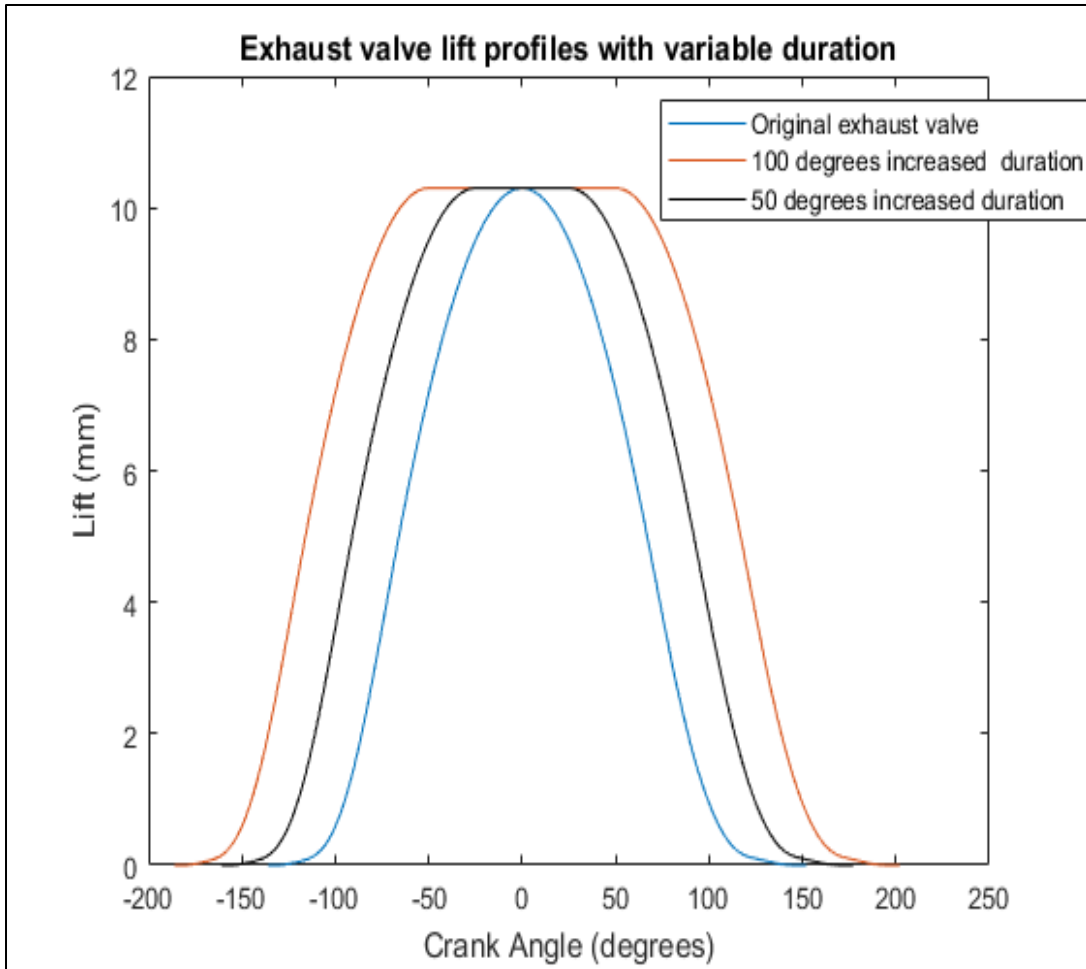


Figure 9: Valve lift profile comparison

There is a physical limit to how late EVC can be. Too late of an EVC leads to valve-to-piston contact, which will quickly destroy the engine. The initial data for this clearance was measured on a previous project with the stock camshafts in their fully retarded position. From that initial data, figure 10 was developed, allowing the determination of how late of an EVC was considered acceptable. The clearance of 1.5 mm at an EVC increase of 15° was considered to be too small if anything were to cause some instability in the valvetrain, so a 10° increase was chosen.

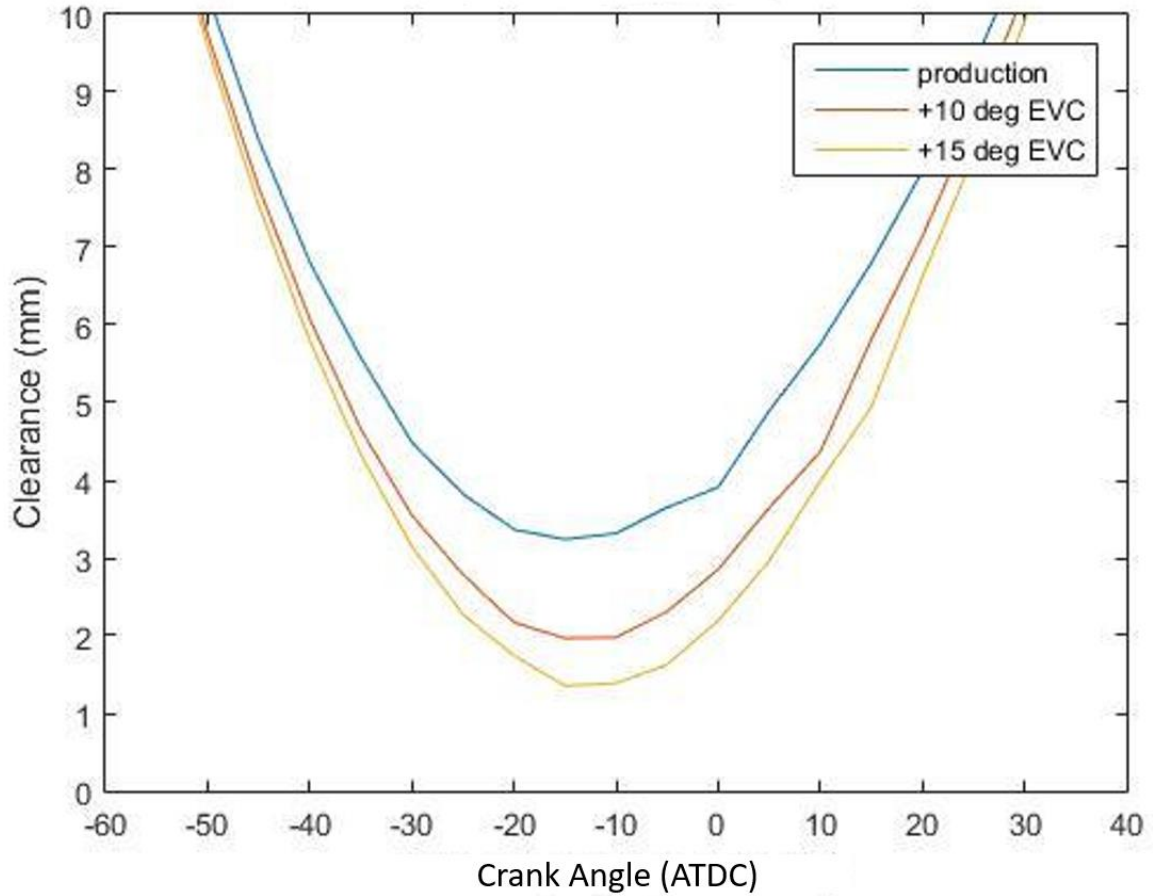


Figure 10: Valve to piston clearance from later EVC cause by longer duration camshaft

Once the camshaft centerlines were determined, the simulations in GT-Power were run. The NMEP produced by each of the camshafts tested can be seen in figure 11. Based on these simulations, it was concluded that the best choice for producing peak power was an increase of 35° CA. This duration increase and the corresponding difference in the cam profile is directly compared with the stock camshaft in figure 12.

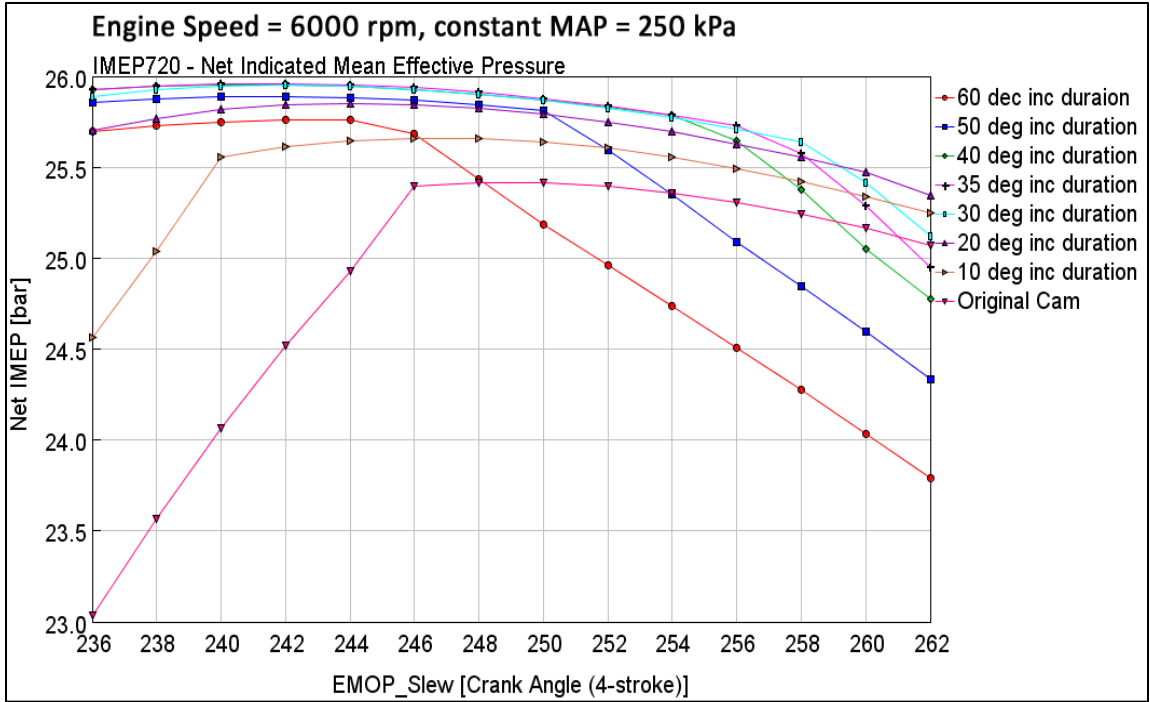


Figure 11: NMEP at 6,000 RPM with different max lift dwell duration increases

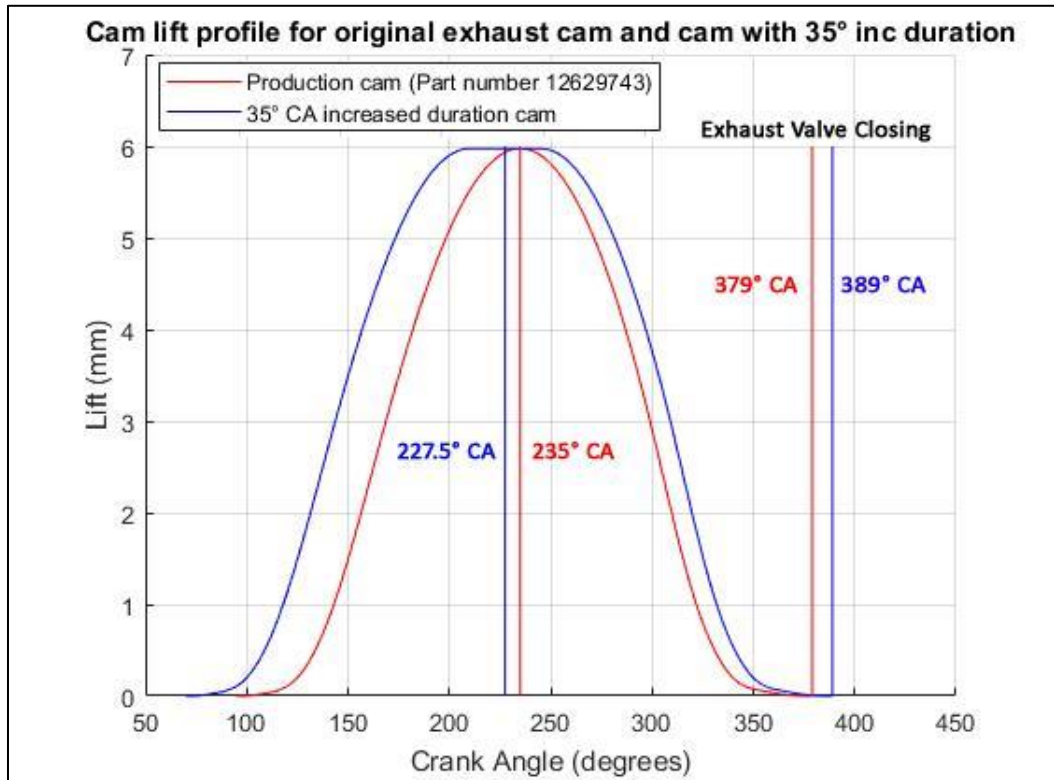


Figure 12: Cam lift profile comparison between stock exhaust camshaft and mid duration camshaft

As further evidence that this new cam duration is useful for power at more than just peak operating speed, a group of simulations was also performed to compare the 35° camshaft to the stock camshaft at 3 different operational speeds of 4,000, 5,000, and the 6,000 RPM. As seen in figure 13, there is a clear advantage in power output at all of the higher speeds at which the engine could be operated.

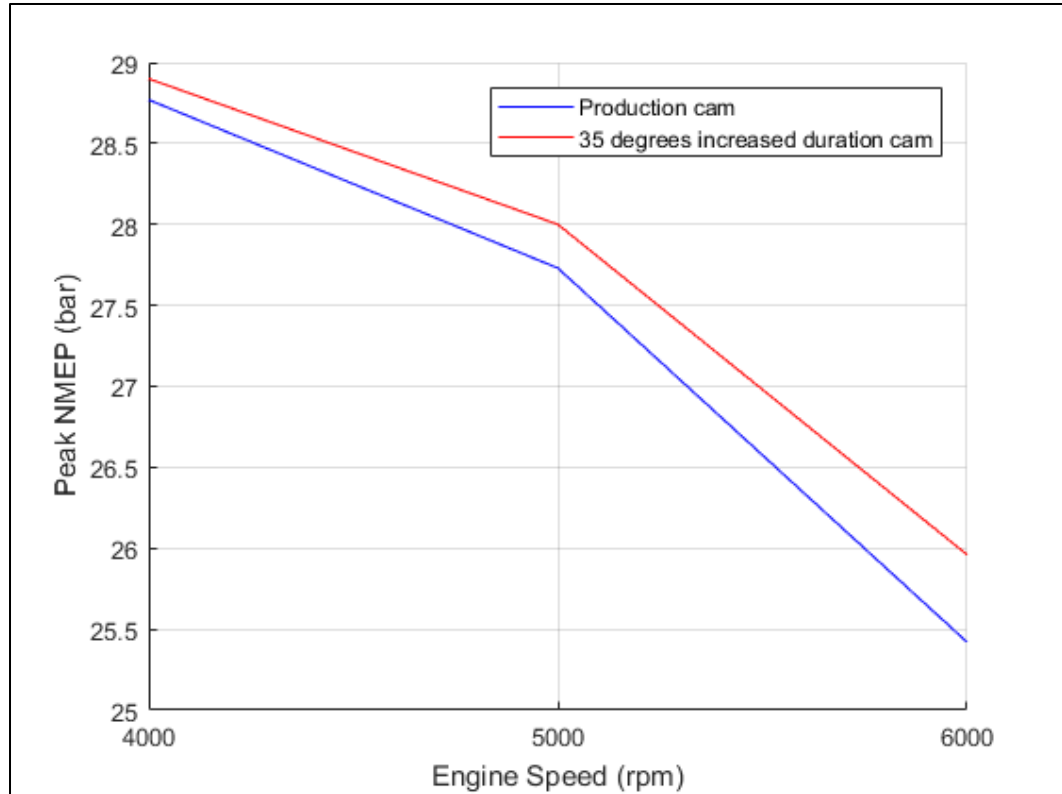


Figure 13: NMEP comparison between final mid duration camshaft design and stock camshaft at different engine speeds

4.1.2 Long Duration

After the development process of the mid-duration camshaft, the longer duration cam was a much faster and more straightforward process. The only constraint with this cam was that the engine was still able to meet the engine load requirement of 250 kPa NMEP. To maintain the valve-to-piston safety margin discussed in 4.1.1.4, the EVC for the longer duration camshaft was matched to that of the mid-duration cam. With these two parameters determined, GT-Power was used again to find the duration with the earliest EVO possible while still maintaining load. These GT-Power simulations showed that an increase of up to 100° did not cause any issues, and the engine was still able to meet load. A 60° increase in duration was chosen, as it would position EVO at 40° ATDC. This is within the target CA50 range, which will be addressed later.

The next step was to check this increase in cam duration at a more retarded cam position. To do this, a test, seen in figure 14, was performed with the camshaft at a position 45° retarded from the home position with SOIs of 280° and 253° BTDC at 1500 RPM and 250 kPa NMEP at $\lambda=1$. This was chosen as a representative point for the engine with later exhaust cam phasing. With the cam in this position, EVO would be at 85° ATDC. Using the data in figure 14, it was determined that this later EVO would allow for complete combustion at later combustion phasing, as CA90 was at 78° ATDC. These result is a camshaft that could theoretically place EVO anywhere from before CA50 to after a complete burn.

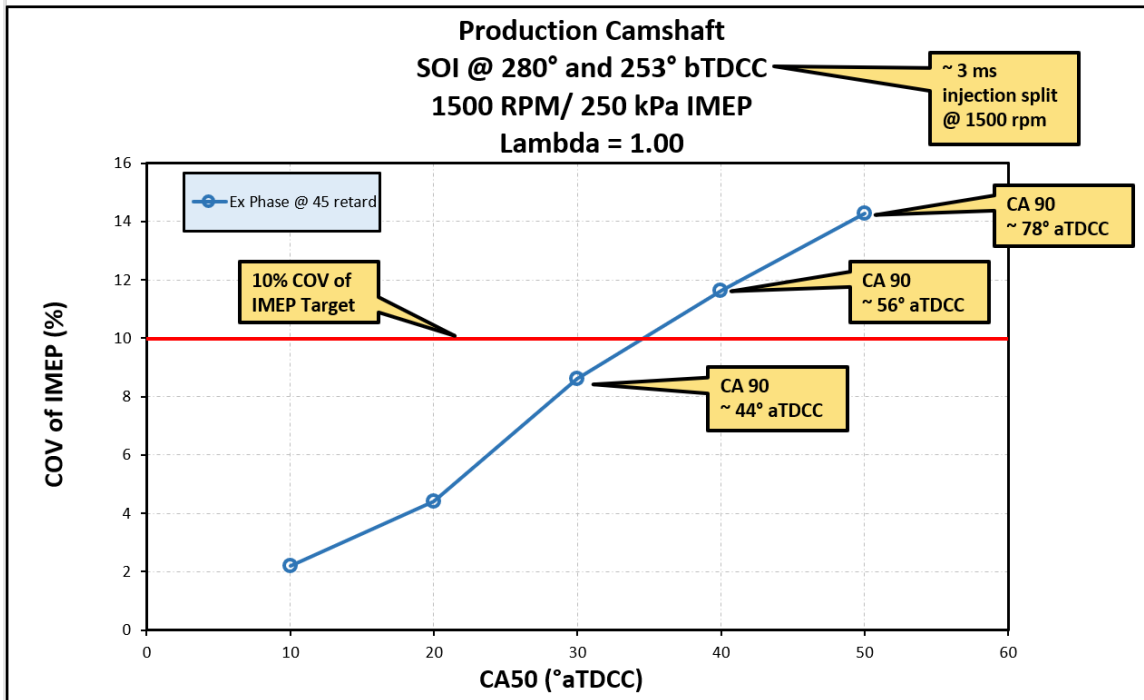


Figure 14: CA90 analysis to determine long duration camshaft duration increase

4.2 Test Matrix

The heart of this project was to determine the effects of valve activation changes on the exhaust enthalpy rate and the emissions produced. With the conventional valvetrain used for testing, there are few options left. The first was to retard the exhaust cam incrementally. The second was to increase the duration of the camshaft. The final option was to deactivate one of the valves. Additionally, CA50 would be swept, as retarding spark is currently the most common method for catalyst heating, and it could easily be replicated on the hardware available.

For the increase in cam duration, it was decided that the stock camshaft, a mid-duration camshaft, and a long duration camshaft would fit within the scope of the project and provide enough resolution to understand the physics behind the changes observed. For

exhaust cam retard, the engine used has a range of 50° CA that it can retard. This was broken into a number of equal steps of 0, 12.5, 25, 37.5, and 50° CA of retard. Again, this number of steps provides enough resolution to understand the physics, but still fell within the time allotted for the project.

Additionally, each camshaft was run in both 1 and dual valve configurations. This was done to allow for a direct comparison of the effects of valve deactivation on an otherwise stock configuration as well as to see how the combination of cam duration and valve deactivation affected each other. A CA50 of 10° ATDC was chosen to represent MBT [18] for the earliest portion of the CA50 sweep. The latest combustion phasing was limited by two factors, misfire and an EGT limit. Misfires are a limit because any misfire on startup will immediately fail emissions and it can also drastically skew the data collected. An EGT limit was set to avoid damaging the turbocharger or the engine. 950°C was determined to be a safe limit.

To ensure load was met for as many points as possible, the engine was operated at WOT for the latest combustion phasings. If the engine was at WOT and load was met, the other limits of misfire and EGT were to apply. If the engine was at WOT and load could not be met spark advance was increased until it could be, and that was the point taken for the CA50 sweep. The final test matrix can be seen in table 4 below.

Table 4: Project test matrix

Camshaft	CA50 Sweep	ECCL Sweep	Active Port	# Test Points
Stock Duration	10, 30, 45,60, Misfire -2° SA or EGT 950°C	0, 12.5, 25, 37.5, 50	1 valve, 2 valve	50
+35° Duration	10, 30, 45,60, Misfire -2° SA or EGT 950°C	0, 12.5, 25, 37.5, 50	1 valve, 2 valve	50
+60° Duration	10, 30, 45,60, Misfire -2° SA or EGT 950°C	0, 12.5, 25, 37.5, 50	1 valve, 2 valve	50
			Total	150

4.3 Test Procedure

4.3.1 Testing

At the beginning of every day of testing, 3 control points were run. The first of these was an all-off control point with the engine at ambient temperature before the first firing event. The engine and all components are room temperature, and so this is a good way to check for any inconsistencies in data acquisition methods. The second was a reference point, with both camshafts in their home positions, $\lambda=1$, an engine speed of 1,300 RPM and a load of 330 kPa NMEP at a CA50 of 8° ATDC. The last control point before testing was a motoring point (engine off, but being spun by the dynamometer) at a MAP measurement of 95 kPa and 1,300 RPM. For all testing, the matrix was randomized to

minimize trends in data. At the end of each day, the second set of control points were taken, including the 1,300/330 point and the motoring point.

4.3.2 Engine Cleaning Procedures

To help minimize the effects of carbon build-up inside the engine absorbing or desorbing hydrocarbons [19], a cleaner made by Wynn's was used before testing began and before each cam switch procedure. This was done with the engine running at 3,000 RPM, a MAP of 80 kPa, and a spark advance of 36° BTDC. Additionally, in-cylinder pressure transducers were removed and cleaned before testing began.

5 Experimental Setup

5.1 Engine Test Bed

5.1.1 Engine

For this study, an LHM 2.0L engine was used. These engines can be found in a variety of GM vehicles from 2011 to 2013. This engine was chosen because it has dual cam phasing, direct injection, and is turbocharged; all of which are common on high-feature engines found in modern vehicles. All of the relevant physical dimensions can be found in table 5.

Table 5: Test engine physical dimensions

GM I4 LHM	
Bore (mm)	86
Stroke (mm)	86
Connecting Rod Length (mm)	145.5
Wrist Pin Offset (mm)	0.8
Number of Cylinders	4
Compression Ratio (-)	9.2
Total Displacement Volume (L)	1.9984
Cylinder Clearance Volume (L)	0.0609
Firing Order	1-3-4-2
Valvetrain specification	DOHC
Camshaft Phasing Ranges	50° Intake/Exhaust Crank Angle IMOP: 436-486° ATDC EMOP: 235-285° ATDC
Intake Charge Delivery	Turbocharged and Intercooled
Fuel Delivery	Direct Injection
Ignition System	Coil-On-Plug
Oil Cooling	Block Mount Cooler

5.1.2 Fluids

5.1.2.1 Fuel

VP Racing Fuel's C9 was the spec fuel used for testing. It represents a premium pump fuel, but without the variation in additives from seasonal changes and the differences in manufacturers. The full specifications for the fuel can be found in Appendix A.

5.1.2.2 Oil

The oil used for the duration of the project was 5W-30 Valvoline Advanced Full Synthetic, as it meets all requirements set by the manufacturer of the engine. [20] [21] There were no additional additives in the oil.

5.1.2.3 Coolant

The coolant used for the duration of the project was a 50/50 mixture of Prestone brand Dex-Cool and water. This coolant was also used because it is the manufacturer's recommendation for this engine. [21] There were no additional additives in the coolant.

5.1.3 Engine Controller

To control the engine, a Bosch Motorsports MS6.3 was used. This controller is fully configurable and has a variety of features that allow for the testing performed. The fuel model used for testing was a volumetric efficiency-based speed density model with closed loop fueling via a Bosch LSU 4.9 lambda sensor. This model uses a combination of intake manifold pressure, temperature, and other engine data to estimate the air charge inside the cylinder for each combustion event. The amount of fuel injected for the event is calculated using this air charge estimate and a target lambda.

5.1.3.1 Split Injection

The initial plan for this project was to run split injection. However, the Bosch unit doesn't have this feature. In an effort to circumvent this, the injectors were re-wired so that the ECU would effectively see 2 banks of 4 injectors, seen in figure 15. The injection timing was controlled by the phasing of these additional 4 ghost cylinders relative to the actual 4 cylinders on the engine. This would have allowed for a 50/50 split between injection pulses. While this solution worked from a hardware and calibration perspective, the injection duration for the speed and load run in testing proved to be too low. To meet the target lambda of 1.01, the injection duration was around 0.7 ms, but the factory injectors in the engine become unstable below a 1 ms. The end result was lambda variations of ± 0.03 , which was unacceptable. In an effort to try to retain split injection, the fuel pressure was lowered until lambda was stable. The resulting fuel pressure was 13

bar, which is far too low for proper atomization of the fuel. Because of this, split injection was not a viable option for testing.

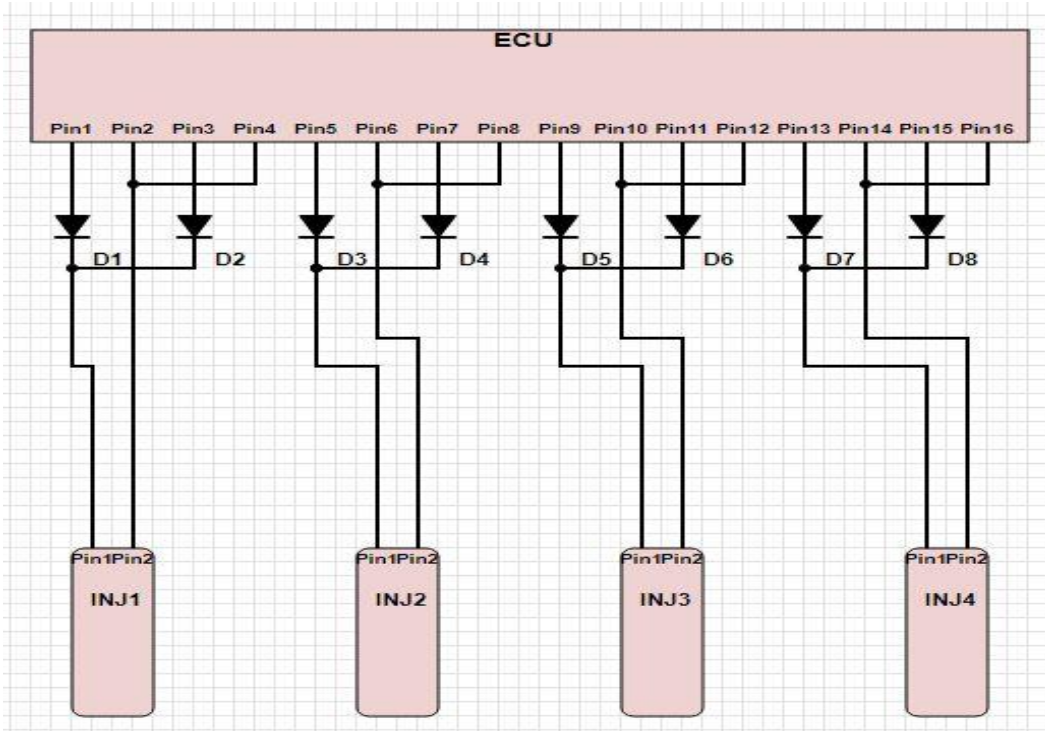


Figure 15: Alternative injector wiring

5.2 Instrumentation

5.2.1 Engine Dynamometer

The dynamometer used for controlling the engine is an adjustable speed A/C dynamometer made by GE Motors. The model number is 5TKF44SDC03AQ04 and the max absorption for the dyno is 460 hp with a max speed of 8,000 RPM.

5.2.2 Test Cell Control and Low-Speed DAQ

The core operating system for this project was NI Veristand 2016 [22]. The chassis used was a PXIe-1078 [23]. Veristand performed all of the core operations of the test cell such as controlling the dyno, switching all power to the engine, and logging all of the lower frequency inputs as well as the atmospheric conditions inside the cell.

5.2.3 In-Cylinder Pressure Transducers

The in-cylinder pressure transducers used were a mix of AVL GH12D and PCB 115A04. While the transducers were mixed across cylinders, they were not changed for the duration of the testing.

5.2.4 Combustion Analyzer

CAS Redline [24] was used for combustion analysis. The encoder used to track crank position for this project was an H20 made by BEI Sensors (Part # XH20DB-37-SS-360-ABZC-28V/V-SM18). The full specifications for this encoder can be determined from the datasheet in Appendix B. All data was taken in 1° increments.

5.3 Emissions Equipment

5.3.1 Fast Response Analyzers

Combustion fast-response analyzers were used for HC and CO/CO₂ [25] for the duration of this project. More detailed specifications can be found in Appendix C.

5.3.1.1 Fast FID

For high-speed HC measurements, a Combustion HFR 500, seen in figure 16, was used. This allows for tracking of HC emissions on a crank angle basis and was primarily used to capture the rebreathing effects. This machine outputs a ppm value that was scaled to a 0-10V output which was then fed into CAS via a BNC cable. The signal was then rescaled in CAS back to ppm for recording into data. One of these signals was taken at the port, the other after the turbine of the turbocharger, as can be seen in figure 21.



Figure 16: Cambustion HFR500 Fast FID

5.3.1.2 Fast CO/CO₂

For the purposes of measuring CO and CO₂, a Cambustion NDIR500 was used, seen in figure 17. The fast analyzer was used because it was available and would help indicate when a misfire occurred. These misfires would lead to large spikes on the CO traces, even if they were not detected by other means. Much like the HFR, the machine was configured to output a 0-10V signal and that signal was processed within CAS.



Figure 17: Combustion NDIR500 Fast CO/CO2

The calibration for both of these was according to the combustion manual. Upper and lower span gases were used with a zero gas to develop a linear correlation around all test points being analyzed. These gases can be seen in table 6.

Table 6: Combustion Span Gases

<u>Gas</u>	<u>Span</u>
CO	1% and 5% CO
CO2	4% and 16% CO2
HC	600ppm and 2500ppm
Zero	N2

5.3.2 PM/PN

For exhaust particle emissions measurements a TSI EEPS 3090 [26], seen in figure 18, was used. Only post-turbine measurements were performed. The unit was disassembled, cleaned, and calibrated before testing began. The primary use of the PM measurement was to determine the best SOI for this operating condition, more details on this are in section 5.7. It was cleaned again before each of the camshafts were tested. However, when running the longer duration camshafts, the machine repeatedly clogged almost immediately. Because of this, the bench was disconnected and no longer used in an effort to prevent damage.



Figure 18: TSI EEPS 3090

5.3.3 Horiba 5-Gas

For the measurements used in the parameter sweeps and the verification of the Cummins NOx sensor, a Horiba MEXA 1600D was employed. This bench is the baseline for all emissions testing performed at the lab as it is an industry standard. The measurements available include CO, CO₂, HC, NO_x, and O₂.

5.3.4 Cummins NOx Sensor

With HC, CO, and CO₂ being measured by the Combustion benches, the only other desired emissions measurements were NO_x and O₂. For the purposes of this project, fast NO_x was deemed to not be value added. These two factors combined with the increased potential for error to be introduced by using another complex machine lead to the use of an OEM NO_x sensor from Cummins (Part # 5293295RX) which reads both NO_x (ppm) and O₂ (%). This sensor was integrated into Veristand via decoded CAN communications.

To check the validity of the OEM sensor, data was taken over a cam sweep and compared to the Horiba 5-Gas. As can be seen in figure 19, there is a good correlation between the two methods of NO_x measurement. The only significant difference between the two is a bias that is reasonably consistent throughout the sweep. This bias can be more clearly seen in figure 20. Because it was a consistent bias at and immediately surrounding the operating conditions in testing and the goal of this project was to make comparisons within this small region, it was deemed appropriate to use the OEM sensor.

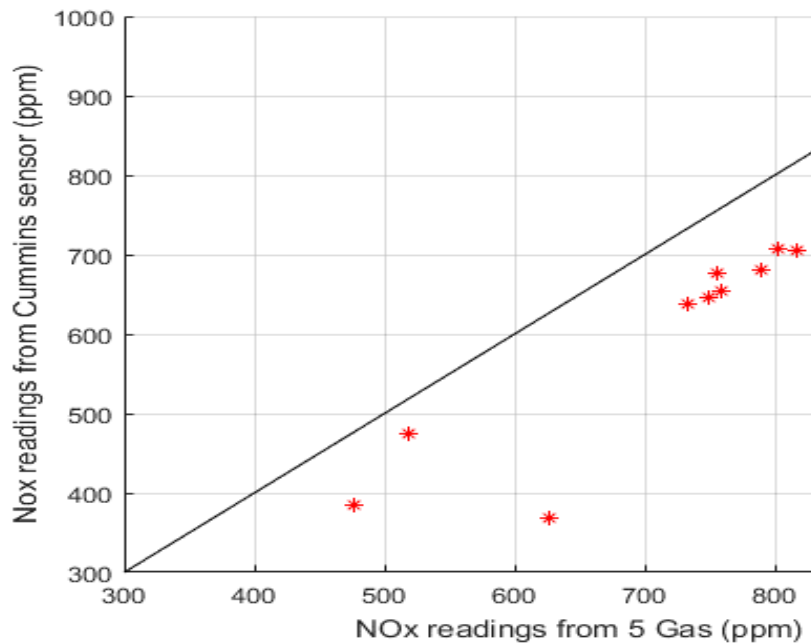


Figure 19: NO_x reading of Horiba 5-Gas bench vs OEM Cummins NO_x sensor

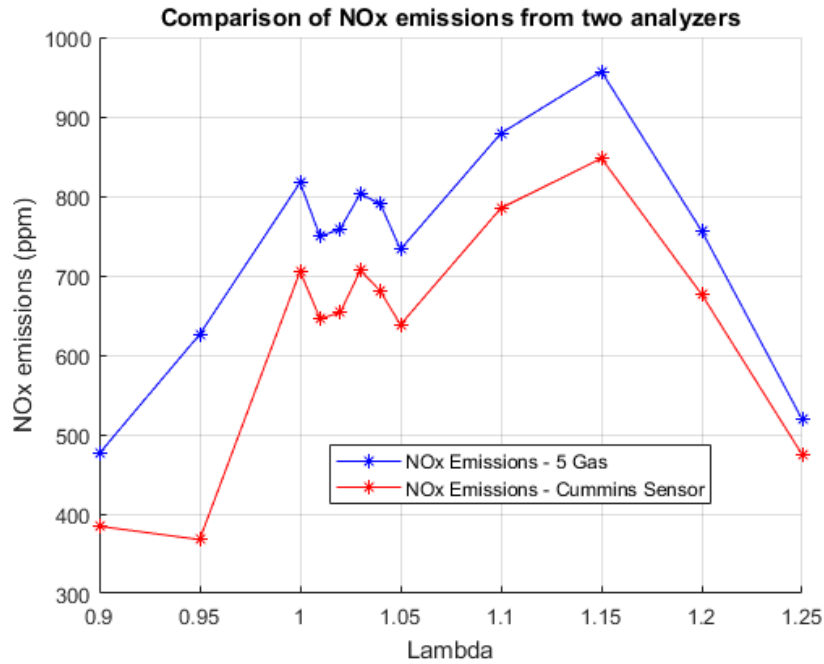


Figure 20: NOx reading comparison between Horiba 5-Gas bench and Cummins OEM NOx sensor for a lambda sweep **Lines are assumed trends**

5.3.5 Probe Location

All probe sampling locations can be seen in figure 20.

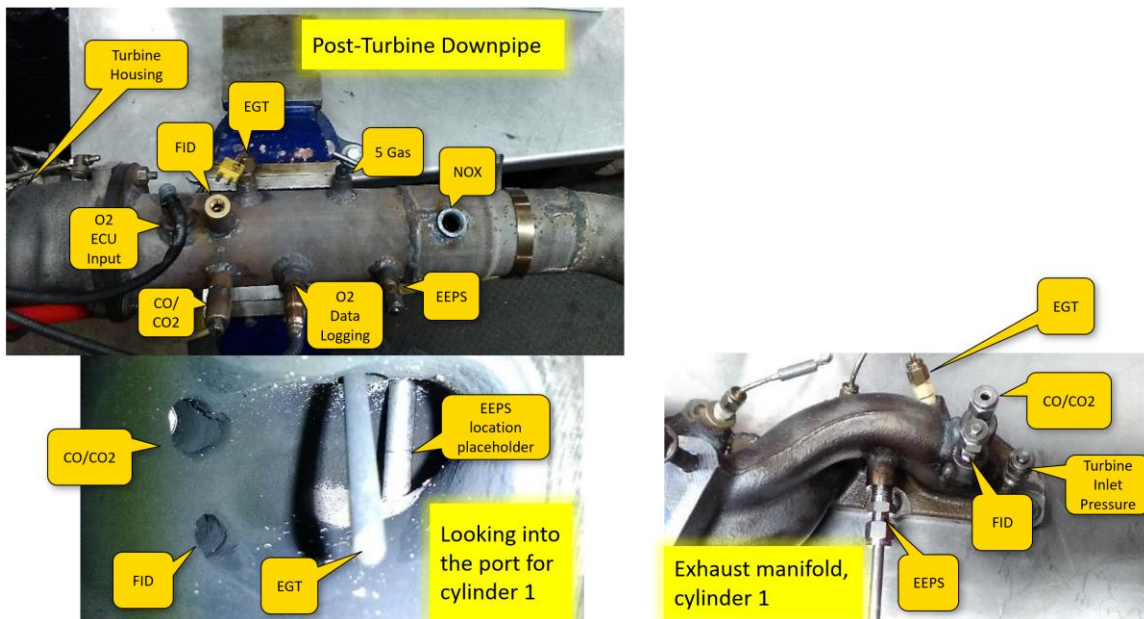


Figure 21: Emissions probe locations

5.4 Camshaft Procurement

The original plan for acquiring the longer duration exhaust cams was to send a stock cam to a large aftermarket cam supplier and have them manufacture two prototypes using additional data developed in sections 4.1.1 and 4.1.2. However, as it turned out, this was not a viable option. Because of this, a search began to find another supplier. As it turned out, this search was significantly more difficult than anticipated.

There were several core issues with finding a camshaft supplier for this project. The first was that none of the companies contacted had any cores to grind. This left only the option of welding more material onto the lobes of a stock camshaft and regrinding them with the new lobe profiles. After contacting many different suppliers, having Andrew's Products design a camshaft that Web Cams could grind was the only viable option. Working with both companies was a necessity because Andrew's cannot weld and grind the camshafts as needed and Web uses masters designed and manufactured by Andrew's to grind their camshafts.

While working with Andrew's, it was discovered that there were two major issues with the fabrication of these cam profiles. The first of these was that the small negative RoC on the cams required a diameter of grinding wheel that was smaller than anything that Web was currently capable of using. A negative RoC is the radius of the curve the must be ground into the camshaft. The grinding wheel radius must be smaller than this value for it to be able to cut into the wheel instead of grinding away the lobe for an "external" curve. This "internal" curve can be seen in figure 22, where the roller wheel is contacting the cam lobe. Web had a new machine that would be capable of performing this operation within months, but this lead time was far too long for this project.

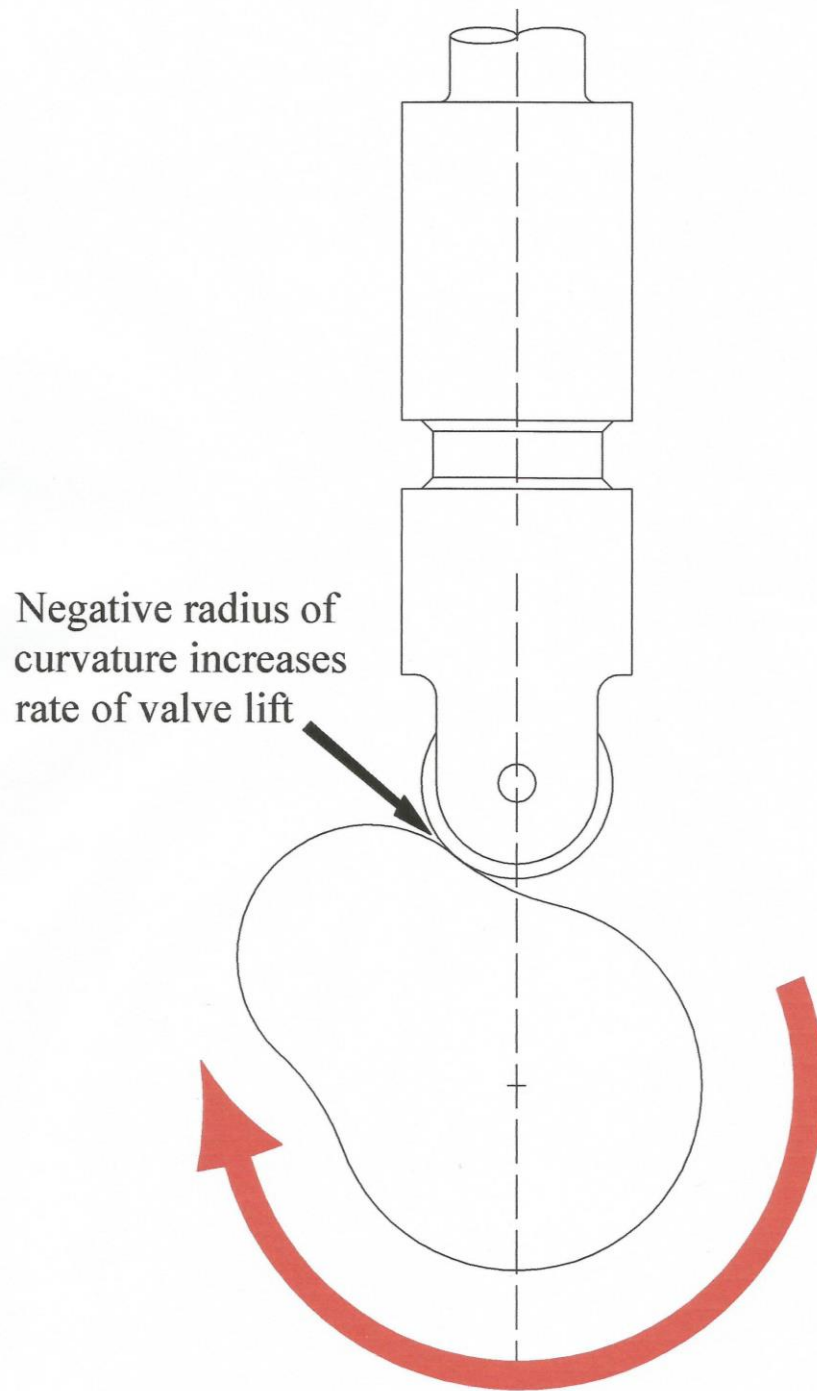


Figure 22: RoC diagram [27]

The second was that there was concern about the dynamics of the valvetrain. There was significant jerk at the transition points between the ramps and peak lift. All of this can be seen in figure 23.

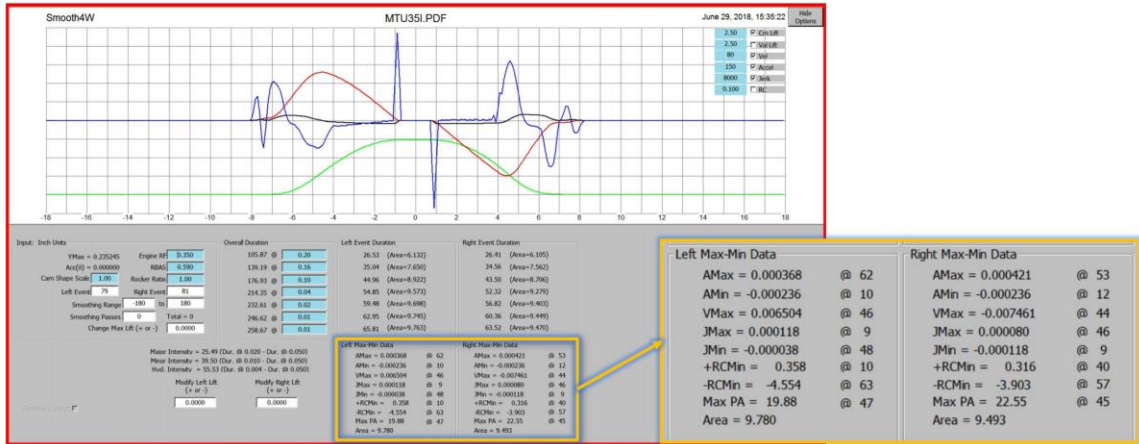


Figure 23: Acceleration curve for mid duration camshaft and stock RoC

Fortunately, these difficulties were being communicated to the consortium during this search, and GM volunteered to redesign the cams to allow for the larger RoC that Web was capable of grinding. The change in RoC was an increase from a baseline of 101 mm to 150 mm on the new design. Once this data was returned to us, simulations were performed to verify that the change in RoC would not cause any significant changes in the results of the project. The first of these checks was to verify that there was no significant change in mass flow across the valve with the new RoC. As can be seen in figure 24, the mass flow is nearly line-on-line, so it was determined that there was no significant difference.

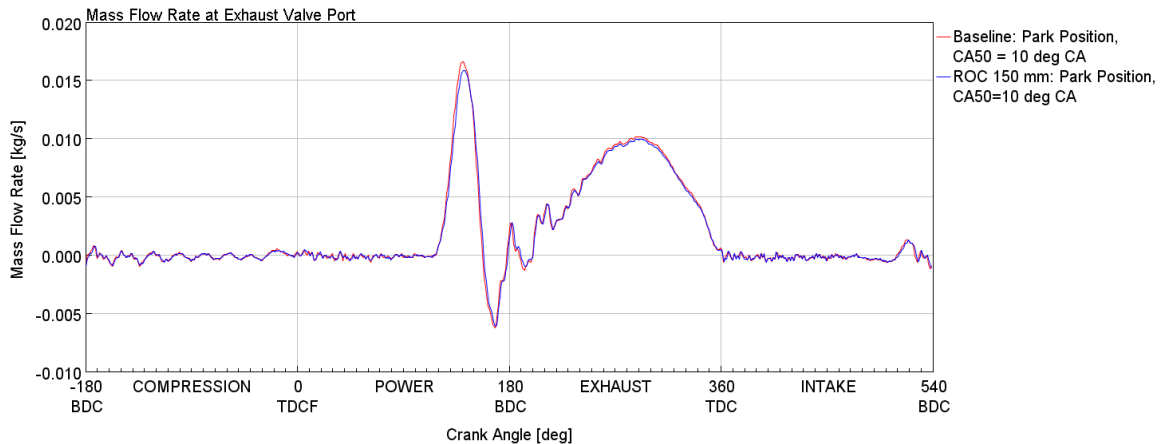


Figure 24: Mass flow rate at exhaust valve port comparing different RoC

After seeing insignificant changes in mass flow across the valve, the simulated LogP-LogV diagrams for each cam design were compared. Based on the results seen in figure 25, it was determined that there was no significant difference from the change in RoC. Between these two metrics, it was determined that the change in RoC had no significant effect on combustion or, theoretically, emissions.

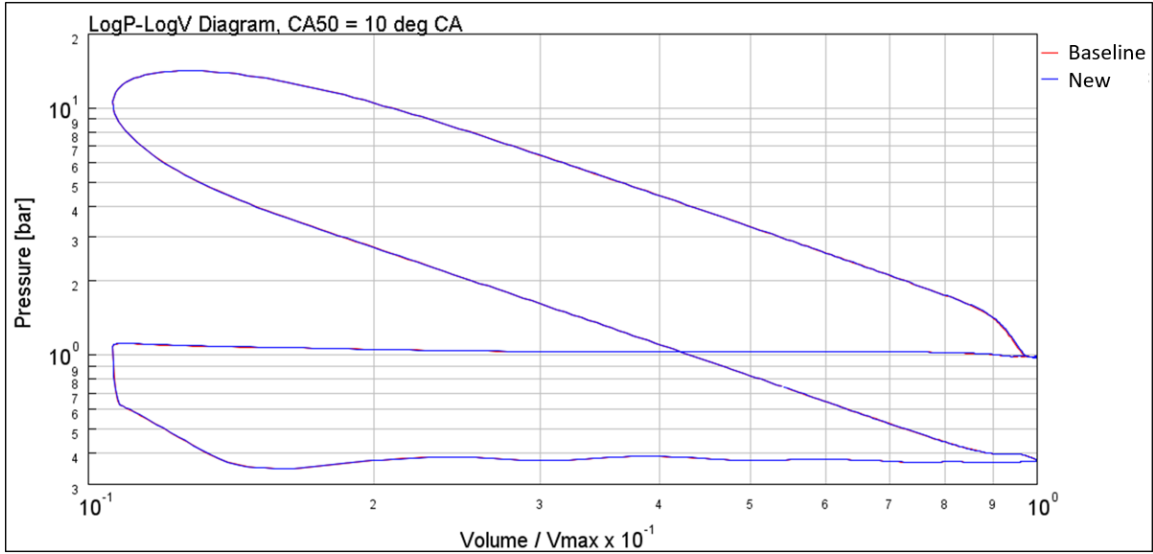


Figure 25: LogP-LogV diagram from GT-Power to verify RoC change doesn't cause other issues

After all of their work redesigning the cams, GM additionally volunteered to manufacture the prototypes. This meant that the cams used in testing would not have any concerns of the welds cracking, coming apart, interrupting testing, and potentially damaging the engine.

In the end, procuring the camshafts for this project went from a simple 12-week process to a nearly 12-month ordeal. There were several suppliers involved, several different complications, and a lot of communication back and forth to find a company that could do the work. A short summary of this process can be seen in table 6.

Table 7: Camshaft procurement summary

<u>Company</u>	<u>Lead Time</u>	<u>Cost</u>	<u>Capability</u>	<u>Notes</u>
GM	4 Weeks	GM Donation	Can grind prototype cams and have cores	Slightly increased RoC
Web Cams & Andrew's Products	5 Mnths	\$2,100	Claimed to be a routine process	Required either RoC change or extremely long lead time. Andrews not responsive for RoC change.
Comp Cams	12 Wks	\$3,000	Expressed Concerns	Comp said they had concerns, but won't elaborate on what those concerns are. No response to many requests for an engineering meeting.
MegaCycle	N/A	Unknown	Could grind small radius	Required specialized masters and camshafts in-hand before quoting or guaranteeing capability
Engine Power Components			Low	They have never done this cam, or one similar. They don't have any cores.
Edelbrock			None	They use Comp for production runs, and Engine Power Components for one-off's
Cam Motion			None	They do not weld, and do not have cores
Schneider Racing Cams			None	They do not weld, and do not have cores
Crane Cams			None	They do not weld, and do not have cores
Brian Crower			No interest	Not interested in taking on this project
Crower Cams			None	They do not weld, and do not have cores
Oregon Camshafts			None	They do not weld, and do not have cores
Delta Cams			None	They do not weld, and do not have cores

5.4.1 Camshaft Install

The longer duration camshafts were designed with the concept that both would have a later EVC than stock to help with rebreathing. However, just before testing began on the longer duration camshafts, it was decided to match EVC as it would eliminate an additional variable. Upon final verification for the prototype camshafts, ECCL was not as expected. In an effort to match EVC as closely as possible, the two prototype cams were advanced by 2 teeth (15.65° CA). The resulting measured valve lift for all three cams can be seen in figure 28. As can be seen in this plot, the stock and the 35° camshaft have a nearly identical EVC at the home position, while the 60° camshaft is slightly off due to the shift in ECCL because the exhaust cam cannot be advanced and is limited to the 50° sweep being used for this project.

As a side note, there was an issue that had to be dealt with in the Bosch software from advancing the camshafts. Because the cam position is measured in the ECU using a toothed wheel that is part of the camshaft, when the cam was advanced, so too was this wheel. This meant that the indexing for the camshafts no longer matched the previous triggering configuration and so the controller was unable to correctly position the cam. To fix this, a correctional offset was implemented in the software. Using this offset and the calibration of the controller, the camshafts had identical EVCs in their fully retarded position.

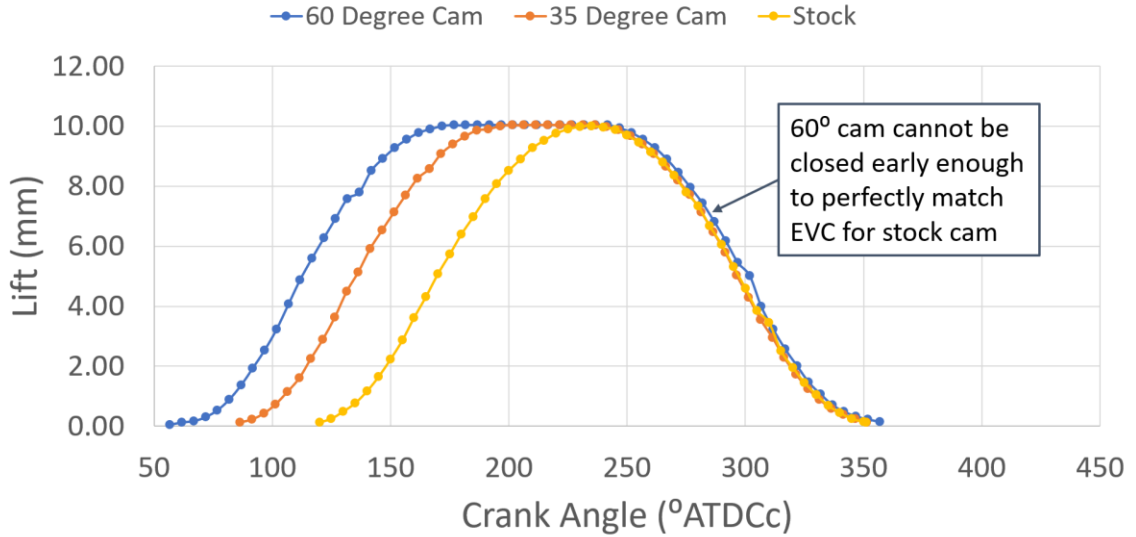


Figure 26: Measured valve lift with the camshaft in the home position

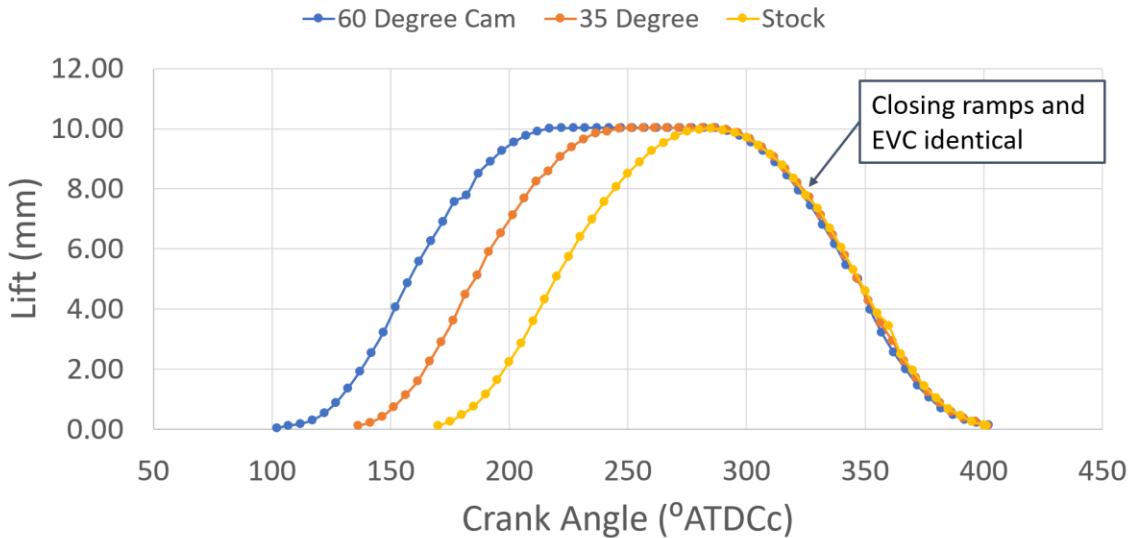


Figure 27: Measured valve lift with the camshaft the fully retarded position

5.5 Valve Deactivation

To deactivate the exhaust valves, the roller followers (RFF in fig. 28) for the valves were removed from the engine. The hydraulic lash adjusters were replaced with units that had been welded shut to avoid oil pressure issues caused by the free flow of oil through the unwelded adjusters. To prevent these adjusters from being displaced via oil pressure and roaming through the engine, hold downs were made. The entire replacement system can be seen in figure 29. This operation was performed on every cylinder when the change was made.

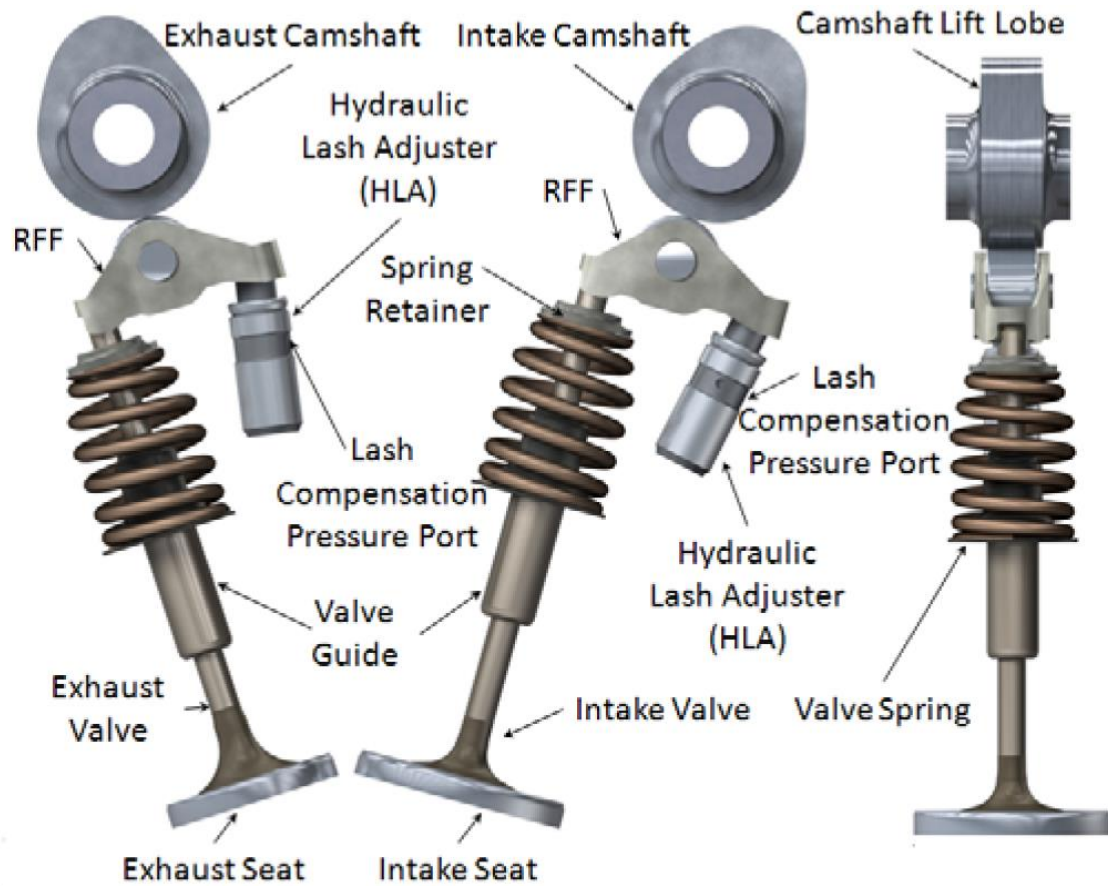


Figure 28: Valvetrain diagram [28]

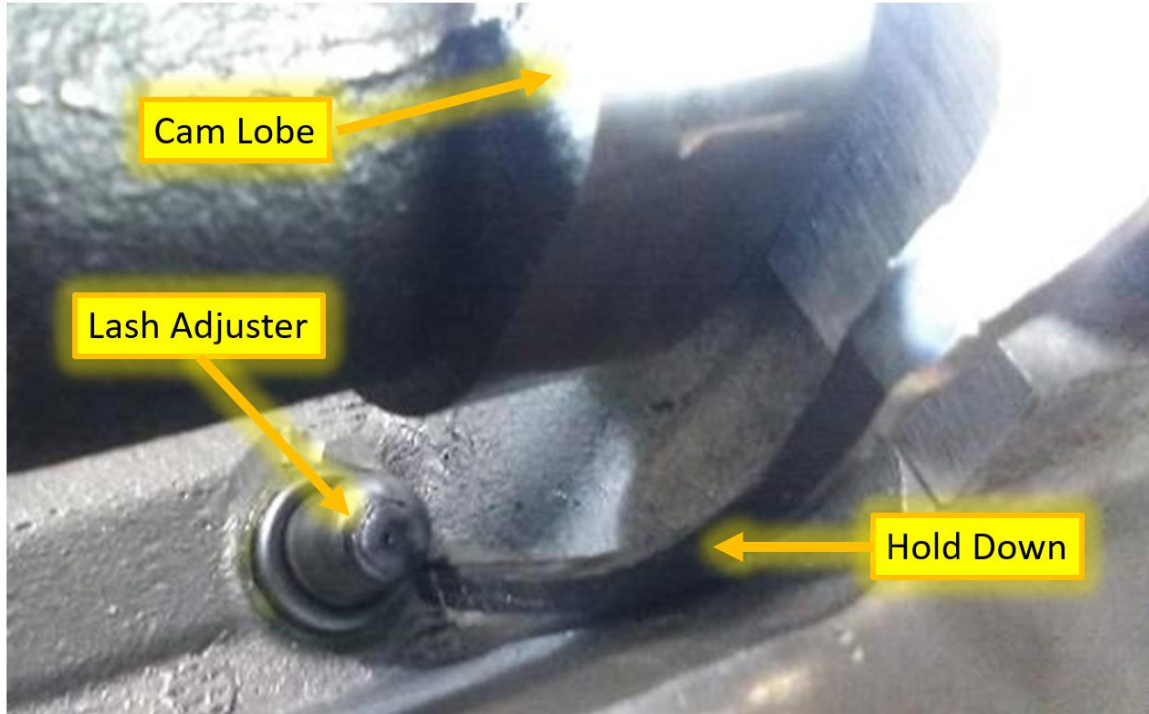


Figure 29: Welded lash adjuster and hold down

5.6 Operational Temperatures

Because the project was for testing the effects at cold start, the minimum temperatures that could be consistently met for all testing had to be determined. The FTP-75 requirement is for an ambient temperature between 20 and 30°C [4]. Because the engine had to be run for long periods of time and hold a constant temperature, these temperatures were not quite achievable. Instead, this data more accurately represent a vehicle that has been parked for a longer duration of time, but not quite the same as a morning startup. After analyzing the data from the parameterization sweeps it was determined to target the temperatures seen in table 7. These temperatures were then measured and controlled for the duration of testing.

Table 8: Temperature set points

Measurement	Oil Temperature	Coolant Temperature	Air Temperature
Set Pont	35° C	35° C	28° C

Oil temperature was measured with a thermocouple at and controlled using a . Coolant temperature was measured with a thermocouple where the coolant exits the engine and controlled using a PID controller in Veristand.

5.7 Parameterization

5.7.1 SOI Sweep

Because SOI changes can have a significant effect on emissions, a sweep was run. This was done with EEPS employed to test for particle emissions changes and the Horiba to check for all other constituents. The results can be seen in figures 30-34. In these figures, the black line with the yellow highlighting is the point at 180° BTDC, or the start of compression. The purple arrows at the bottom indicate the direction in which injection is occurring earlier in the cycle. The dotted red line is the injection angle that was chosen for testing, 240° BTDC. For the purposes of particle mass, the objective was to find a minimum point on figures 30 and 31.

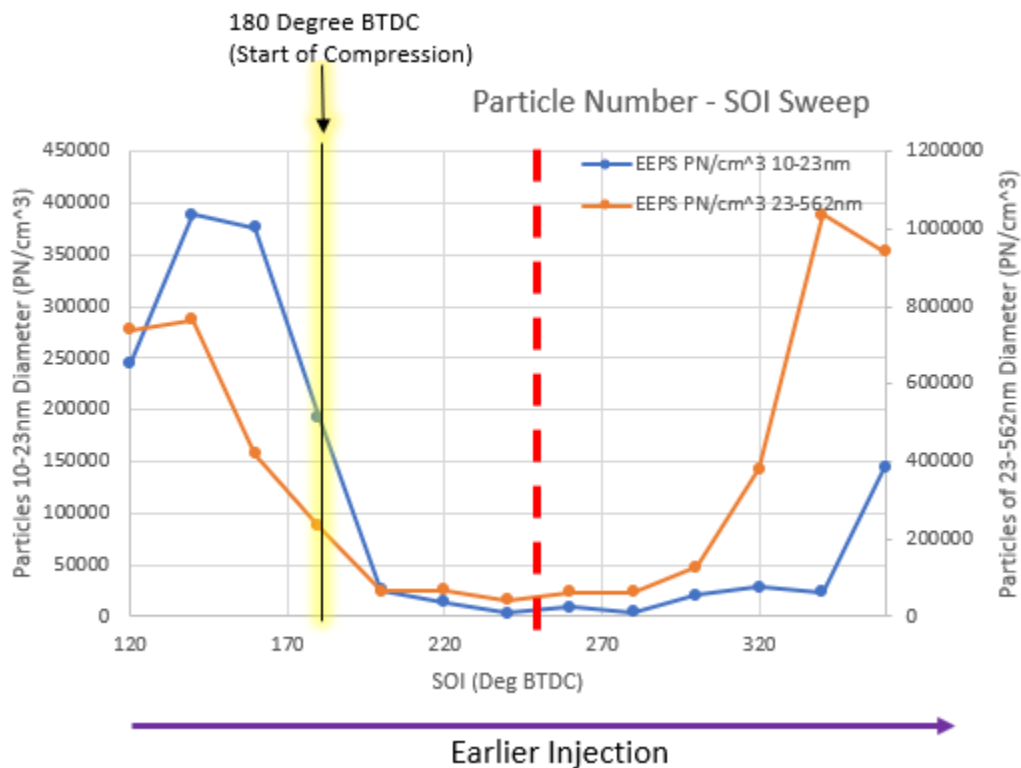


Figure 30: PN from TSI EEPS for SOI sweep **Lines are assumed trends**

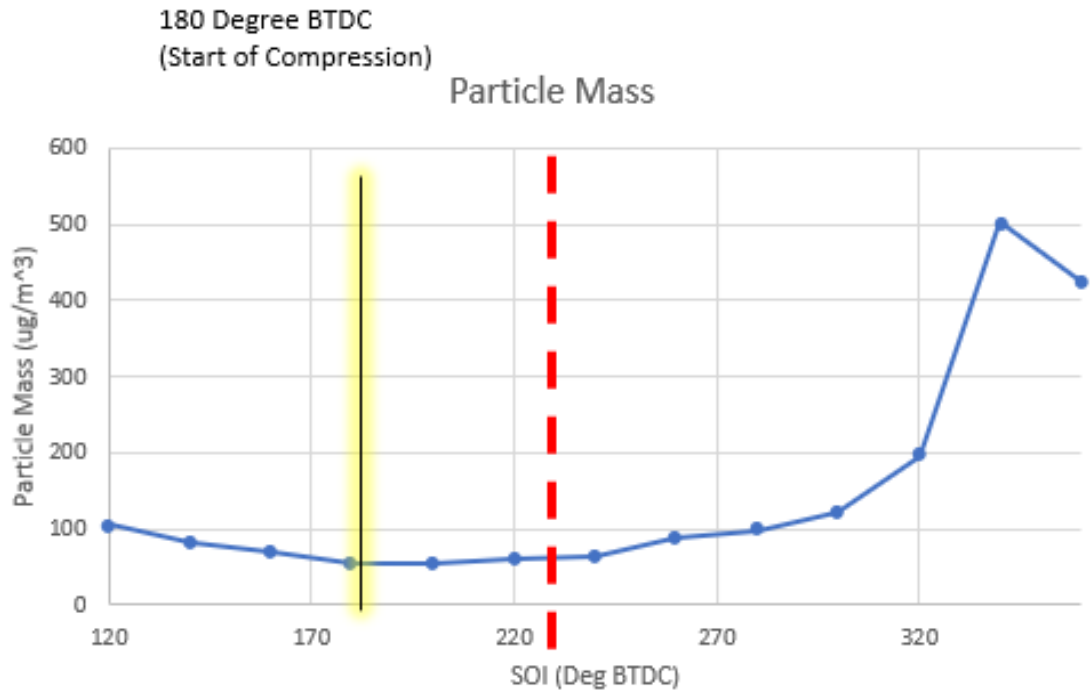


Figure 31: Particle mass from TSI EEPS for SOI Sweep **Lines are assumed trends**

For the rest of the emissions, the objective was to find an SOI that was as flat as possible with no drastic slope in either direction. This was done in an effort to try and mitigate any of the effects that might exist from any errors during testing.

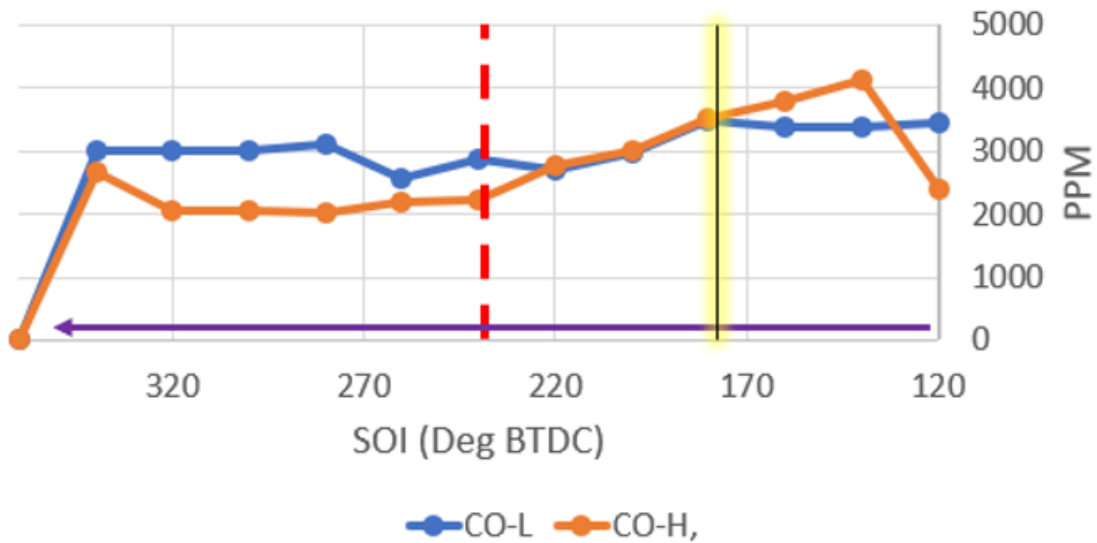


Figure 32: CO from 5-Gas for particle sweep **Lines are assumed trends**

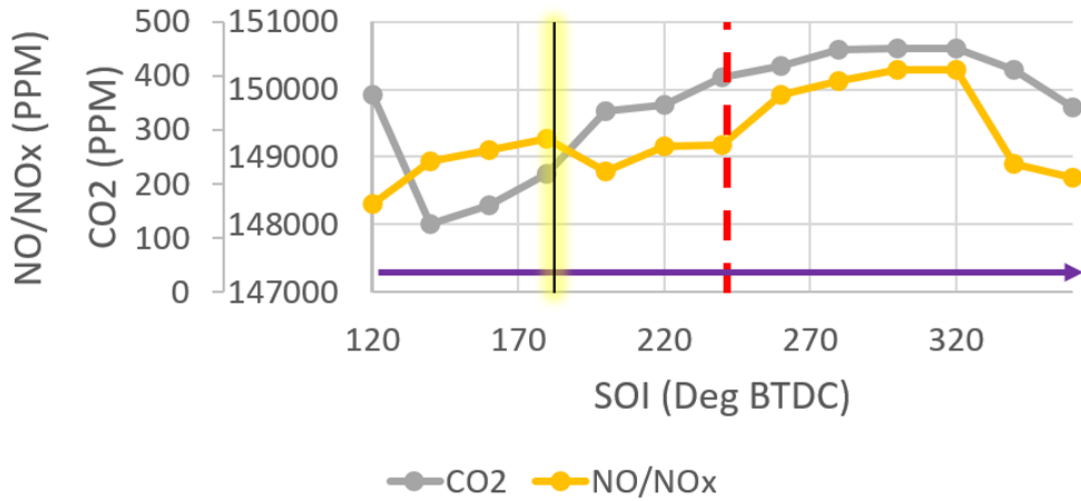


Figure 33: CO2 and NOx from 5-Gas for SOI sweep **Lines are assumed trends**

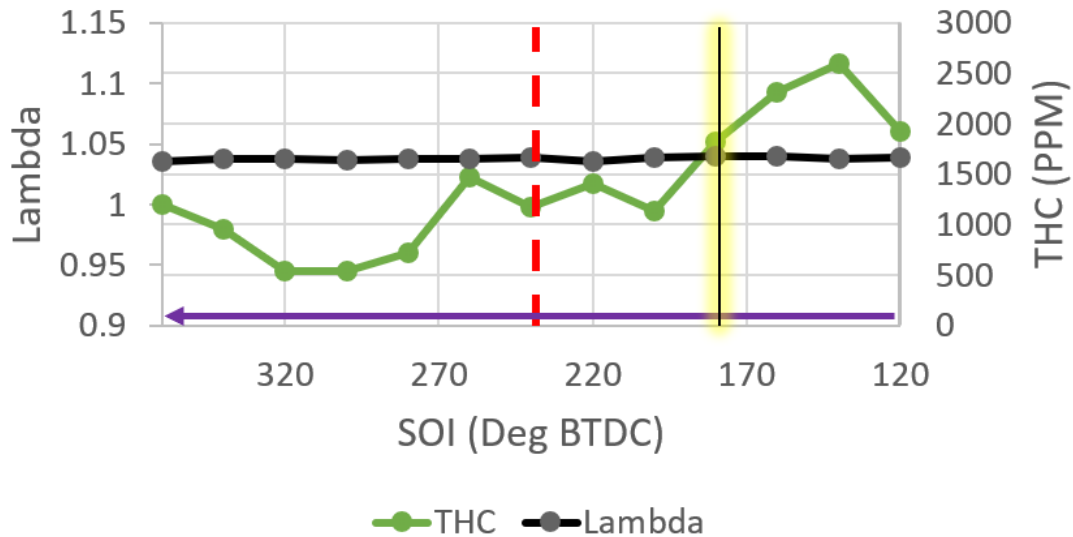


Figure 34: HC and lambda from 5-Gas for SOI sweep **Lines are assumed trends**

5.7.2 Lambda Sweep

After SOI was determined, a lambda sweep was performed. Again, the objective was to minimize the sensitivity on either side of the set point. As can be seen in figure 35, there is a drastic switching effect around $\lambda=1$, so that was not an option, with a significant decrease in CO2 and NOx as the fuel mix becomes richer. Additionally, too drastic of a change towards lean operation causes a significant decrease in CO2 and NOx.

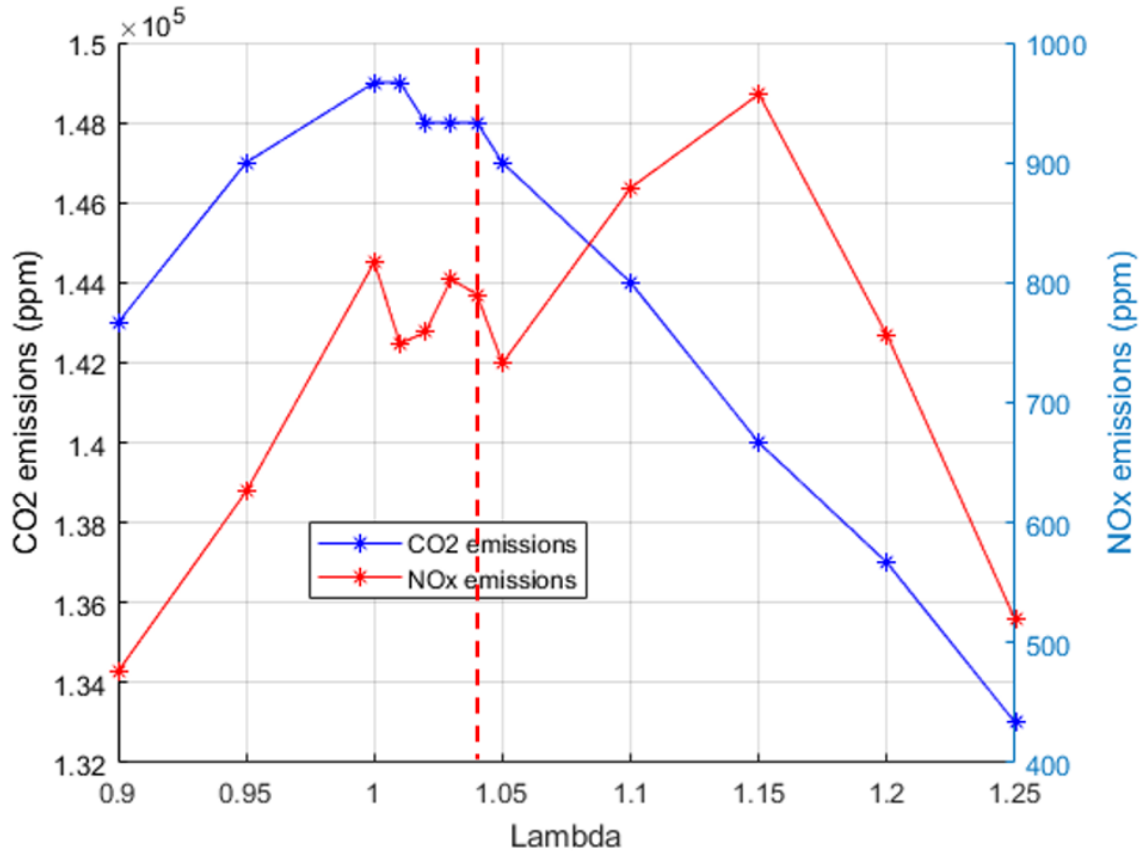


Figure 35: CO2 and NOx for lambda sweep **Lines are assumed trends**

As shown in figure 36, fuel-rich operation proves to have a significant positive slope in HC and CO emissions, as expected, due to the increase in the fuel that has no oxygen to react with. Lean operation changes CO and THC far less, so that was not as much of a concern. Because of this, the final chosen value for testing can be seen in figures 35 and 36 as a dashed red line at $\lambda=1.04$.

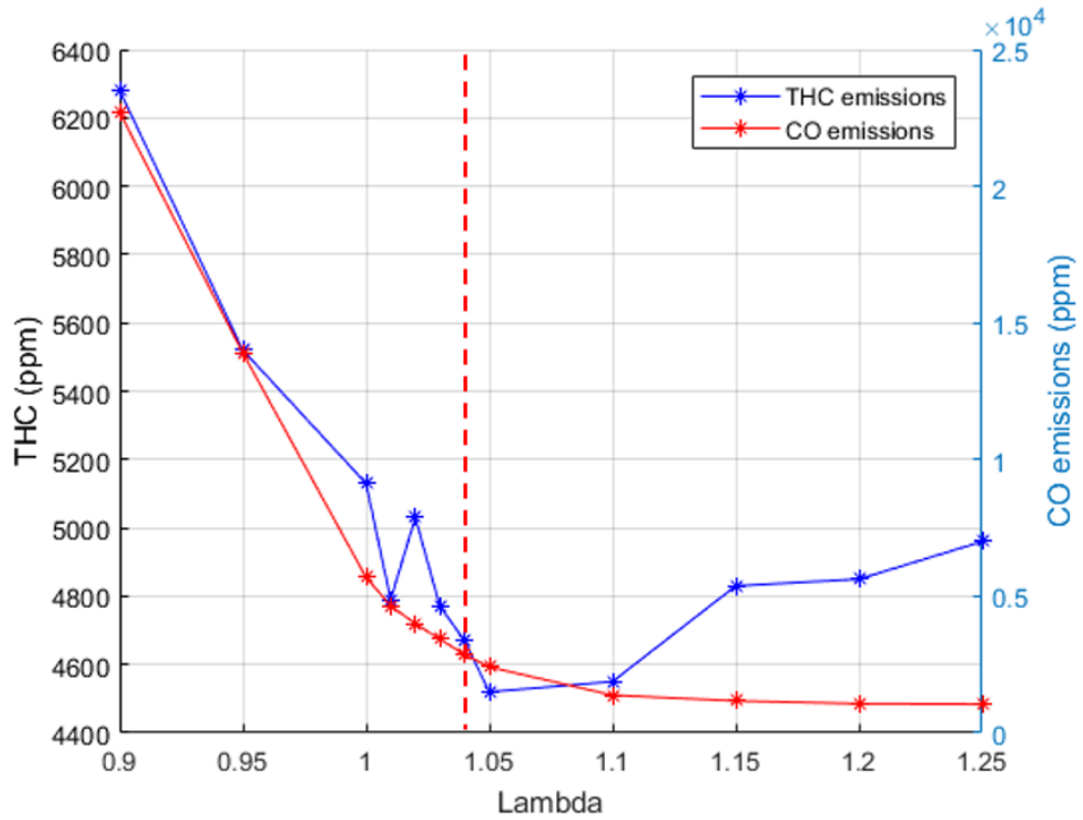


Figure 36: HC and CO for lambda sweep **Lines are assumed trends**

6 Results

To better understand the data and the physics behind it, the analysis was broken down into three major parts. The first is the comparison between single and dual exhaust valves with the stock camshaft. The second is the comparison between the different exhaust cam durations. Finally, the combined effects were examined.

6.1 Rate of Exhaust Enthalpy

Enthalpy was the metric used to measure the exhaust energy that could be transferred into the catalyst for light off. This was because it takes both temperature and mass flow into account which are both measured and can be controlled to some extent. Changing mass flow would result in a change in energy rate and changing the temperature changes the rate of heat transfer. A metric such as exergy would be very difficult, if not impossible to calculate without a catalyst to use for measuring the temperature. The rate of exhaust enthalpy was expected to increase with both the use of valve deactivation and the longer duration camshafts. In general, this was the case, however, the reasoning behind the increase was not as expected.

6.1.1 Single valve vs Dual valve

6.1.1.1 CA50

As a baseline, a sweep of only combustion timing can be seen in figure 37. This sweep was with the factory camshaft in the home position and in the dual valve configuration. As expected, the exhaust enthalpy increases as combustion phasing is retarded. This is due to several factors. The first is that the later CA50 causes the engine to become less efficient, and so more fuel energy is required to meet load. Second, with the drop in expansion work being done comes an increase in EGT. So, there is an increase in mass flow and temperature, leading to an increase in exhaust enthalpy.

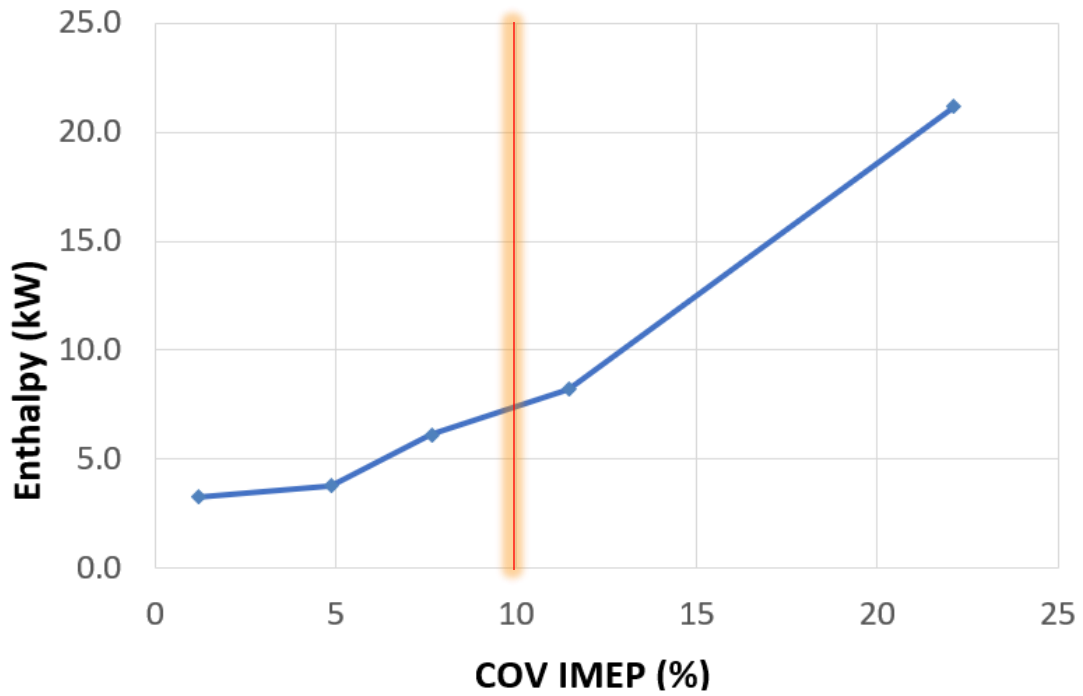
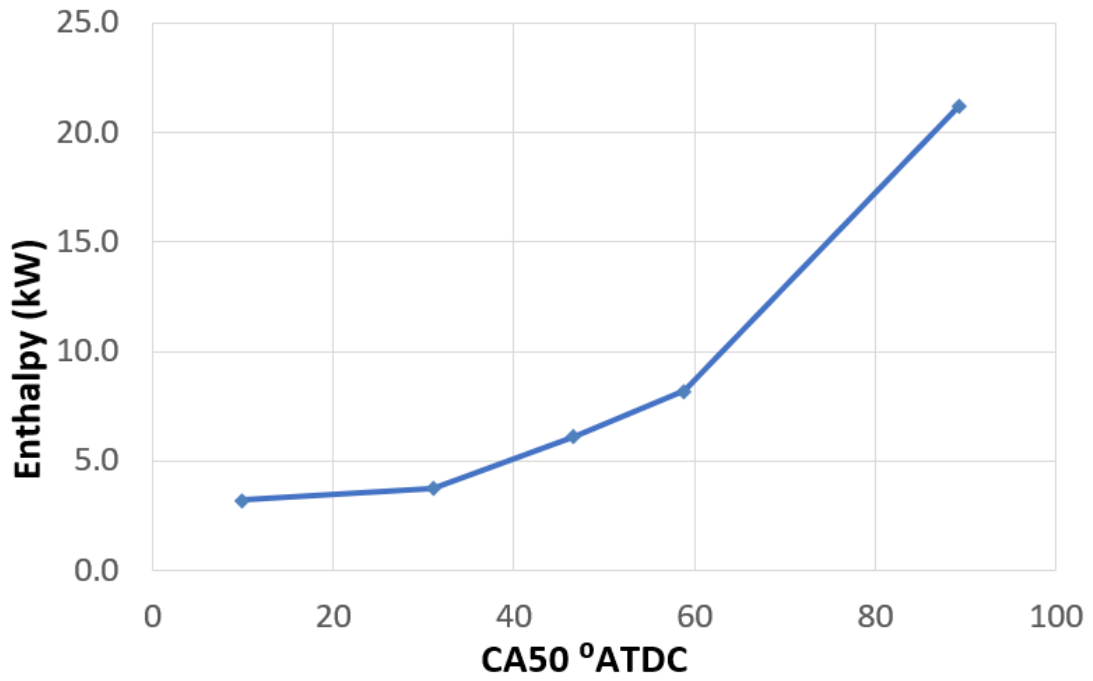


Figure 37: CA50 Sweep with stock cams without cam retard **Lines are assumed trends and red line represents current COV limits**

When comparing single valve and dual valve operation on a CA50 basis, there is a slight increase in the rate of exhaust enthalpy that comes with valve deactivation. However, this difference isn't as great as expected. The differences between the two modes of operation become more evident as cam position becomes more retarded, but the net effect of retarding the cam is generally a negative one, seen in figure 38.

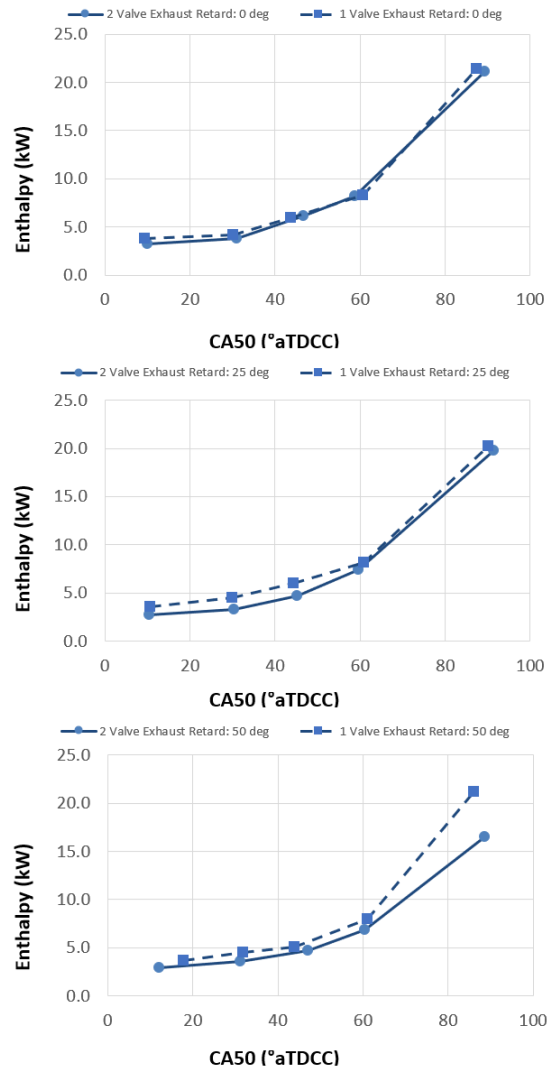


Figure 38: Exhaust enthalpy rate comparison for stock cam single valve and dual valve operation with CA50 as x-axis. **Top:** Camshaft in home position **Middle:** Camshaft retarded by 25° **Bottom:** Camshaft retarded by 50° **Lines are assumed trends and red line represents current COV limits**

6.1.1.2 COV IMEP

In an attempt to better relate the results to actual criteria for the operation of engines in a consumer's vehicle, the x-axis was changed to COV of IMEP, seen in figure 39. This is a

standard metric used to gauge the NVH levels of the engine, calculated using equation 2, and so it is one of the constraints for the final implementation of any technology in a vehicle. Perhaps more importantly though, the change of x-axis makes the overall effect of valve deactivation more clear.

$$\text{COV IMEP} = 100 \times \frac{\sigma_{\text{IMEP}}}{\bar{X}_{\text{IMEP}}} \quad (2)$$

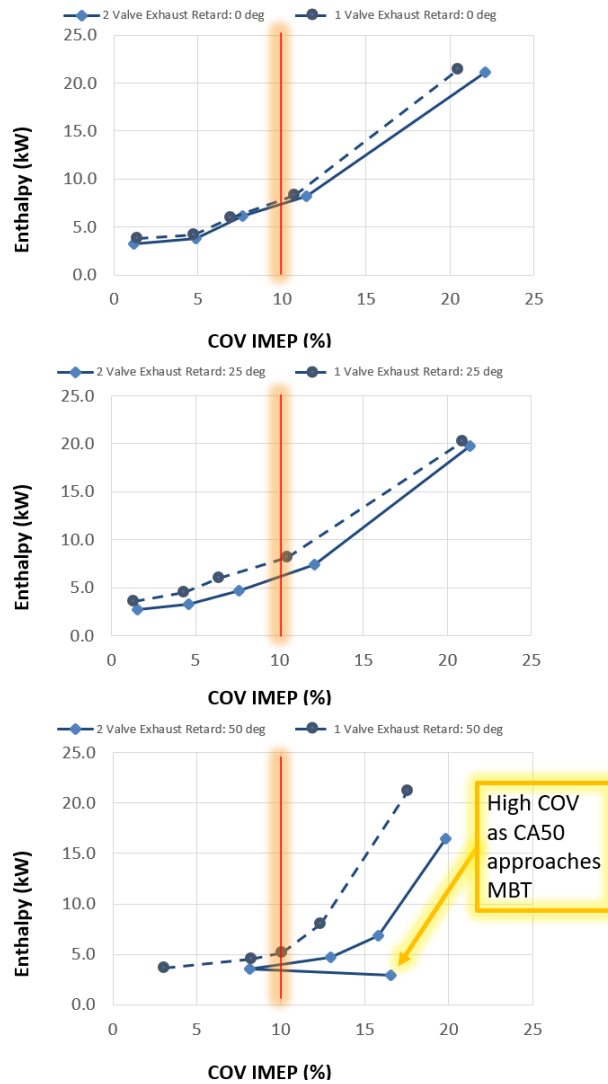


Figure 39: Exhaust enthalpy on a COV of IMEP basis for stock cam single valve and dual valve operation. **Top:** Camshaft in home position **Middle:** Camshaft retarded by 25° **Bottom:** Camshaft retarded by 50° **Note:** Low exhaust enthalpy and high COV point for dual valve operation is due to the engine approaching misfire limit when approaching MBT. Lines are assumed trends and red line represents current COV limits

6.1.2 Exhaust Enthalpy

Equation 3 is the equation for the exhaust enthalpy rate. Going forward, this equation will be broken into its individual components and there will be a comparison made for valve deactivation. For the purposes of this study, the Pv term was considered to be constant as the exhaust was at atmospheric pressure and the specific volume was not measured.

$$\dot{H} = c_p \dot{m} T + P v$$

c_p = Specific heat of the exhaust stream
 \dot{m} = Mass flow of the exhaust stream
 T = Post-turbine EGTs for exhaust stream
 P = Pressure of the exhaust stream
 v = Specific volume of the exhaust stream

(3)

6.1.2.1 Temperature

When initially examining EGTs, the first location of concern was post-turbine. As can be seen in figure 40, the results at this location support the initial theory that the smaller wetted area in the port contributes to less heat transfer. However, when examining the port EGTs, it can be seen that this is not the case. In fact, the temperatures are actually lower for the configuration with the deactivated valve. After further investigation, it was discovered that this is the result of several factors.

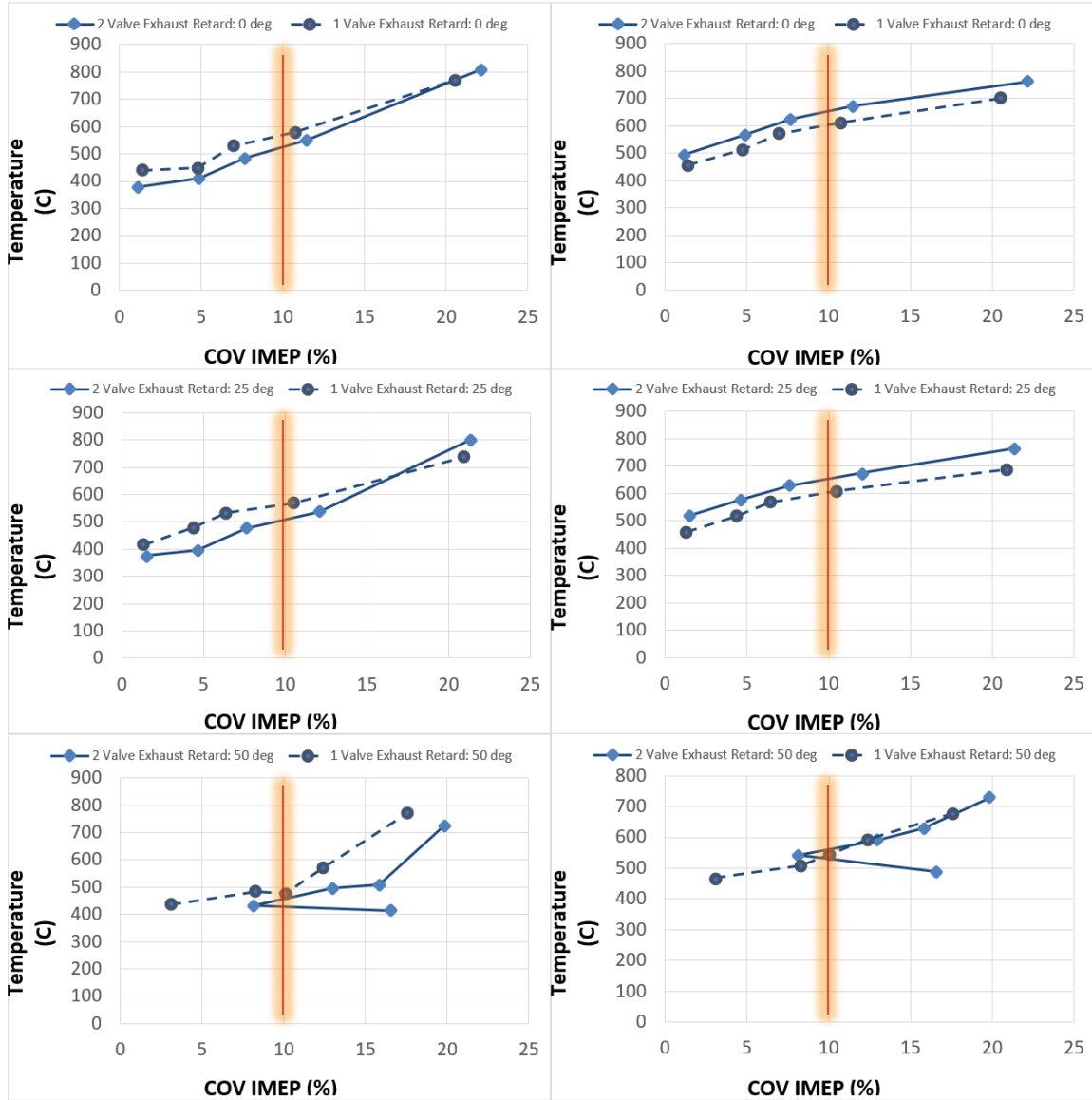


Figure 40: **Left-** Post-turbine EGTs **Right-** Port EGTs **Top:** Camshaft in home position **Middle:** Camshaft retarded by 25° **Bottom:** Camshaft retarded by 50° **Lines are assumed trends and red line represents current COV limits**

6.1.2.1.1 Heat Transfer

First and foremost, the effects of the wetted area do not contribute in the way that was anticipated. To show this, the base equation for heat transfer seen in equation 4 will be broken into its individual components.

$$Q = hA\Delta T$$

h = Heat transfer coefficient (4)

A = Wetted area of port for heat transfer

ΔT = Temperature difference from the exhaust stream to the port wall

GT-Power simulations were used to calculate many of the factors involved in this heat transfer. One of the things that was changing unexpectedly was the heat transfer coefficient, as seen in figure 41.

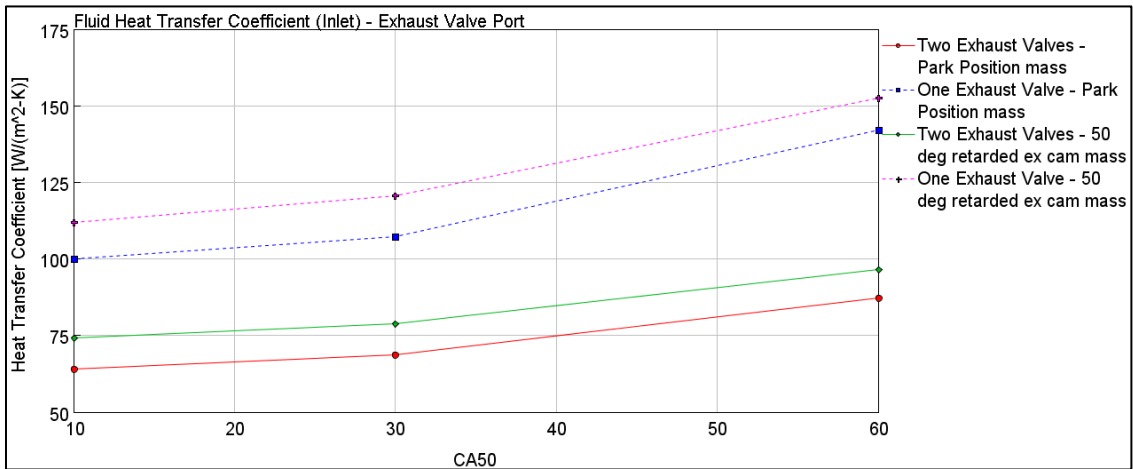


Figure 41: GT-Power heat transfer coefficient comparison

To better understand why this coefficient was changing so drastically, one of the fundamental ratios in fluid heat transfer was used, the Nusselt number. Its relationship with the heat transfer coefficient can be seen in equation 5. The Nusselt number itself is related to both the Reynolds number and the Prandtl number in equation 6.

$$Nu = h_c \frac{D}{k} \quad (5)$$

$$Nu = 0.023(Re)^{0.8}Pr^{0.4} \quad (6)$$

Breaking the Reynolds and Prandtl numbers down into the components that make them up and substituted them into equation 6. Setting this new equation equal to equation 4 and rearranging yields equation 7.

$$h_c = 0.023(k/D)\left(\frac{\rho VD}{\mu}\right)^{0.8}\left(\frac{C_P\mu}{k}\right)^{0.4} \quad (7)$$

After looking through each variable in equation 7 in GT-Power, it was deemed appropriate to assume constant density, viscosity, and specific heat. This was because the changes for each of these was significantly smaller, on a percentage basis, when compared to changes in velocity. By assuming these constants, using equation 7 for each valve configuration, and rearranging the two, the end result is equation 8.

$$\frac{h_{c,1 Valve}}{h_{c,2 Valve}} = \left(\frac{V_{1 Valve}}{V_{2 Valve}}\right)^{0.8} \quad (8)$$

Using the calculated values for velocity in GT-Power from the case with the cam in the park position and the engine operating at MBT, and rearranging the resulting equation leads to equation 9, below. The end result is that the heat transfer coefficient for the single valve configuration is actually higher than that of the dual valve configuration. Based on this calculation, the heat transfer for the single valve configuration is roughly 41% higher in the area of the port before the septum. Unfortunately, while the Prandtl number meets the requirements for this specific correlation, the Reynolds number is a bit low. However, the end result still matches the results seen in the GT-Power simulation.

$$h_{c,1 Valve} = 1.41h_{c,2 Valve} \quad (9)$$

Additionally, the area of the port is not actually half and there are several reasons for this. The first is that the flow itself will cause a low-pressure area in the dead port. This low-pressure area will draw in some of the hot exhaust gases past the septum, increasing the area for heat transfer. The second is that the dead port will also be slightly cooler in temperature, further lowering the pressure and drawing in exhaust gases, increasing the effective heat transfer area again. Last, and this is somewhat definition-dependent, even if this low-pressure area did nothing, the most significant area of the port is after the septum, where the flow paths for each exhaust valve combine into a single larger exhaust flow path, and so the overall area of the port still wouldn't be cut in half, but more comparable to a 1/3 decrease in area. The diagram in figure 42 is helpful in visualizing

the effect. As a reference point, the dashed red line represents a plane that would divide the port in half.

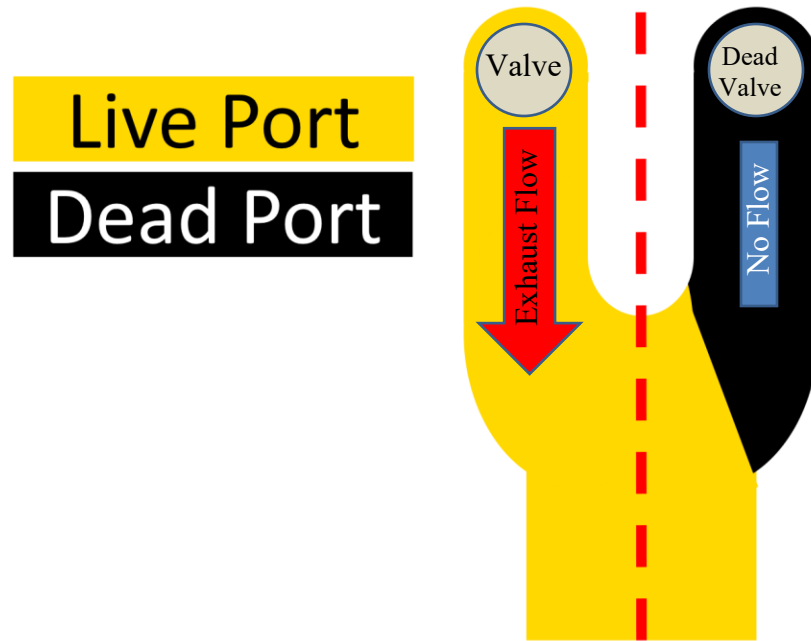


Figure 42: Diagram of port area after valve deactivation

6.1.2.1.2 Increased Expansion Work

The second factor is that the deactivated valve chokes flow during the blowdown process. This choked flow leads to further expansion of the exhaust gases, and the result is lower EGTs. This expansion can be seen in the highlighted circle in figure 43. The operating point used in this figure is for one of the more extreme cases of combustion, but the effects are seen in all cases.

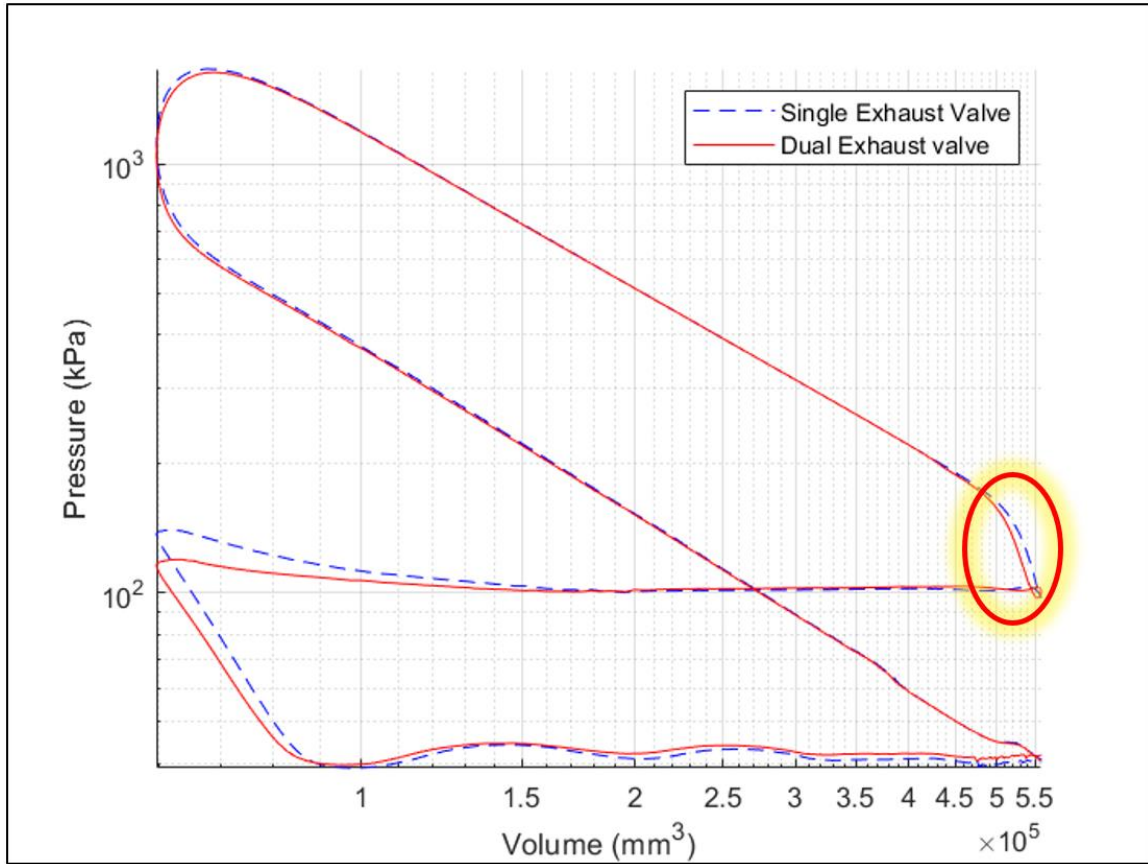


Figure 43: LogP-LogV Diagram of experimental engine for fully exhaust cam and a CA50 at MBT

However, even with all of these factors contributing to lower EGTs at the port, the single valve configuration was surprisingly better at maintaining higher EGTs post-turbine, where the catalyst is positioned, seen in figure 44. This is likely due to the occurrence of post-oxidation, as there were unburned HC in the exhaust stream and the temperature of the stream was significantly higher than the auto-ignition temperature of the fuel. This leads to a further decrease in temperature drop in the exhaust stream.

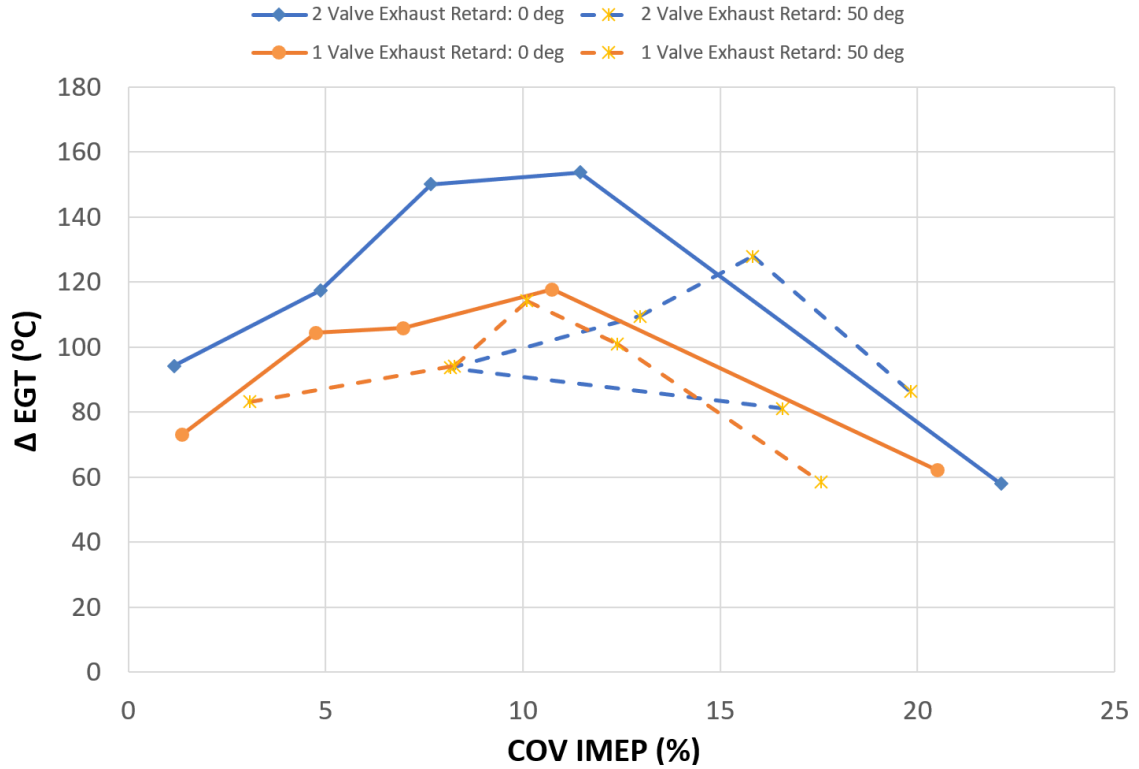


Figure 44: EGT drop from port to post-turbine **Lines are assumed trends**

6.1.2.1.3 EGT Measurement

Lastly, the measurement of the EGTs is slightly skewed. The port thermocouples only have exhaust flowing across them for a portion of the cycle. During the other portion of the cycle the thermocouples are actually cooling. The data rate used for recording in Veristand was not high enough to measure this fluctuation, and so the port temperatures were averaged within each data set.

This effect can also be seen in the comparison between the port and post-turbine EGTs. The post-turbine thermocouple has a nearly constant stream of exhaust gases flowing across it and so it does not have the cooling portion of the cycle that the port thermocouples experienced.

6.1.2.2 Mass Flow Rate

Mass flow rate is a critical component in the exhaust enthalpy rate as the rate of exhaust enthalpy scales directly with mass flow rate. One of the benefits to single valve operation is the increase in mass flow. This increase can be seen in figure 45.

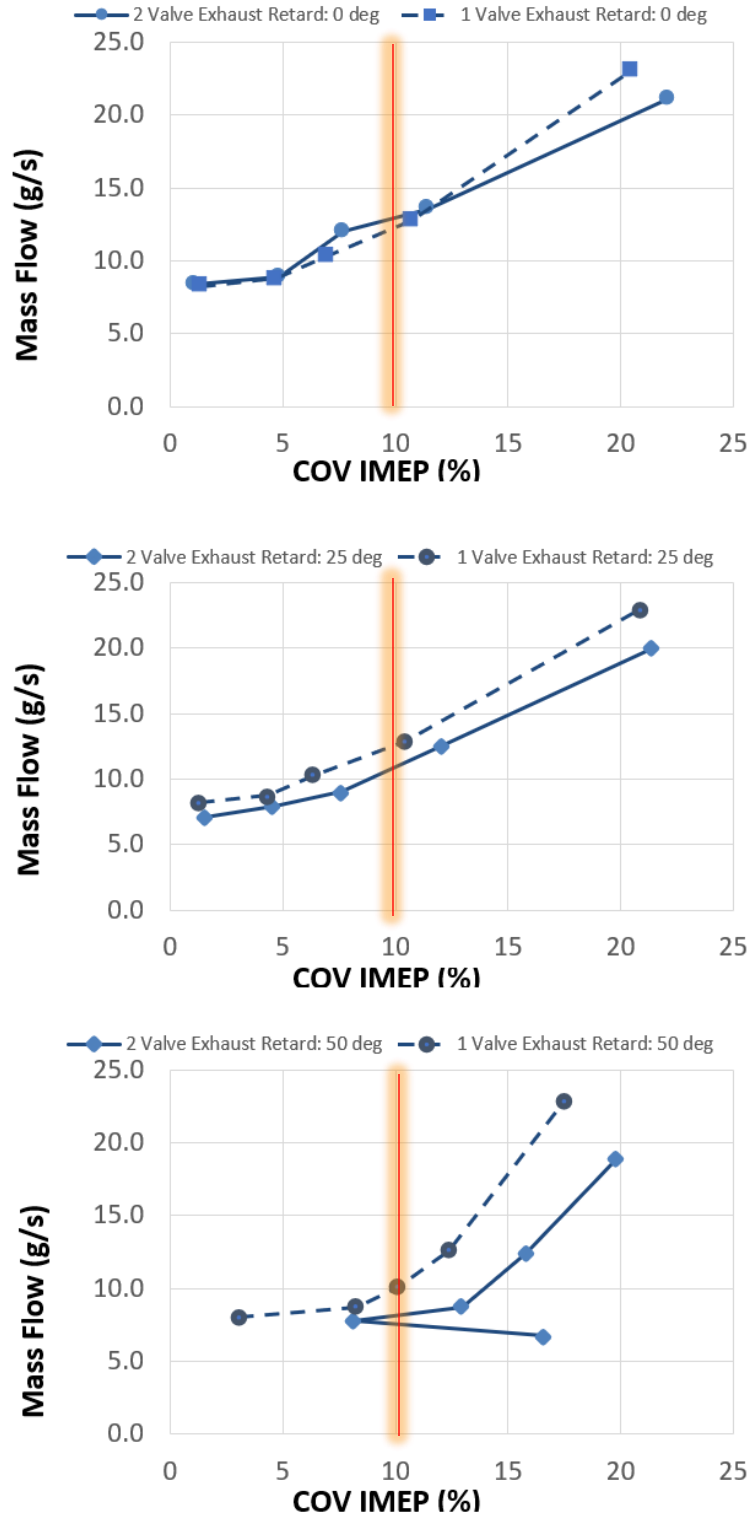


Figure 45: Mass flow comparison for stock cam single valve and dual valve operation. **Top:** Camshaft in home position **Middle:** Camshaft retarded by 25° **Bottom:** Camshaft retarded by 50° **Lines are assumed trends and red line represents current COV limits**

This increase in mass flow is largely contributed to three different effects seen in figure 46. Zone 1 shows the decrease in curtain area causing higher cylinder pressure during the exhaust stroke, which increases pumping work. Zone 2 shows the restriction of backflow into the cylinder, decreasing cylinder pressure and increasing pumping work in the early part of the intake stroke. This lower pressure also indicates lower in-cylinder residuals. Zone 3 shows how the decrease in residuals leads to the need to increase throttling to meet the target load, further increasing pumping losses.

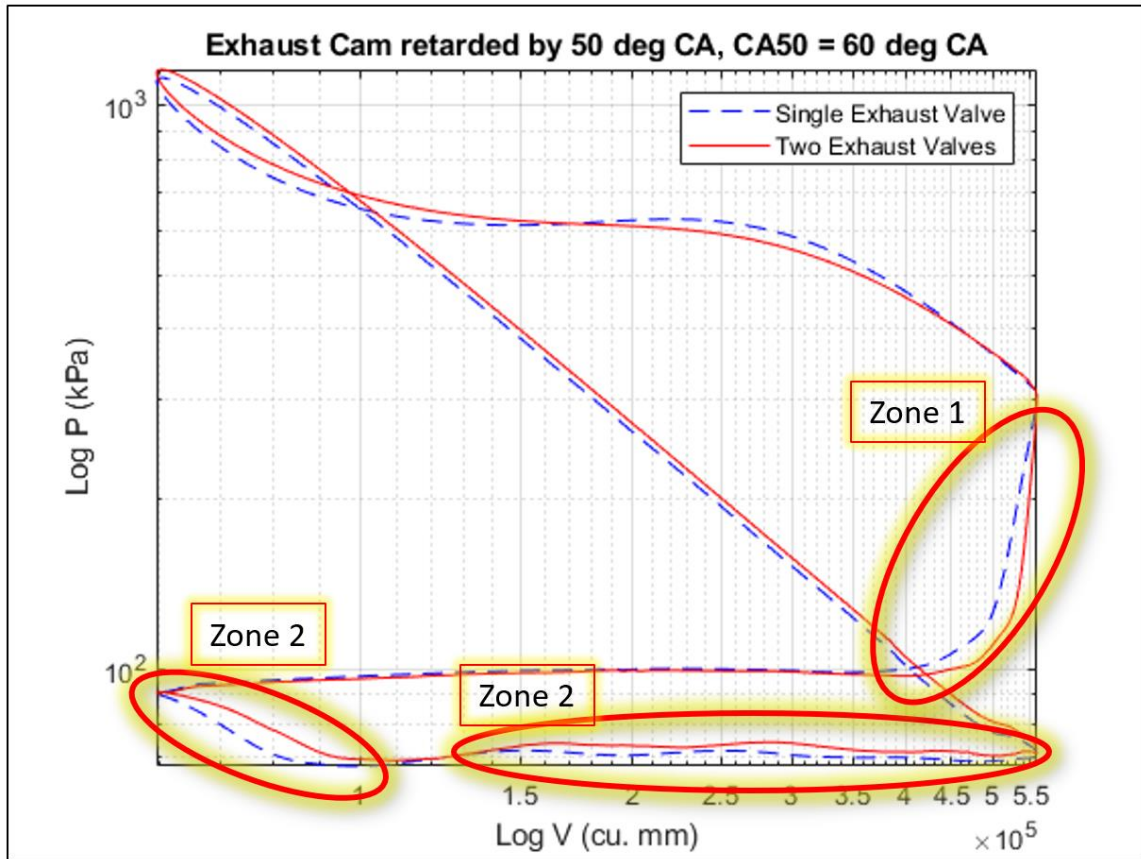


Figure 46: LogP-LogV with cam retarded by 50° and CA50 of 60° to show pumping losses

6.1.2.3 Specific Heat

Calculating the specific heat for the flow is relatively simple. In equation 10, the mass fraction of each constituent is multiplied by the specific heat for that constituent. The sum of each of these different values is the specific heat for the exhaust flow.

$$c_p = \sum x_i c_{p,i} \quad (10)$$

In this study, most of the contributing constituents were directly measured. However, H₂O and H₂ could not be directly measured, and so were calculated using the water gas

shift reaction found in equation 4.63 of [1]. The constant K used was 3.5, as it is a commonly accepted constant for this equation to be valid. For the HC term, it was assumed that this was the same molecular makeup as the fuel being used, as this is also a common practice.

6.1.2.4 Residuals

As previously alluded to, the key to all of these effects is the changes in in-cylinder residuals. Because residuals cannot be measured directly in the experiment, they were calculated using GT-Power. The results can be seen in table 8. In this table, the red and green represent a relative scale of residuals with dark red indicating the highest relative residuals and green the lowest. The third section of the table the difference between dual valve and single valve operation, with red indicating an increase with the switch to single valve and blue indicating a decrease. When the cam is in the home position, the residuals for single valve are actually slightly higher than those for the dual valve configuration. This is a reflection of figure 45 when the mass flow for the two configurations was similar. However, once the cam is retarded to 25° and 50°, the results become much more clear. The residuals for dual valve have increased by over 13%.

Table 9: Cam Residual Comparison. All Values are in % The green and red plots correspond to lowest and highest values, respectively. The blue and red colors in the delta table correspond to decreased residuals from dual to single valve and increased residuals, respectively. Dual valve operation with stock, 35° duration increase, and 60° duration increase

2 Valve	Cam Position	Stock Cam			
		CA50			
		10	30	45	60
0		11.4	9.7	8	6.5
25		17.1	15.4	13.2	10.9
50		30.9	27.9	23.8	19.2
1 Valve	Cam Position	Stock Cam			
		CA50			
		10	30	45	60
0		12.8	10.7	8.8	7
25		14.5	12.8	10.8	8.7
50		26.5	23.7	20.3	16.4
Delta (2V-1V)	Cam Position	Stock Cam			
		CA50			
		10	30	45	60
0		-1.4	-1	-0.8	-0.5
25		2.6	2.6	2.4	2.2
50		4.4	4.2	3.5	2.8

6.1.3 Combined Effects of Port Deactivation and Longer Duration Camshaft on Rate of Enthalpy

As can be seen in figure 47, there is generally an increase in the rate of enthalpy with the 60° camshaft and single valve operation. The single valve configuration is slightly better due to the reasons previously examined. The longer duration camshaft provides a slight increase in the rate of exhaust enthalpy because the mass flow is slightly higher overall when compared to the stock camshaft, seen in figure 48.

Additionally, as cam duration increases, the in-cylinder residuals decrease. This is especially evident with the use of the deactivated valve, and is presented in table 9, an expansion of table 8 used to compare all operational configurations and their respective residuals. In fact, with the valve deactivated and the 60° camshaft, there is a 42% reduction in residuals with this configuration. This leads to an increase in combustion temperatures and, theoretically, higher EGTs. However, as seen previously, the single valve configuration leads to increased expansion work, so the EGTs are relatively similar between the two.

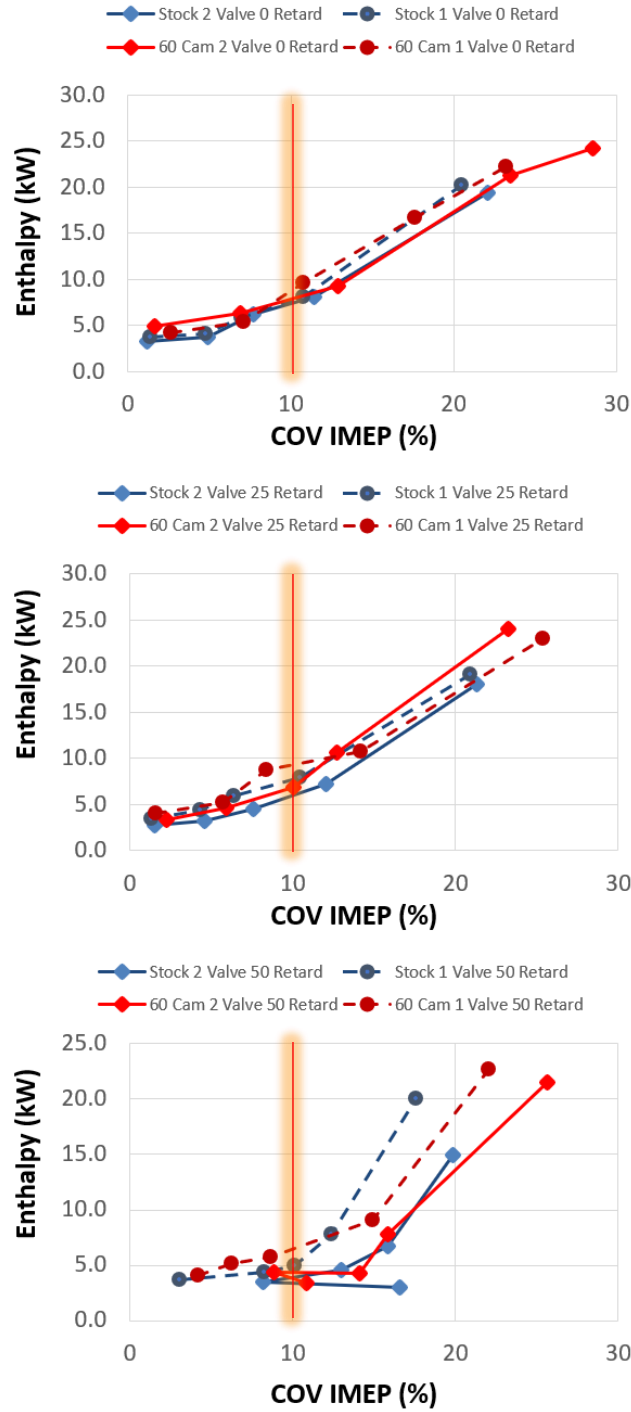


Figure 47: Enthalpy comparison for single valve and dual valve with the stock and 60° camshafts **Top:** Camshaft in home position **Middle:** Camshaft retarded by 25° **Bottom:** Camshaft retarded by 50° **Lines are assumed trends and red line represents current COV limits**

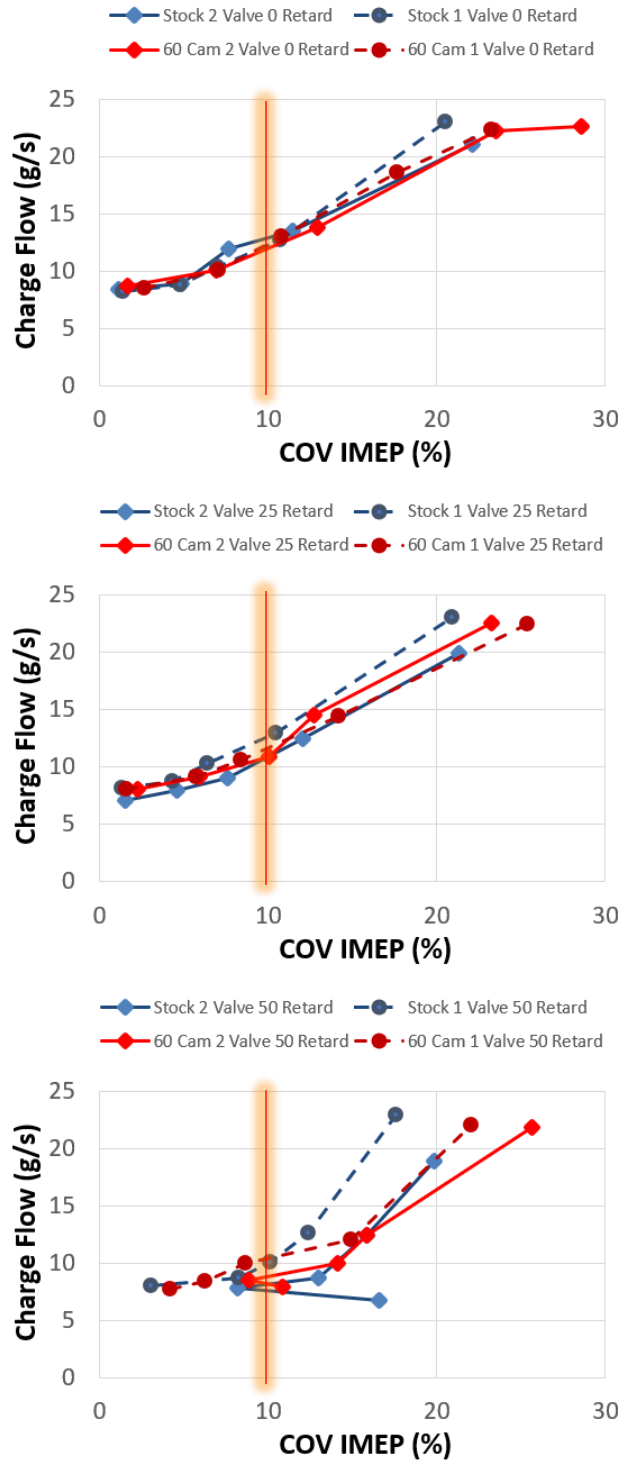


Figure 48: Mass flow comparison for single valve and dual valve with the stock and 60° camshafts **Top:** Camshaft in home position **Middle:** Camshaft retarded by 25° **Bottom:** Camshaft retarded by 50° **Lines are assumed trends and red line represents current COV limits**

Table 10: Residuals comparison for all configurations All values are in %. The green and red plots correspond to lowest and highest values, respectively. The blue and red colors in the delta table correspond to decreased residuals from dual to single valve and increased residuals, respectively. **Left:** dual valve operation with stock, 35° duration increase, and 60° duration increase **Middle:** single valve operation with stock, 35° duration increase, and 60° duration increase **Right:** Difference between dual valve and single valve operation with stock, 35° duration increase, and 60° duration increase

	Stock Cam						Stock Cam						Stock Cam				
	CA50						CA50						CA50				
	10 30 45 60						10 30 45 60						10 30 45 60				
	Cam Position	0	25	50			Cam Position	0	25	50			Cam Position	0	25	50	
2 Valve	35 Cam					1 Valve	35 Cam					Delta (2V-1V)	35 Cam				
	CA50						CA50						CA50				
	10 30 45 60						10 30 45 60						10 30 45 60				
	Cam Position	0	25	50			Cam Position	0	25	50			Cam Position	0	25	50	
		11.4	17.1	30.9	9.7			12.8	14.5	26.5	10.7			-1.4	2.6	4.4	-1.0
		9.7	15.4	27.9	8.0			10.7	12.8	23.7	8.8			-1.0	2.6	4.2	-0.8
		8.0	13.2	23.8	6.5			8.8	10.8	20.3	7.0			-0.8	2.4	3.5	-0.5
		6.5	10.9	19.2				7.0	8.7	16.4				-0.5	2.2	2.8	
		10.8	18.2	29.5	4.3			16.0	25.6	35.2	5.4			-5.3	-7.5	-5.7	-2.5
60 Cam					60 Cam					60 Cam							
CA50					CA50					CA50							
10 30 45 60					10 30 45 60					10 30 45 60							
Cam Position	0	25	50		Cam Position	0	25	50		Cam Position	0	25	50				
	10.6	16.4	30.4	8.6		5.1	9.9	15.3	2.1		5.5	6.5	15.2	6.6			
	8.6	14.2	27.2	6.5		2.0	4.6	13.4	2.7		6.6	9.6	13.8	4.4			
	6.5	11.7	23.1	6.2		2.1	2.6	8.6	2.7		4.4	9.1	14.5	3.6			
	6.2	9.0	18.2			2.7	3.4	5.0			3.6	5.6	13.2	5.6			

6.2 Emissions

6.2.1 Single valve vs. Dual valve

While enthalpy increases with the deactivation of a valve, so to do some of the measured emissions. Figure 49 shows the increase in HC for different configurations. For the earlier cam timings, the single valve configuration is worse from an emissions perspective. This is because the curtain area of the single valve is restricting the rebreathing that would normally draw the HC back into the cylinder and completing the combustion process with the previously unburned HC. For the later cam timing, however, this is not necessarily the case. This is because the COV for the dual valve configuration is much higher with the later cam timing than it is with the earlier cam timing and is even greater than the single valve configuration at times.

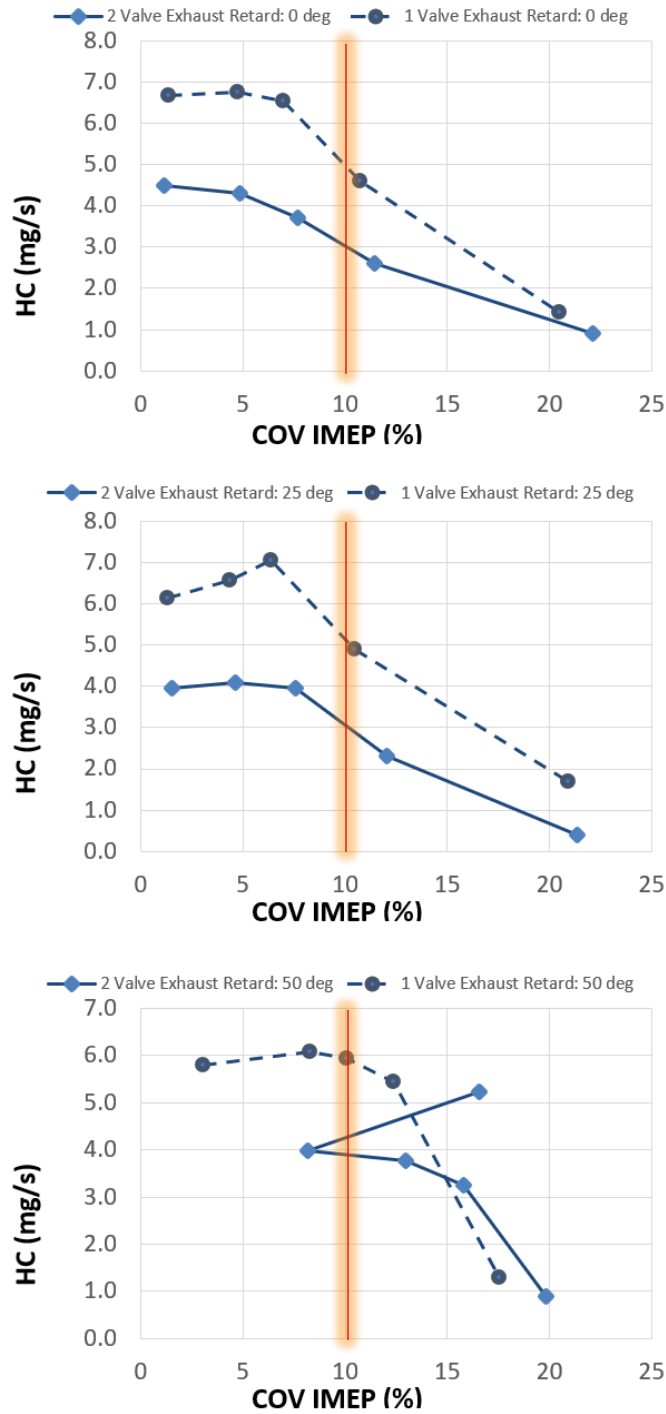


Figure 49: HC emissions comparison for single valve and dual valve with the stock camshaft **Top**: Camshaft in home position **Middle**: Camshaft retarded by 25° **Bottom**: Camshaft retarded by 50° **Lines are assumed trends and red line represents current COV limits**

On the other hand, CO is lower for most of the cases with the single valve configuration, seen in figure 50. There is generally a trade-off between HC and CO though because the reaction is being cut short during different stages of combustion. This means that the reaction is not only stopping before the constituents reach the point of becoming CO₂, it is stopping before the fuel fully dissociates and the carbon begins to combine with the available oxygen atoms.

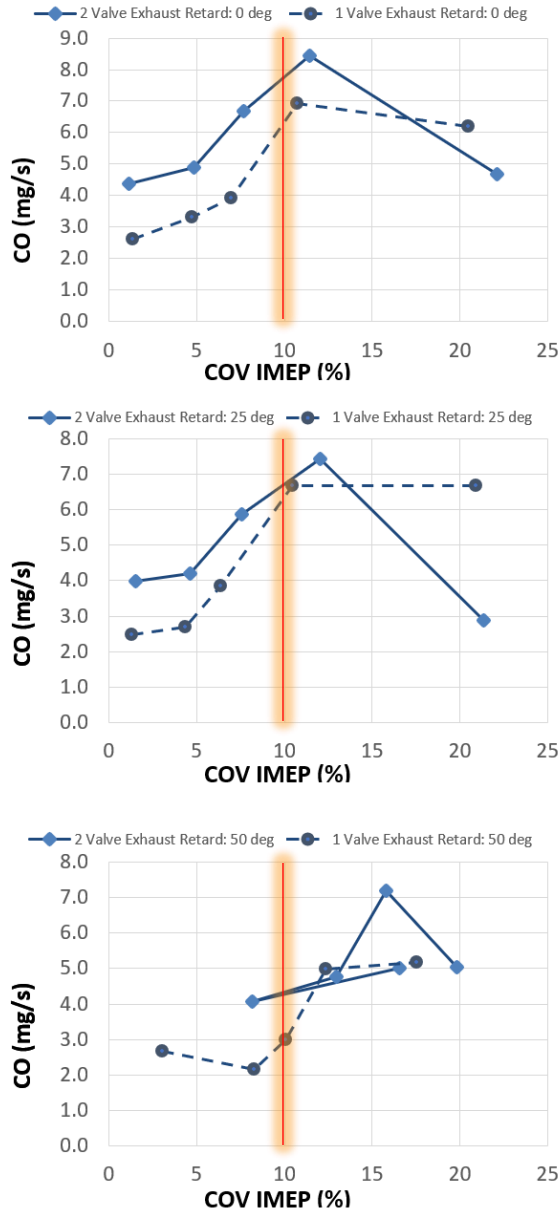


Figure 50: CO emissions comparison for single valve and dual valve with the stock camshaft **Top**: Camshaft in home position **Middle**: Camshaft retarded by 25° **Bottom**: Camshaft retarded by 50° **Lines are assumed trends and red line represents current COV limits**

NOx appears similar between the two configurations in figure 51, but this is generally an artifact created by the use of COV on the x-axis. The total NOx output for similar set points is similar between the two, but the single valve configuration is operating at a lower COV, and so the values appear to be higher. The overall trend also matches the residuals trend seen in table 10 because the decrease in residuals leads to a higher combustion temperature and, therefore, more NOx is formed. This can be seen in figure 52.

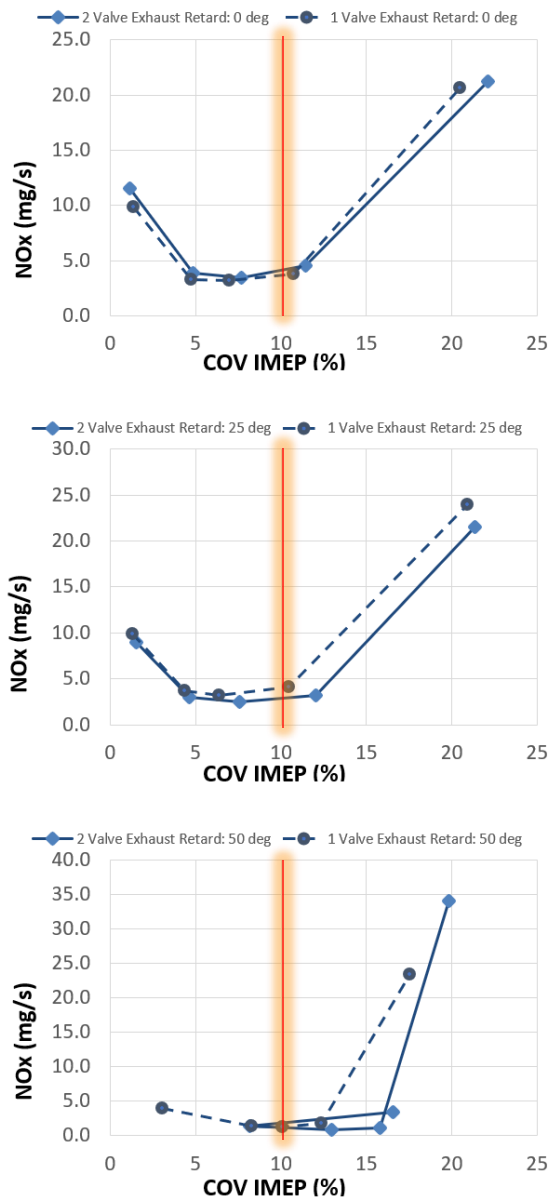


Figure 51: NOx emissions comparison for single valve and dual valve with the stock camshaft **Top**: Camshaft in home position **Middle**: Camshaft retarded by 25° **Bottom**: Camshaft retarded by 50° **Lines are assumed trends and red line represents current COV limits**

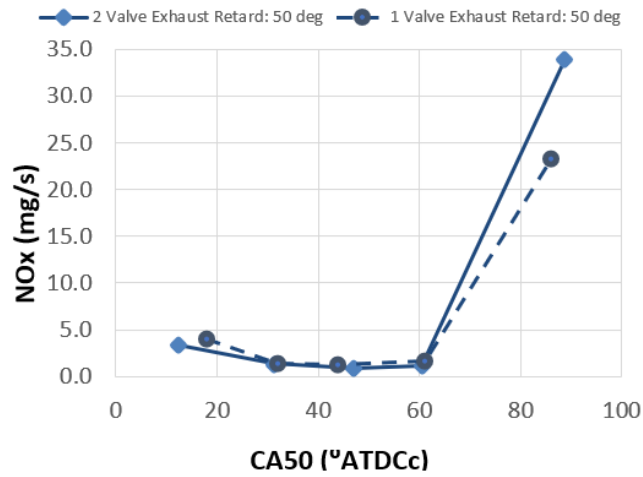
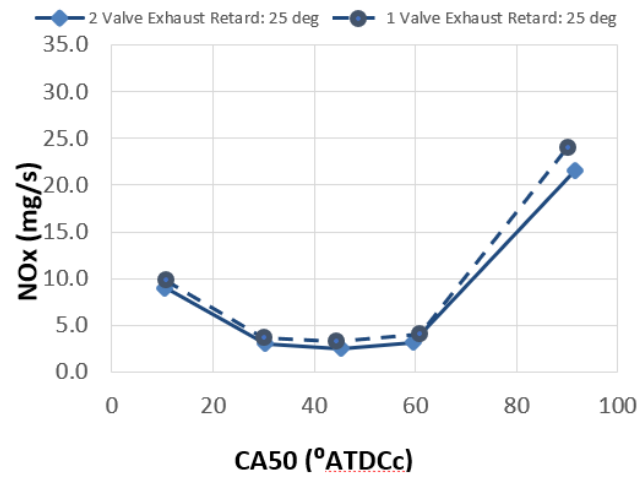
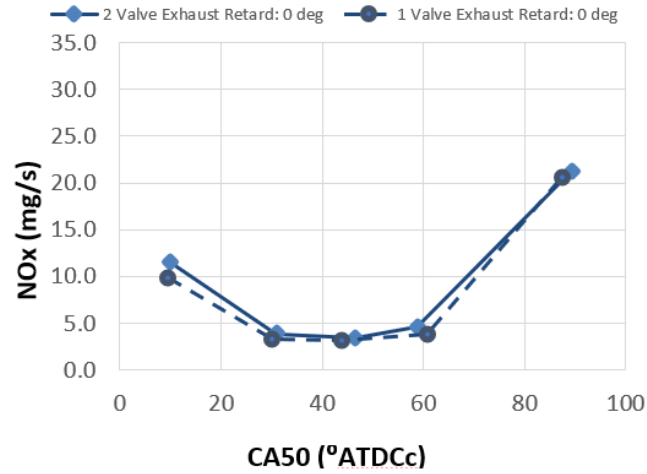


Figure 52: NOx emissions comparison for single valve and dual valve with the stock camshaft on a CA50 basis **Top**: Camshaft in home position **Middle**: Camshaft retarded by 25° **Bottom**: Camshaft retarded by 50° **Lines are assumed trends**

6.2.2 Combined Effects of Port Deactivation and Cam Duration Increase on Emissions

As seen in figure 53, HC is higher for the longer duration camshaft at earlier cam timings. The longer duration camshaft has an earlier EVO, which effectively cuts combustion short. This results in an increase in unburned fuel, resulting in an increase in HC mass flow from the engine. Once the camshaft was retarded into the later combustion phases, this becomes less of a factor, as EVO has been moved back towards where the stock cam was at earlier cam timings.

Much like HC, CO is increased with the longer duration camshaft. Figure 54 shows this clearly, especially at earlier cam timing. In fact, the reasoning for this is the same. The earlier EVO cuts combustion short and the reactants that were in the CO state have been essentially trapped in this mid-reaction state.

NO_x, on the other hand, is very similar between the two camshafts, with an increase in NO_x for the stock camshaft at the extreme points, shown in figure 55. This is likely due to the combustion process ending with the earlier EVO and the resulting combustion temperatures being lower for the longer duration camshaft.

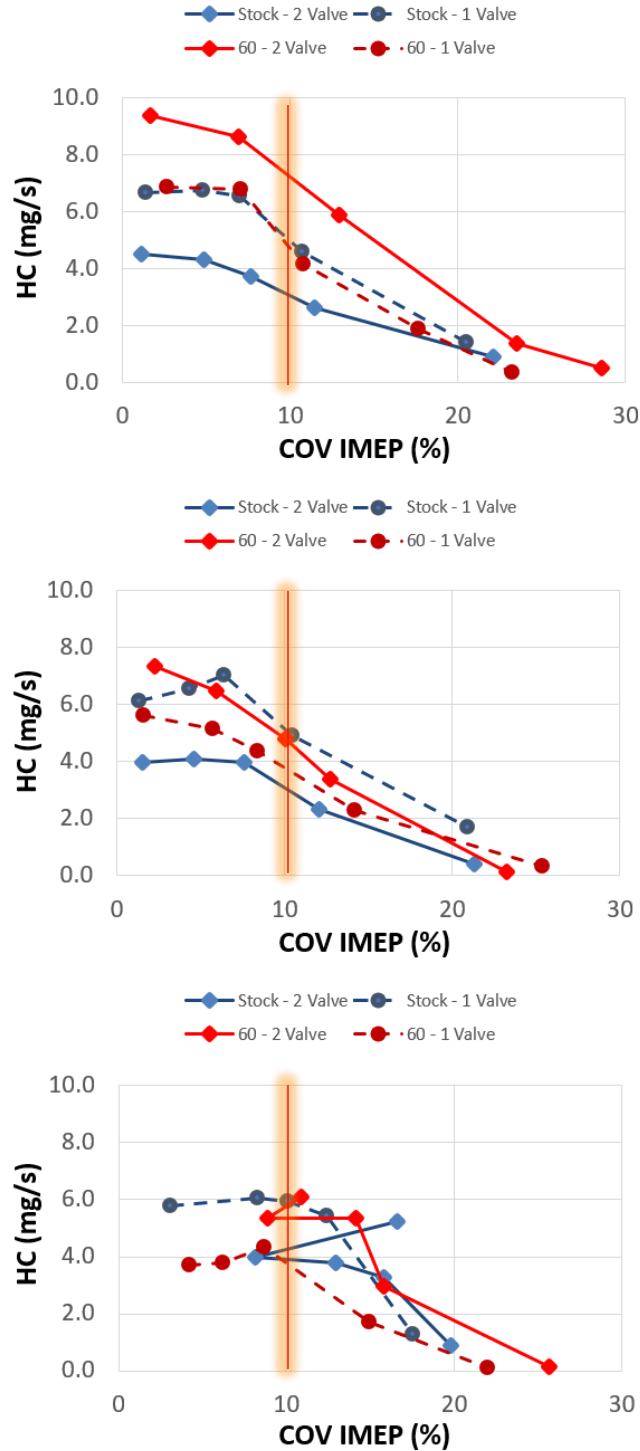


Figure 53: HC emissions comparison for single valve and dual valve with the stock and 60° camshafts **Top**: Camshaft in home position **Middle**: Camshaft retarded by 25° **Bottom**: Camshaft retarded by 50° **Lines are assumed trends and red line represents current COV limits**

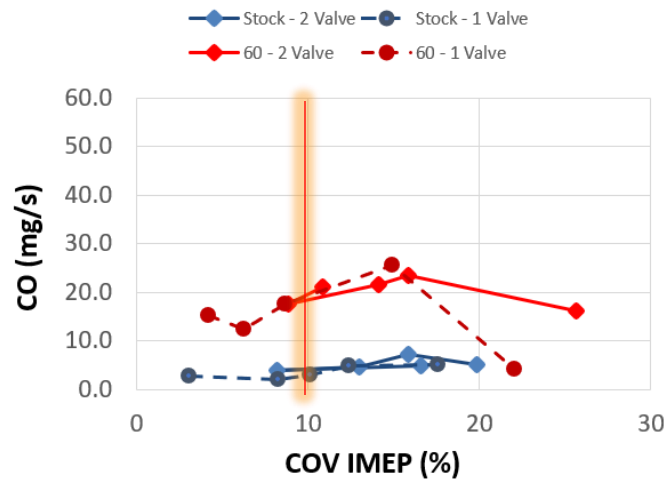
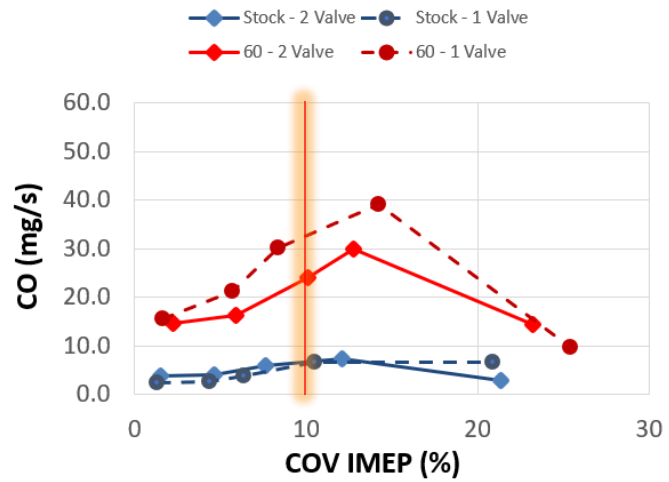
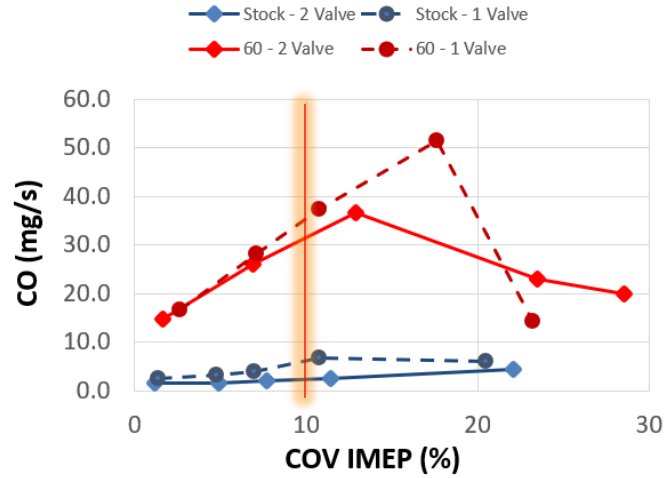


Figure 54: CO emissions comparison for single valve and dual valve with the stock and 60° camshafts **Top**: Camshaft in home position **Middle**: Camshaft retarded by 25° **Bottom**: Camshaft retarded by 50° **Lines are assumed trends and red line represents current COV limits**

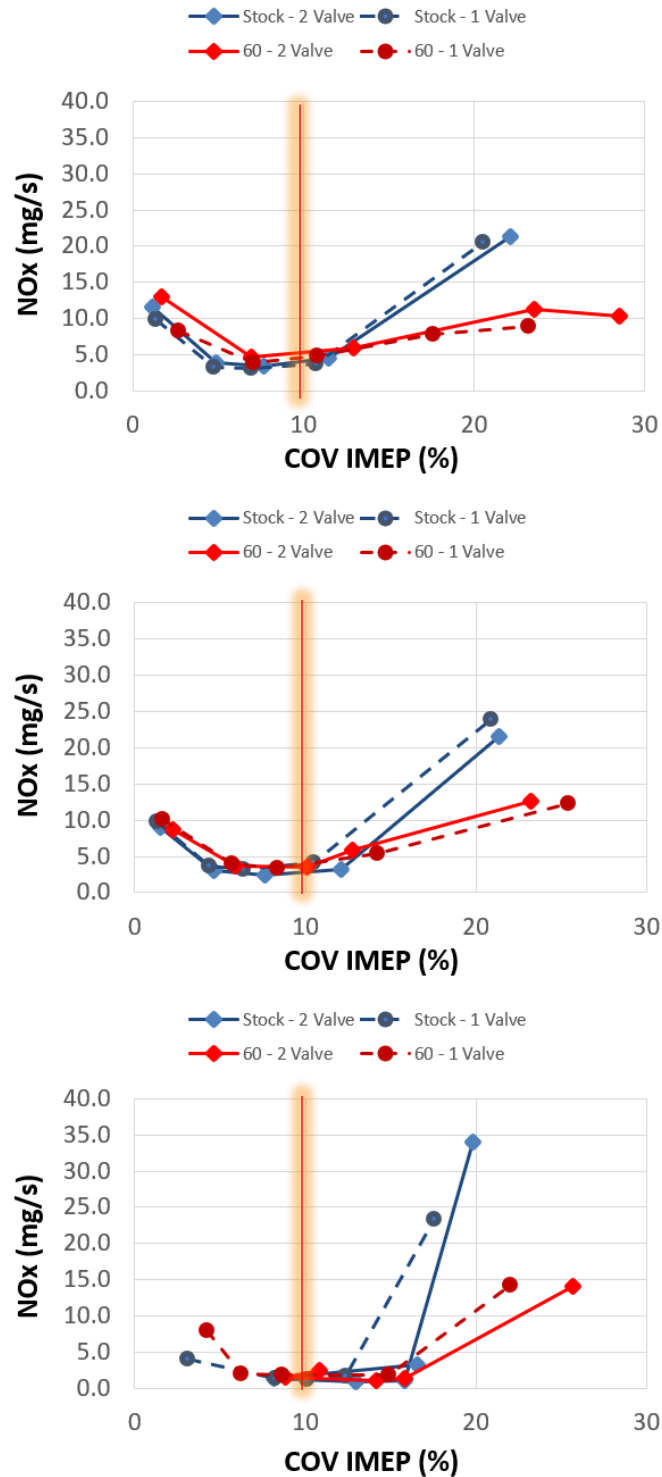


Figure 55: NOx emissions comparison for single valve and dual valve with the stock and 60° camshafts **Top**: Camshaft in home position **Middle**: Camshaft retarded by 25° **Bottom**: Camshaft retarded by 50° **Lines are assumed trends and red line represents current COV limits**

6.3 Mass Fraction Burn Analysis

With combustion occurring as late as it is, analysis was performed to ensure that the CA50 being calculated in real time by CAS was accurate. This was done by post-processing the cylinder pressure data and comparing it to the CAS data in a cross plot. This verification was only done with the stock camshaft. The results can be seen in figure 56.

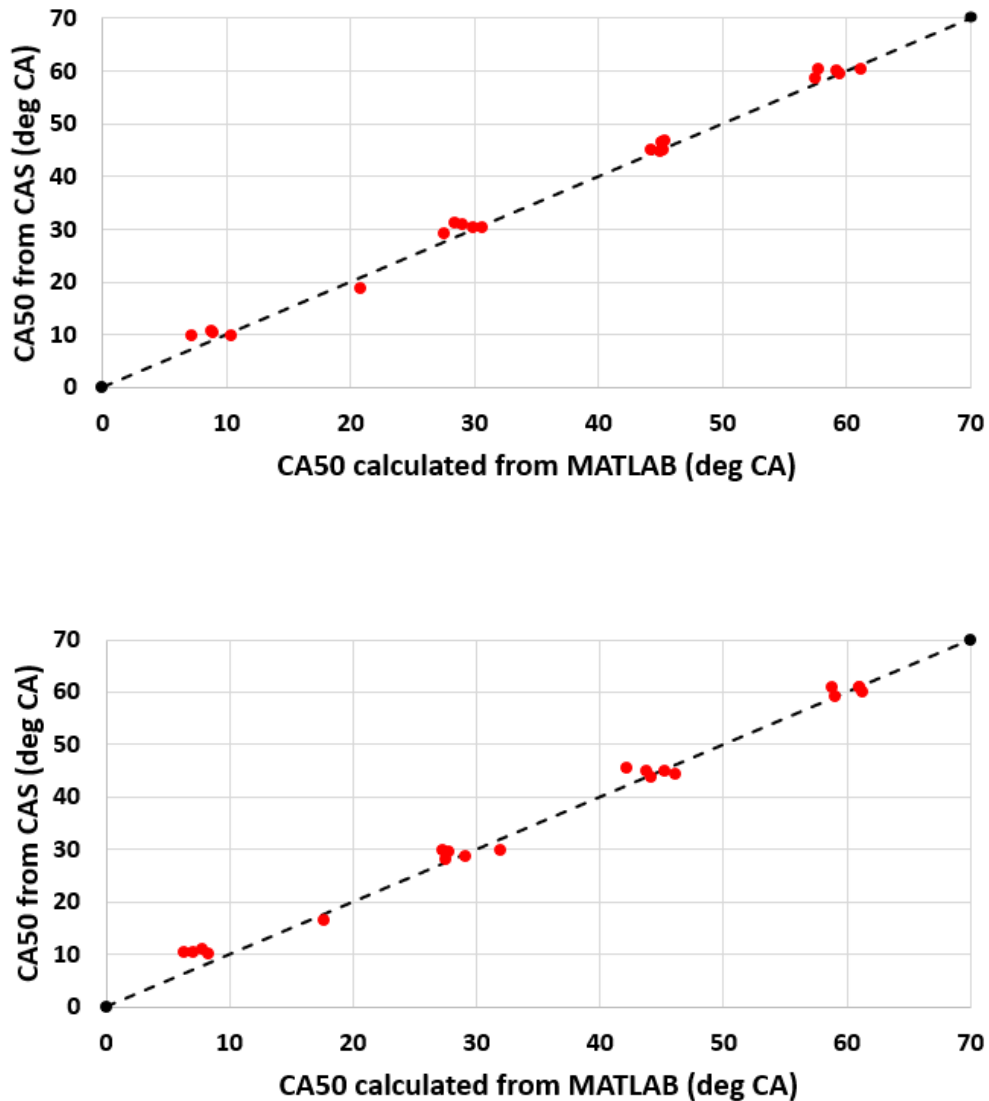


Figure 56: CAS CA50 comparison with post-processed CA50 **Top:** Dual valve operation
Bottom: Single valve operation **Lines represent perfect correlation**

However, there is an issue with calculating MFB for the longer duration camshafts. It was initially planned that with the longer duration camshafts EVO could be pushed into the combusting mixture, but by matching EVC across all camshafts, this option of pushing EVO into combustion became a requirement. This is especially true for the 60° camshaft. Referring back to figures 26 and 27, it can be seen that EVO for the 60° camshaft can be as early as 57° ATDC, or as late as 102° ATDC. Figure 57 is data from the engine under testing conditions with the stock camshaft in the park position to help show how variances in CA50 effect COV and CA90. In figure 57 it can be seen that for a CA50 of 30°, CA90 is 73°. This means that the 60° camshaft interrupts the combustion event for all test points shown. The result is that combustion phasing becomes very difficult to measure or estimate, and so there was some error in the combustion phasing calculations for some points with the longer duration camshafts.

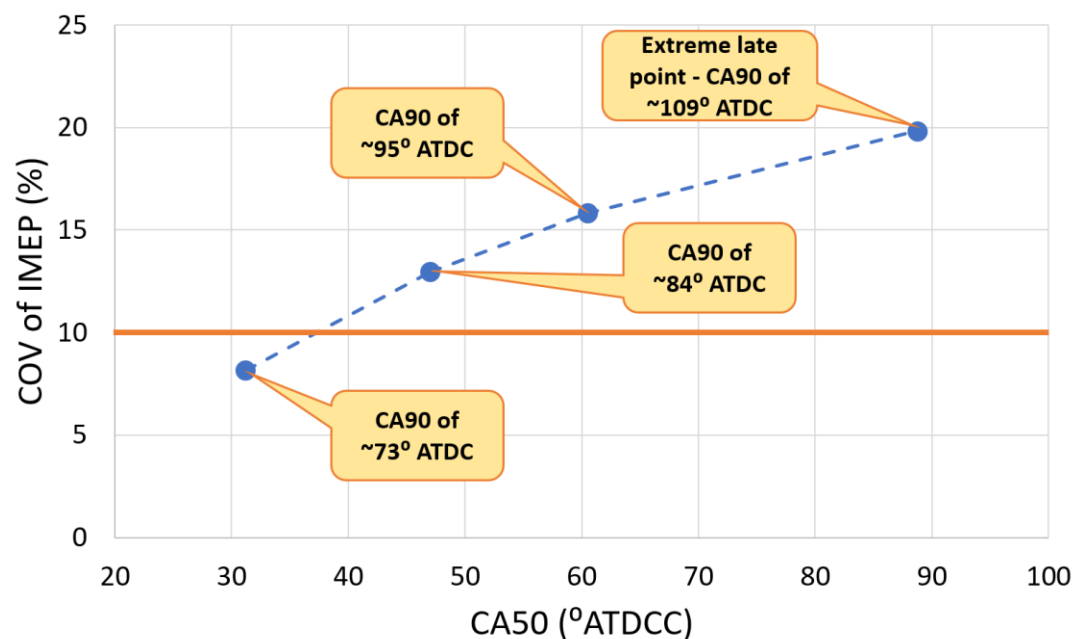


Figure 57: Home position, stock cam, dual valve operation CA50 sweep **Lines are assumed trends**

7 Conclusions

In the end, there are two sets of conclusions that can be made. One is for the comparison of single and dual valve operation and the other is on the effects of the duration increase of the exhaust cam. For the single and dual valve comparison, the results of the single valve operation were:

- The decrease in heat transfer in the dead port was partially offset by an increase in heat transfer in the live port (increased h coefficient)
- Mass flow rate increased (increasing the rate of enthalpy) due to increased pumping work early and late in the exhaust stroke resulting from reduced curtain area
- The decreased residual of single valve operation would enable later CA50 for a given COV of IMEP
 - The later CA50 would further increase EGT, while requiring increased mass flow to meet the load
- The downside of the reduced rebreathing is a significant increase in HC
- ***Bottom Line: 1-Valve does increase the rate of enthalpy slightly, but at the cost of increased engine out HC***

For the increase in cam duration:

- As expected, longer cam duration (at fixed EVC) leads to earlier EVO and an increased rate of enthalpy on a CA50 basis
- Early EVO increases the sensitivity between normal combustion variation and extracted work and can end combustion early, causing an increase in engine-out emissions
 - Retarding the cam doesn't help, as residual is increased, driving an increase in combustion variation
- ***Bottom Line: COV is inherently higher at all cam timing with the long duration cam, therefore on a COV basis there is only a slight increase in the rate of enthalpy***

Table 10 is a summary of everything found in this project. The arrows indicated a relative difference between the new configuration and the stock camshaft. Green arrows means either an increase in the rate of enthalpy or a decrease in emissions, which is the desired effect. Red arrows indicated the opposite. A single arrow represents a smaller change and dual arrows represents a larger change. The blue boxes represent no change.

Table 11: Final summary of results

Camshaft	Cam Position °CA Retarded From Park	Residuals	Port EGT	Post EGT	HC	CO	CO2	NOx	H2	CP	Enthalpy
Stock	2 Valve	■	■	■	■	■	■	■	■	■	■
	1 Valve	↓	↓↓	↑	↑↑	↓	↑	↑	↓	↑	↑
35°	2 Valve	↓	■	■	↑↑	↑	↑	↑	↑↑	↑	↑
	1 Valve	↑↑	↓	↑	↑↑	↑	↑	↑	↑	↑	↑
60°	2 Valve	↓	■	↑	↑↑	↑↑	↑	↑	↑↑	↑	■
	1 Valve	↓↓	↓	↑↑	↑	↑↑	↑	↑	↑↑	↑	↑



8 Future Work

For future iterations of this project, there are several routes that could be taken:

- Integration of a system similar to FIAT / Schaeffler “UniAir” technology or Koenigsegg’s Freevalve technology to allow an increased resolution for testing different valve activation configurations
- Test the engine under transient conditions to better represent the operating conditions of the FTP-75 and real world operation
- Test with as late of an EVC as possible to help increase rebreathing potential for the longer duration camshafts. This would potentially recapture HC and decrease engine-out HC when the catalyst is cold and non-functional
- More in-depth analysis of higher COV operational conditions as better NVH damping allows for the use in application. This would allow for the effects of this study to be drastically increased.

Reference List

- [1 J. B. Heywood, Internal Combustion Engine Fundamentals, New York: McGraw Hill, 1988.
- [2 U. S. E. P. Agency, "Vehicle and Fuel Emissions Testing," [Online]. Available: <https://www.epa.gov/vehicle-and-fuel-emissions-testing>. [Accessed 2019].
- [3 DieselNet, "United States: Cars and Light-Duty Trucks: Tier 3," [Online]. Available: https://www.dieselnet.com/standards/us/ld_t3.php. [Accessed 5 May 2019].
- [4 EPA, "Federal and California Light-Duty Vehicle," 19 January 2017. [Online]. Available: <https://19january2017snapshot.epa.gov/sites/production/files/2016-02/documents/420f16002.pdf>. [Accessed 5 May 2019].
- [5 S. J. Cornelius, N. Collings, K. Glover and D. E. Davidson, "Air-to-fuel Ratio Modulation Experiments over a Pd/Rh Three-way Catalyst," SAE Technical Paper 2001-01-3539, 2001.
- [6 F. R. Fernando, "Downstream Lambda Sensor Control Optimized to Fuel Blend," SAE Technical Paper 2008-36-0082, 2008.
- [7 C. Amann, "Control of the Homogeneous-Charge Passenger-Car Engine—Defining the Problem," SAE Paper 801440, 1980.
- [8 P. Bielaczyc, A. Szcotka and J. Woodburn, "The effect of a low ambient temperature on the cold-start emissions and fuel consumption of passenger cars," *Journal of Automobile Engineering*, vol. 225, no. 9, pp. 1253-1264, 2011.
- [9 P. Langen, M. Theissen, J. Mallog and R. Zielinski, "Heated Catalytic Converter Competing Technologies to Meet LEV Emission Standards," SAE Technical Paper 940470, 1994.
- [1 S. H. Chan and J. Zhu, "The Significance of High Value of Ignition Retard Control on the Catalyst Lightoff," SAE Technical Paper 962077, 1996.
- [1 J. E. Kubsh and G. W. Brunson, "EHC Design Options and Performance," SAE Technical Paper 960341, 1996.
- [1 Auto Batteries, "Cold Cranking Amps (CCA)," Auto Batteries, [Online]. Available: <https://www.autobatteries.com/en-us/how-to-choose-your-car-battery-replacement/battery-cold-cranking-amps-cca>. [Accessed 5 May 2019].

- [1] Optima Batteries, "WHAT DOES COLD CRANKING AMPS (CCA) MEAN?,"
3] [Online]. Available: <https://www.optimabatteries.com/en-us/experience/2014/01/what-does-cold-cranking-amps-cca-mean>. [Accessed 5 May 2019].
- [1] T. Ma, N. Collings and T. Hands, "Exhaust Gas Ignition (EGI) - A New," SAE
4] Technical Paper 920400, Detroit, 1992.
- [1] W. Gottschalk, G. Kirstein, O. Magnor, M. Schultalbers and R. Wetten,
5] "Investigations on a Catalyst Heating Strategy by Variable Valve Train for SI Engines," SAE Technical Paper 2012-01-1142, 2012.
- [1] K. Min, W. K. Cheng and J. B. Heywood, "The Effects of Crevices on the Engine-
6] Out," SAE Technical Paper 940306, 1994.
- [1] M. Ashford, R. Matthews, M. Hall, T. Kiehne, W. Dai, E. Curtis and G. Davis, "An
7] On-Board Distillation System to Reduce Cold-Start Hydrocarbon Emissions," SAE Technical Paper 2003-01-3239, 2003.
- [1] J. J. Worm, P. Dice, F. Jehlik, J. McFarland and S. A. Miers, "The Effect of
8] Individual Cylinder Fuel and Air Mixing in a High Performance Automotive Engine," ASME, 2013.
- [1] H. J. V. Schmidt, "THE EFFECT OF SOLID DEPOSIT FORMATIONS ON SI PFI
9] ENGINE PERFORMANCE AND CONTROL," Michigan Technological University, Houghton, 2014.
- [2] Valvoline, "Product Information: Valvoline Advanced Full Synthetic Motor Oils,"
0] [Online]. Available: <https://sharena21.springcm.com/Public/Document/18452/f1d157d1-0f7e-e711-9c10-ac162d889bd3/3aa410a1-0bbd-e711-9c12-ac162d889bd1>. [Accessed 6 May 2019].
- [2] General Motors, "2012 Buick Regal Owners Manual," [Online]. Available:
1] https://my.buick.com/content/dam/gmownercenter/gmna/dynamic/manuals/2012/buick/regal/2012_buick_regal_owners.pdf. [Accessed 6 May 2019].
- [2] National Instruments, "Veristand," National Instruments, [Online]. Available:
2] <http://www.ni.com/veristand/>. [Accessed 14 May 2019].
- [2] National Instruments, "NI PXIe-1078 User Manual," National Instruments, 2012.
3]

- [2 MTS Powertrain Technology Division, "CAS Software Manual," MTS Systems
4] Corporation, 2000.
- [2 Cambustion, [Online]. Available: <https://www.cambustion.com/>. [Accessed 2019].
5]
- [2 TSI Incorporated, "Model 3090/3090AK: Engine Exhaust Particle Sizer
6] Spectrometer Operation and Service Manual Rev. H," TSI Incorporated, 2011.
- [2 J. Coxon, "Slip sliding away," High Power Media Ltd., 09 July 2014. [Online].
7] Available: <https://www.highpowermedia.com/blog/3914/slip-sliding-away>.
[Accessed 23 May 2019].
- [2 A. Radulescu, J. McCarthy and S. Brownwell, "Development of a Switching Roller
8] Finger Follower for Cylinder Deactivation in Gasoline Engine Applications," SAE
Technical Paper 2013-01-0589, 2013.

Appendix A: Fuel Properties



MAKIN' POWER!™
www.vpracingfuels.com

Specification Sheet: C9

(TYPICAL VALUES)

Specific Gravity: 0.718@ 60°F/15.6°C

Color: Red

MON: 90.4

RON: 97.5

R+M/2: 94

RVP: 8.1 psi, 55.9 kpa

Oxygenated: No

Distillation:

10% evap @ 140.2°F/60.1°C

50% evap @ 209.8°F/98.8°C

90% evap @ 214.7°F/101.5°C

E.P. @ 229.1°F/109.5°C


H:C ratio = 2.06


O:C ratio = 0.09

Stoichiometric Ratio = 14.82

9 Appendix B: Crank Position Encoder

Model H20® Incremental Encoder





Mechanical Specifications

Shaft Diameter: 1/4" thru 3/8" and metric versions. Hollow shaft, hub shaft or thru-shaft versions available.

Flat On Shaft: 0.75 x 0.03 deep

Shaft Loading: up to 40 lbs. axial and 40 lbs. radial

Shaft Runout: .001 T.I.R. maximum

Starting Torque at 25°C: 1.0 in-oz maximum without shaft seal; 2.5 in-oz maximum with shaft seal; 4.0 in-oz thru-shaft

Bearings: 52100 bearing steel

Shaft material: 303 stainless steel

Bearing Housing: Die cast aluminum with iridite finish; stainless steel (special feature)

Cover: Die cast aluminum with protective finish (For MS or CS terminations), otherwise drawn aluminum with protective finish; stainless steel (special feature)

Bearing Life: 1.5 X 10⁶ revs at rated load (10,000 hrs at 2500 RPM)

Maximum RPM: 8,000 (see Frequency Response)

Moment of Inertia: 2.0 x 10⁻⁴ oz-in-sec²

Weight: 9 oz. typical

Cycles per Shaft Turn: 1 to 4096 (see table A) For resolutions above 1024 contact BEI for interpolation options

Supply Voltage: 5 to 28 VDC available

Current Requirements: 100 mA typical + output load, 250 mA (max)

Voltage/Output: (see note 5)
 28V/L: Line Driver, 5-28 VDC in, V_{out} = V_{in}
 28V/S: Line Driver, 5-28 VDC in, V_{out} = 5 VDC
 28V/OC: Open Collector, 5-28 VDC in, OCout

Protection Level: reverse, overvoltage and output short circuit (see note 5)







Frequency Response: 100 KHz (up to 1024 cpt; 400 KHz with interpolation option (see note 7))

Output Terminations: see Table 1

Note: Consult factory for other electrical options

The H20 is an extremely rugged encoder designed to economically fill the resolution range up to 4096 cycles per turn. This compact unit features a shock resistant disc, heavy duty bearings, and EMI shielding. The H20 conforms to NEMA 4 and 13 requirements. The H20 is also available in a hub shaft style with a flexmount (inset) for easy mounting directly to small motors. Typical applications of the H20 include machine control, process control, agricultural machinery, textile equipment, robotics, food processing, and metering.

Special Models of the H20 Incremental Encoder are available with one or more of the following certifications. Consult factory for details.

 EN 55011 and EN 61000-6-2	 U.S. Standards Class I, Group A,B,C & D; Class II Group E,F & G	 Canadian Standards Class I, Zone 0, Group IIC
 UL 12.0035X UL 12.0082X	 Class I, Div 2, Group A,B,C & D; Class II, Div 2, Group F & G	
 CENELEC II G Ex ia IIB/IIC T4 II 3 G Ex nA IIB T3 Gc II 3 G Ex nA IIB T4 Gc		

Electrical Specifications

Code: Incremental

Output Format: 2 channels in quadrature, 1/2 cycle index gated with negative B channel as standard. Ungated index when 3904 is specified as the output device

Environmental Specifications

Enclosure Rating: NEMA 4 & 13 (IP66) when ordered with shaft seal (on units with an MS connector) and a cable gland (on units with cable termination)

Temperature: Operating, 0° to 70°C; extended temperature testing available (see note 8); Storage, -25° to 90°C unless extended temperature option called out

Shock: 50 g's for 11 msec duration

Vibration: 5 to 2000 Hz @ 20 g's

Humidity: 98% RH without condensation

NOTES & TABLES: All notes and tables referred to in the text can be found on the back of this page.

H20 Incremental Ordering Options

for assistance call 800-350-2727

Use this diagram, working from left to right to construct your model number (example: H20DB-37-SS-500-ABZC-28V/V-SM18).

All notes and tables referred to can be found on pages the back of this page.

<div style="border: 1px solid black; padding: 2px; margin-bottom: 5px; text-align: center;">H20</div> <p>TYPE: H = Heavy Duty 20 = 2.00" DIA.</p> <p>HOUSING CONFIG: D = Square Flange E = 2.00 Dia. <i>See Dimensions</i></p>	<p>SHAFT DIA: 25 = 0.2497 37 = 0.3747 39 = 0.3935 39 = 0.3932</p> <p>PILOT CONFIG: A = 1.181 (30mm) Female (No shaft seal available) B = 1.25</p>	<p>FACE MOUNT: F5, F12, F28 Blank = None <i>See Dimensions</i></p> <p>SHAFT TYPE: TS = Thru Shaft HS = Hollow Shaft HS = Hub Shaft Blank = single ended shaft (standard)</p> <p>SHAFT SEAL: SS = Shaft Seal (must use pilot B, except HBS units can take SS with pilot A) <i>See note 2</i></p>	<p>CYCLES PER TURN: (Enter Cycles) <i>See table A</i></p> <p>NO. OF CHANNELS: A = Single Channel AB = Dual Quad. Ch. ABZ = Dual with Index AZ = Single with Index <i>See note 3</i></p>	<p>VOLTAGE/OUTPUT: 28V/L = 5-28V_{in}/out 28V/S = 5-28V_{in}/5V_{out} 28V/OC = 5-28V_{in}/OC_{out}</p> <p>COMPLEMENTS: C = Complementary Outputs Blank = None <i>See note 4</i></p>	<p>OUTPUT TERMINATION LOCATION: E = End S = Side</p> <p>HAZARDOUS AREA RATINGS: Blank = None EX = Intrinsically Safe NI = Non-Incendive Contact factory for voltage options</p> <p>SPECIAL FEATURES: S = Special features specified on purchase order. (Consult factory) <i>See note 6</i></p> <p>OUTPUT TERMINATION: M14 = MS3102R14S-6P M16 = MS3102R16S-1P M18 = MS3102R18-1P C = Pigtail Cable CS = Cable with Seal (Side or End Term) Add cable length (i.e., C18=18" cable) <i>See table 1 & note 9</i></p>
---	---	--	---	---	---

EXPRESS ENCODERS® Items highlighted with are standard Express Encoders and ship in one to three days.

T2 option is available as a standard H20 Express Encoder.

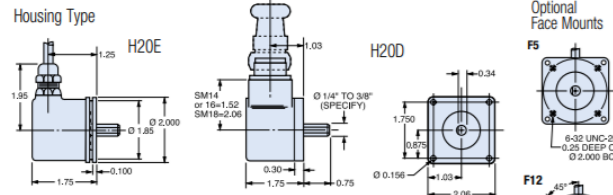
BEI SENSORS

Tel: 805-968-0782 / 800-350-2727 | Fax: 805-968-3154 / 800-960-2726
 7230 Hollister Ave., Goleta, CA 93117-2807 | www.beisensors.com

Model H20[®] Incremental Encoder



Dimensions



Special Shaft Options

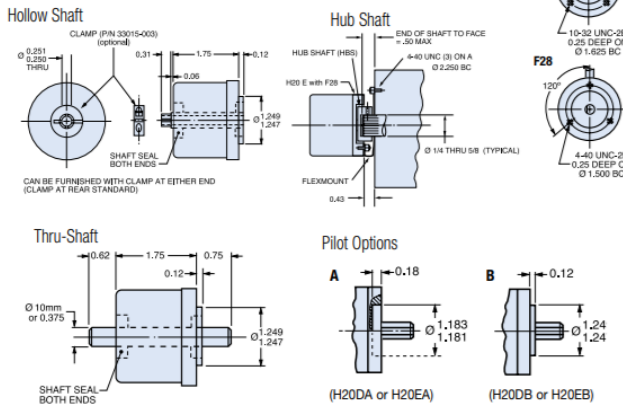


Figure 1

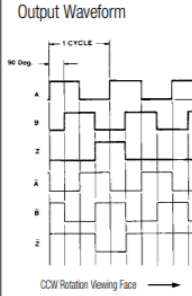


Table A

H20 Disc Resolutions							
1*	2	3	5	6	8	10	
11	12	24	25	30			
32	40	50	60	64			
75	80	95	100	105	115		
120	125	150	192	200			
240	250	256	300	336			
360	400	500	510	512			
600	625	635	720	785			
1000	1024	1200**					

Resolutions Shown in RED are not available as Express Encoders
 *No index. For interpolation please specify the multiplied output (up to 4,096 for H20) in the model number, i.e. 4,096-T4.
 **Consult factory for this resolution

Notes

- Mounting is usually done either using the D-style square flange mount, E- or G-style servo mounts, or one of the standard face mounts, F1 for example. Consult factory for additional face mount options.
- The shaft seal is recommended in virtually all installations. The most common exceptions are applications requiring a very low starting torque or those requiring operation at both high temperature and high speed.
- Non-standard index widths and multiple indices are available by special order. Consult factory.
- Complementary outputs are recommended for use with line driver type (source/sink) outputs. When used with differential receivers, this combination provides a high degree of noise immunity.
- Output IC's:** Output IC's are available as either Line Driver (LD) or NPN Open Collector (OC) types. Open Collectors require pull-up resistors, resulting in higher output source impedance (sink impedance is similar to that of line drivers). In general, use of a Line Driver style output is recommended. Line Drivers source or sink current and their lower impedance mean better noise immunity and faster switching times. **Warning:** Do not connect any line driver outputs directly to circuit common/OV, which may damage the driver. Unused outputs should be isolated and left floating. Our applications specialists would be pleased to discuss your system requirements and the compatibility of your receiving electronics with Line Driver type outputs. **28V/I:** Multi-voltage Line Driver (7272*); 100 mA source/sink. Input voltage 5 to 28 VDC +/- 5% standard (Note: $V_{out} = V_{in}$). This driver is TTL compatible when used with 5 volt supply. Supply lines are protected against overvoltage to 60 volts and reverse voltage. Outputs are short circuit protected for one minute. Supply current is 120 mA typical (plus load current). This is the recommended replacement for 3904R and 7406R open collector outputs with internal pull-up resistors. It is also a direct replacement for any 4469, 88C30, 8830 or 28LS31 line driver. **28V/O:** Multi-voltage Line Driver (7272*); 100 mA source/sink. Input voltage 5 to 28 VDC +/- 5% standard. Internally regulated with 5V (TTL compatible) logic out. Supply lines are protected against overvoltage to 60 volts and reverse voltage. Outputs are short circuit protected for one minute. Supply current is 90 mA typical (plus load current). **15V/V:** Multi-voltage Line Driver (4469*); 100 mA source/sink. Input voltage 5 to 15 VDC +/- 5% standard (Note: $V_{out} = V_{in}$). TTL compatible when used with 5 volt supply. Supply lines are protected against overvoltage to 60 volts and reverse voltage. Outputs are short circuit protected for one minute. Supply current is 90 mA typical (plus load current). This is a direct replacement for the 4469 Line Driver. **28V/OC:** NPN Open Collector (3904*, 7273*). Current sink of 80 mA max. Current sourced by external pull-up resistor. Output can be pulled up to voltage other than supply voltage (30 V max). Input voltage 5 to 28 VDC +/- 5% standard. Supply current is 120 mA typical. This replaces prior IC's with designations of 3904, 7406, 3302, 681 and 689. **5V/OCR, 15V/OCR, 24V/OCR:** Open Collector (3904R*, 7406R*, 7273R*). Current sink of 70 mA max. Includes internal pull-ups sized at approximately 100 ohms/volt. Max current source is 10 mA. Supply current is 100 mA typical, 120 mA with internal pull-ups. 5V/V, 5V/OC, 5V/OCR and 9V/OC can be intrinsically safe line driver and open collector outputs available on certain model variations. They are intrinsically safe only when installed per the control drawing noted on the certification label affixed to the encoder body.
- Special -S at the end of the model number is used to define a variety of non-standard features such as special shaft lengths, voltage options, or special testing. Please consult the factory to discuss your special requirements.
- Higher frequency response may be available. Please consult with the factory.
- Extended temperature ratings are available in the following ranges: -40 to 70°C, -40 to 85°C, -20 to 105°C and -40 to 105°C depending on the particular model. Some models can operate down to -55°C. Extended temperature ranges can affect other performance factors. Consult with factory for more specific information.
- Mating straight plug receptacles may be ordered from the factory:
 For M12 use MS3116F12-10S, For M14 use MS3106F14S-6S
 For M14/19 use MS3116J14-19S, For M16 use MS3106F16S-1S
 For M18 use MS3106F18-1S, For M20 use MS3106F20-2S

Table 1

Incremental Output Terminations

The connector style will determine pinouts. For example, an encoder with ABC channels and an M18 connector uses the table to the right.

M14 CONNECTOR	M16 CONNECTOR	CHANNELS DESIGNATED IN MODEL NO.		
PIN	PIN	ABZ	ABC	ABC
E	A	A	A	A
D	B	B	B	B
C	C	Z	Z	A
B	D	+V (SUPPLY VOLTAGE)		
F	E	—	—	B
A	F	0 V (CIRCUIT COMMON)		
	G	CASE GROUND (CG) (Except H20)		

M18 CONNECTOR	
PIN	CHANNEL
A	A
B	B
C	Z
D	+V
E	—
F	OV
G	—
H	A
I	B
J	Z

WIRE COLOR (22AWG)	DA 15P CONNECTOR	CHANNELS DESIGNATED IN MODEL NO.		
		ABZ	ABC	ABZC
YEL	13	A	A	A
BLUE	14	B	B	B
ORN	15	Z	—	Z
W-YEL	10	—	A	A
W-BLU	11	—	B	B
W-OM	12	—	—	Z
RED	6	+V (SUPPLY VOLTAGE)		
BLK	1	0 V (CIRCUIT COMMON)		
GRN	9	CASE GROUND (CG) (Except H20)		
WHITE		SHIELD DRAIN (Shielded cable only)		



Tel: 805-968-0782 / 800-350-2727 | Fax: 805-968-3154 / 800-960-2726 | 7230 Hollister Ave., Goleta, CA 93117-2807
 www.beisensors.com

10 Appendix C: Combustion Fast Analyzer Specifications

Specifications	HFR500 HC analyzer	CLD500 NO _x analyzer	NDIR500 CO & CO ₂ analyzer
Measurement principle	Flame Ionisation Detector	Chemiluminescence Detector	Non-Dispersive Infra-Red
Component(s) measured	Total Hydrocarbons (THC)	NO, NO ₂ (with NO ₂ converter)	Carbon monoxide (CO), Carbon dioxide (CO ₂)
Number of channels	2	2	2
Measurement ranges	0-2000 to 0-1,000,000 ppm C1	0-100 ppm to 0-5,000 ppm (extendable to 0-10,000 ppm)	0-5%, 0-10%, 0-15% and 0-20%
Fastest response time T _{90-10%} (sample probe length dependent)	0.9 ms	2 ms (8 ms with NO ₂ converter)	8 ms
Zero drift	<1% FS / hour	<5 ppm / hour	<2% FS / hour
Span drift	<1% FS / hour	<1% FS / hour	<2% FS / hour
Sample gas flow (1 channel including bypass)	6 litres per minute (1 bara)	6 litres per minute (1 bara) 4 lpm with NO ₂ converter	6 litres per minute (1 bara)
Power supply	50/60Hz 100-240VAC		
Max power requirement (single phase)	1.7 kVA	2.6 kVA	1.7 kVA
Gases required (all at 2 bar gauge)	40% H ₂ /He or H ₂ /N ₂ fuel HC span gas, Zero air & N ₂	NO (NO ₂) span gas, N ₂	2 each of CO & CO ₂ span gases, N ₂
Cabinet dimensions	(w x d x h) 550 x 780 x 1,140 mm including wheels		
Approx cabinet weight (incl. vac pumps)	125 kg	150 kg	125 kg
Operating conditions	0 - 40° C. Sub-zero sampling option available		
Conduit length	10 metres (detector to cabinet). Custom lengths available		
Connection to control PC	RS232 or RS485		
Test cell interface	Analog data outputs with AK and digital remote control optional		

Figure 58: Specifications for Combustion Fast Analyzers [21]

11 Appendix D: Copyright Documentation

11.1 Permission to use screen images and plots from GT-Power and GT-Post software produced by Gamma Technologies Incorporated

5/8/2019

Michigan Technological University Mail - Permission to use GT-Power and GT-Post information for a master's thesis



Michigan Tech

Zak Parker <zrparker@mtu.edu>

Permission to use GT-Power and GT-Post information for a master's thesis

2 messages

Zak Parker <zrparker@mtu.edu>
To: C.Contag@gtisoft.com

Wed, May 8, 2019 at 4:29 PM

Hello,

I am currently writing my master's thesis and I would like to request permission to use GT-Power model screen-shots and GT-Post plots. If you could grant me permission to use these in my thesis, I would greatly appreciate it.

Thanks,
Zak

Zakarie Parker

Masters Student-Michigan Technological University
Mechanical Engineering
APS Labs Graduate Research Assistant
Former Vice President, MTU Archery Club
Email: zrparker@mtu.edu
Phone: (231) 730-2642

Christopher Contag <C.Contag@gtisoft.com>
To: Zak Parker <zrparker@mtu.edu>

Wed, May 8, 2019 at 4:42 PM

Hello Zak,

Sure, you have permission to use screen shots of the models and plots in your thesis. We are always interested in academic work done with our software, so if you can share your thesis with us, it would be greatly appreciated – but no worries if you cannot share the work. I will take the opportunity to point you to our careers section, in case you are looking for a job after finishing your thesis, and have not checked it out yet: <https://www.gtisoft.com/about-gt/careers/>

Best Regards,

Chris

Christopher A. Contag
Account Manager

System Solutions Engineering
Direct: 1 (630) 537-9214 | Main: 1 (630) 325-5848
[601 Oakmont Lane, Suite 220, Westmont, IL, 60559](#)

Gamma Technologies [Website](#) | [Publications](#) | [Training](#)

[Quoted text hidden]

11.2 Permission to use Equation 1, Table 1, and Figure 2 from [8]

5/10/2019

Michigan Technological University Mail - Journal of Automobile Engineering, vol. 225, no. 9, pp. 1253-1264, 2012 Permissions



Zak Parker <zrparker@mtu.edu>

Journal of Automobile Engineering, vol. 225, no. 9, pp. 1253-1264, 2012 Permissions

2 messages

Zak Parker <zrparker@mtu.edu>
To: piotr.bielaczyc@bosmal.com.pl

Fri, May 10, 2019 at 9:22 AM

Hello,

I am currently working on my master's thesis and was wondering if I could be given permission to use the following from "The effect of a low ambient temperature on the cold-start emissions and fuel consumption of passenger cars":

Equation 1
Table 1
Figure 2

Thanks,
Zak

Zakarie Parker

Masters Student-Michigan Technological University
Mechanical Engineering
APS Labs Graduate Research Assistant
Former Vice President, MTU Archery Club
Email: zrparker@mtu.edu
Phone: (231) 730-2642

Piotr Bielaczyc <Piotr.Bielaczyc@bosmal.com.pl>
To: Zak Parker <zrparker@mtu.edu>

Fri, May 10, 2019 at 9:41 AM

Yes, please feel free to use this data. Thanks for your email.

Best regards,

Piotr Bielaczyc, PhD
Department Head

Engine Research Department
cell.: +48 698637991
tel.: +48 33 813 0598
e-mail: piotr.bielaczyc@bosmal.com.pl
web: www.bosmal.com.pl



BOSMAL Automotive Research and Development Institute Ltd
93 Sami Stok, 43-300 Bielsko-Biala, Poland
tel.: +48 33 813 0 539
Regional Court in Bielsko-Biala, VIII Commercial Department of National Court's Register
National Court Registry No.: 0000221979, EU VAT No.: PL5472013159
Basic capital: PLN 5.150.000

11.3 Permission to use the image from [27]

5/23/2019

Michigan Technological University Mail - Using an image for my thesis



Zak Parker <zrparker@mtu.edu>

Using an image for my thesis

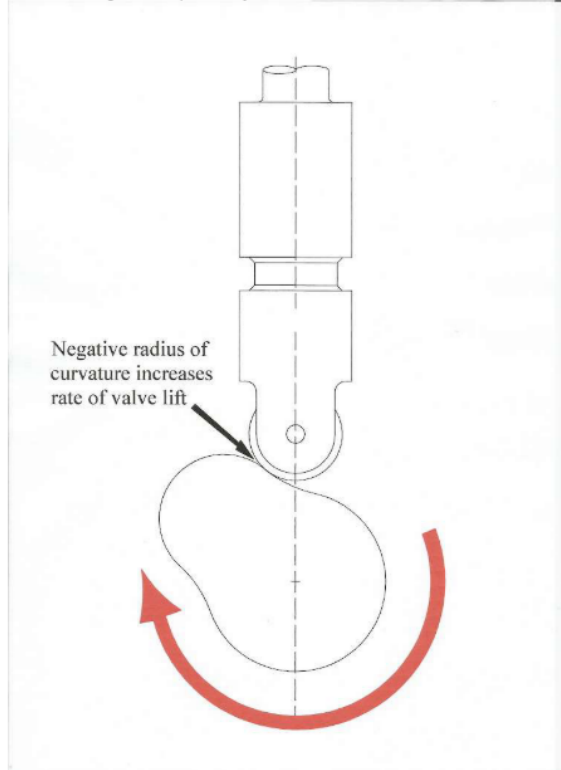
2 messages

Zak Parker <zrparker@mtu.edu>
To: info@highpowermedia.com

Wed, May 22, 2019 at 9:03 PM

Hello,

I am working to complete my master's thesis and I would like to use this image:



from: <https://www.highpowermedia.com/blog/3914/slip-sliding-away> May I please have your permission to do so?

Thanks,
Zak

Zakarie Parker

Masters Student-Michigan Technological University
Mechanical Engineering
APS Labs Graduate Research Assistant
Former Vice President, MTU Archery Club
Email: zrparker@mtu.edu
Phone: (231) 730-2642

<https://mail.google.com/mail/u/1?ik=bf1f43657b&view=pt&search=all&permthid=thread-a%3Ar-5320571852276361155&simpl=msg-a%3Ar-528573805...> 1/2

5/23/2019

Michigan Technological University Mail - Using an image for my thesis

Chris Perry <chris@highpowermedia.com>
To: Zak Parker <zrparker@mtu.edu>

Thu, May 23, 2019 at 4:15 AM

Hi Zak,

No problem to use the image for the purposes of your thesis. Well done for asking and good luck with the master's.

Kind regards,

Chris.

Chris Perry

High Power Media Ltd

Office: +44 (0) 1934 713957

Mobile/Cell: +44 (0) 7793 597315

Fax: +44 (0) 208 497 2102

Email: chris@highpowermedia.com

Web: www.highpowermedia.com

High Power Media Ltd, Whitfield House, Cheddar Road, Wedmore, Somerset, BS28 4EJ, England
Registered in England and Wales No. 5666309


VAT Registration No. 888253574

The contents of this email and any attachments are strictly confidential. They may not be disclosed to someone who is not a named or authorized recipient. They may also be subject to professional privilege and unauthorized disclosure, copying or use is prohibited. If you receive this e-mail in error please notify the sender by replying using the words Misdirected E-mail in the subject, and then delete the message and any attachments from your system. Although this e-mail and any attachments have been scanned for viruses, the success of scanning products is not guaranteed. The recipient's should therefore carry out any checks that they believe to be appropriate in this respect. Opinions expressed in this email may not be official policy.

[Quoted text hidden]

<https://mail.google.com/mail/u/1?ik=bf1f43657b&view=pt&search=all&permthid=thread-a%3Ar-5320571852276361155&simpl=msg-a%3Ar-528573805...> 2/2

11.4 Permissions to use Figures 3, 4, 6, 7, 28



Note: Copyright.com supplies permissions but not the copyrighted content itself.

1 PAYMENT 2 REVIEW 3 **CONFIRMATION**

Step 3: Order Confirmation

Thank you for your order! A confirmation for your order will be sent to your account email address. If you have questions about your order, you can call us 24 hrs/day, M-F at +1.855.239.3415 Toll Free, or write to us at info@copyright.com. This is not an invoice.

Confirmation Number: 11840448
Order Date: 08/11/2019

If you paid by credit card, your order will be finalized and your card will be charged within 24 hours. If you choose to be invoiced, you can change or cancel your order until the invoice is generated.


Payment Information

Alex Normand
apslabs@mtu.edu
+1 (906) 487-1131
Payment Method: invoice
PO#: Zak Parker-Thesis

Billing address:
23199 Airpark Blvd
Advanced Power Systems
Calumet, MI 49913
US

Order Details


Development of a Switching Roller Finger Follower for Cylinder Deactivation in Gasoline Engine Applications

Order detail ID: 71977027	Permission Status:  Granted
Order License Id: 4646010275836	Permission type: Republish or display content
Report ID: 2013-01-0589	Type of use: Thesis/Dissertation
Publication Type: Report	Requestor type: Academic institution
Volume:	Format: Electronic
Issue:	Portion: chart/graph/table/figure
Start page:	Number of charts/graphs/tables /figures: 1
Publisher: SAE International	The requesting person/organization: Zak Parker
Author/Editor: Radulescu, Andrei	Title or numeric reference of the portion(s): Figure 6

Note: This item will be invoiced or charged separately through CCC's **RightsLink** service. [More info](#) **\$ 67.25**

On-Board Distillation System to Reduce Cold-Start Hydrocarbon Emissions

Order detail ID: 71977028
Order License Id: 4646010277092
Report ID: 2003-01-3239
Publication Type: Report
Volume:
Issue:
Start page:
Publisher: SAE International
Author/Editor: Ashford, Marcus

Permission Status:  **Granted**

Permission type: Republish or display content
Type of use: Thesis/Dissertation

Requestor type: Academic institution
Format: Electronic
Portion: chart/graph/table/figure
Number of charts/graphs/tables/figures: 1
The requesting person/organization: Zak Parker/Michigan Technological University
Title or numeric reference of the portion(s): Figure 11
Title of the article or chapter the portion is from: PHASE II. CALIBRATION DEVELOPMENT
Editor of portion(s): Ashford, Marcus
Author of portion(s): Ashford, Marcus
Volume of serial or monograph: N/A
Page range of portion: 8
Publication date of portion: 2003
Rights for: Main product
Duration of use: Current edition and up to 5 years
Creation of copies for the disabled: no
With minor editing privileges: no

For distribution to: Worldwide
RightsLink service: [More info](#)

Note: This item will be invoiced or charged separately through CCC's **RightsLink** service. [More info](#)

\$ 67.25

Heated Catalytic Converter Competing Technologies to Meet LEV Emission Standards

Order detail ID: 71977029
Order License Id: 4646010278300
Report ID: 940470
Publication Type: Report
Volume:
Issue:
Start page:
Publisher: SAE International
Author/Editor: Langen, Peter

Permission Status:  **Granted**

Permission type: Republish or display content
Type of use: Thesis/Dissertation


Requestor type	Academic institution
Format	Electronic
Portion	chart/graph/table/figure
Number of charts/graphs/tables/figures	1
The requesting person/organization	Zak Parker/Michigan Technological University
Title or numeric reference of the portion(s)	Figure 3
Title of the article or chapter the portion is from	3.2 External measures outside the engine
Editor of portion(s)	Langen, Peter
Author of portion(s)	Langen, Peter
Volume of serial or monograph	N/A
Page range of portion	49
Publication date of portion	1994
Rights for	Main product
Duration of use	Current edition and up to 5 years
Creation of copies for the disabled	no
With minor editing privileges	no

Note: This item will be invoiced or charged separately through CCC's **RightsLink** service. [More Info](#) **Worldwide**

\$ 67.25

Control of the Homogeneous-Charge Passenger-Car Engine — Defining the Problem


Order detail ID: 71977031
Order License Id: 4646010279512
Report ID: 801440
Publication Type: Report
Volume:
Issue:
Start page:
Publisher: SAE International
Author/Editor: Amann, Charles A.

Permission Status:  **Granted**
Permission type: Republish or display content
Type of use: Thesis/Dissertation
Requestor type: Academic institution
Format: Electronic
Portion: chart/graph/table/figure
Number of charts/graphs/tables/figures: 1
The requesting person/organization: Zak Parker/Michigan Technological University
Title or numeric reference of the portion(s): Figure 16
Title of the article or chapter the portion is from: OXIDIZING CATALYTIC CONVERTER
Editor of portion(s): Amann, Charles A.
Author of portion(s): Amann, Charles A.
Volume of serial or monograph: N/A
Page range of portion: 10
Publication date of portion: 1980
Rights for: Main product
Duration of use: Current edition and up to 5 years
Creation of copies for the disabled: no
With minor editing privileges: no

Note: This item will be invoiced or charged separately through CCC's [RightsLink](#) service. [More info](#) **Worldwide** **\$ 67.25**

Downstream Lambda Sensor Control Optimized to Fuel Blend

Order detail ID: 71977032
Order License Id: 4646010280638
Report ID: 2008-36-0082
Publication Type: Report
Volume:
Issue:
Start page:
Publisher: SAE International
Author/Editor: Rovai, Fernando Fusco

Permission Status:  **Granted**
Permission type: Republish or display content
Type of use: Thesis/Dissertation

Requestor type: Academic institution

Format: Electronic

Portion: chart/graph/table/figure

Number of charts/graphs/tables/figures: 1

The requesting person/organization: Zak Parker/Michigan Technological University

Title or numeric reference of the portion(s): Figure 3

Title of the article or chapter the portion is from: INTRODUCTION

Editor of portion(s): Rovai, Fernando Fusco

Author of portion(s): Rovai, Fernando Fusco

Volume of serial or monograph: N/A

Page range of portion: 3

Publication date of portion: 2008

Rights for: Main product

Duration of use: Current edition and up to 5 years

Creation of copies for the disabled: no

With minor editing privileges: no

Note: This item will be invoiced or charged separately through CCC's **RightsLink** service. [More info](#)

\$ 67.25